Spring 1-1-2010

Development of an Ultraviolet Point-of-Use Device for Household Disinfection

Christina Kay Barstow
University of Colorado at Boulder, ckbarstow@gmail.com

DEVELOPMENT OF AN ULTRAVIOLET POINT-OF-USE DEVICE

FOR HOUSEHOLD WATER DISINFECTION

By

CHRISTINA KAY BARSTOW

A thesis submitted to the Faculty of the Graduate School of the

University of Colorado at Boulder

in partial fulfillment of the requirements for the degree of

Master of Science

Department of Civil, Environmental, and Architectural Engineering

2010

This thesis entitled:

Development of an Ultraviolet Point-of-Use Device
for Household Water Disinfection

written by Christina Kay Barstow

has been approved for the Department of Civil, Environmental,
and Architectural Engineering

Karl G. Linden

R. Scott Summers

Aaron D. Dotson

Date: ________________

The final copy of this thesis has been examined by the signatories, and we find that both the content and the form meet acceptable presentation standards of scholarly work in the above mentioned discipline.

Barstow, Christina Kay (M.S., Civil Engineering [Department of Civil, Environmental, and Architectural Engineering])

Development of an Ultraviolet Point-of-Use Device for Household Water Disinfection

Thesis directed by Professor Karl G. Linden

Abstract

Point-of-use (POU) disinfection systems have the ability to provide safe drinking water to the millions who lack access to an improved water source. While many POU systems exist in developing communities, there are several concerns that lead to low user acceptability. Concerns include low flow rates, taste and odor issues, high costs, recontamination and ineffectiveness at treating common pathogenic organisms. In response to these concerning issues, an ultraviolet (UV) POU system has been developed consisting of developing community appropriate materials (recycled plastics, recycled aluminum, etc.) and simple construction techniques based around the use of a low-wattage, low pressure UV bulb. Three generations of prototypes were developed and tested for hydraulics and microbicidal effectiveness. The latest prototype has the ability to inactivate 4-log bacteria and protozoa, and 1-2 log viruses.

Acknowledgements

I would first like to thank my advisor, Karl Linden, for his support, patience and allowing me the flexibility to perform this research. Additionally, I owe a great deal of thanks to Aaron Dotson, for your practical mind and support in the lab. Erinn Kunik, who worked on the power supply and many of the tracer studies during a summer research program was extremely helpful and a great student to mentor in the lab. I am also grateful to Jared Leidich for modeling the systems, Tim May for his help with the electrical components, Kevin McCabe for help with the microbiological work and all of the students in the Linden lab group. And lastly, I greatly appreciate my family and friends for keeping me sane and their unconditional support in pursuit of my academic endeavors.

Table of Contents

Table of Tables

Table of Figures

1. Background

1.1 Point-of-Use Water Treatment and Safe Storage

In developing communities there is a daily struggle to consume safe drinking water. While recent estimates by the World Health Organization (WHO) show some progress towards the reduction of those at risk, 1.1 billion people in 2006, to the current estimate of 884 million people, a large problem still exists (WHO 2010). The problem threatens to become worse with problems of overpopulation and displacement of entire communities due to climate change.

The number at risk may also be drastically underestimated. The term, "improved" source is used by WHO to determine if one is at risk. A list of improved sources includes household connection, public standpipe, borehole, protected dug well, protected spring and rainwater collection (WHO 2010). However, many of these improved sources do not provide safe drinking water at the time of consumption. Many community level treatment options such as a protected spring or borehole can be re-contaminated after water collection. This highlights the need for treatment at the point-of-use (POU), directly prior to consumption. Several studies have concluded higher effectiveness through POU treatment options over community treatment options (Clasen et al 2007, Clasen and Bastable 2003, Fewtrell et al 2005, Wright et al 2004).

Recontamination often occurs because a safe storage vessel is not being used. A safe storage vessel prevents the user from coming into contact with the water and contaminating it before it is consumed. This type of vessel will often include a narrow mouth, lid, and a tap

(Murcott 2006). Even while practicing POU water treatment, it is important to have a safe water container if the water is to be stored after treatment.

There are many POU technologies that currently exist in the field. Several lessons can be learned from previous lab and field studies which will help aid in the design of any future POU device.

1.2 POU Technologies

Many POU water treatment technologies have been implemented worldwide in an effort to curb the incidence of diarrheal disease. Many of these technologies have been widely studied by such institutions as The Center for Disease Control and Prevention (CDC), University of North Carolina (UNC), The Swiss Federal Institute of Aquatic Sciences and Technology (EAWAG) and others. Both lab and field based studies have been conducted with varying degrees of success. The more widely known and studied technologies include boiling, chlorination, bio-sand filtration, ceramic filters, solar disinfection (SODIS), and combined coagulation/disinfection systems.

1.2.1 Boiling

Boiling is the most common POU water treatment technology (Rosa and Clasen 2010). Boiling is simple and therefore easily understood by the user. It is often incorporated into everyday cooking and requires materials that are already around the home such as pots and fuel wood. Boiling is also highly effective at killing pathogenic organisms including bacteria, viruses and protozoa. However, boiling can be very expensive. With many homes in the developing world spending the majority of their income on firewood or spending hours a day collecting firewood, boiling is not feasible. Efforts have been made to reduce the cost of boiling by educating users on not bringing the water up to a full boil because most disinfection is possible at lower temperatures. But this requires a thermometer or some indicator that the water has reached a high enough temperature. Additionally if the water is stored, recontamination is possible, especially with users waiting for the water to cool down before drinking. Lastly, the environmental impacts of firewood usage are immense, including rapid deforestation in many countries (Sobsey 2002).

1.2.2 Chlorination

Chlorine is effective against most pathogenic organisms and leaves a residual disinfectant which can prevent recontamination of water for days or weeks at a time. Chlorine is also relatively inexpensive compared with other disinfection technologies.

In the developing world, chlorine is either privately manufactured and shipped in or locally produced using electrolysis of salt water (Mintz et al 2001). Usually it is found in a liquid solution or as a tablet. Chlorine solutions are marketed internationally under several different names including Aquatabs, WaterGuard, Chlorin and many others. A bottle of the solution (usually around half a liter) can treat about 2500 liters of water for about $0.60 depending on the manufacturer (Murcott 2006). However, many users dislike the smell and taste of chlorine (Sobsey 2002, Mintz et al 2001).

Chlorine interventions have been widely studied by the CDC. They have shown POU chlorine interventions to be effective at the reduction of diarrheal disease in many countries including Uzbekistan, Bolivia and Malawi (Semenza et al 1998, Quick et al 1998, Stockman et al

2007). Additional emphasis of this research included the use of household chlorination with safe storage techniques and community education. These additions were shown to be essential to the success of the POU intervention (Quick et al 1998).

1.2.3 Bio-Sand Filtration

Bio-sand filtration is a modified form of slow sand filtration which has been used widely for drinking water disinfection. While slow sand filtration requires a large surface area and low flow rates, a bio-sand filter, is smaller and can provide flow rates up to 1 L/min. Most bio-sand filters consist of a layer of fine sand, coarse sand and gravel which is stored in an approximately 0.9 m high and 0.3 m square concrete container (Lantagne et al 2007). Bio-sand filters operate like a slow sand filter with the formation of a biofilm layer called the Schmutzdecke which uses biological mechanisms to remove pathogenic organisms (Yung 2003).

Bio-sand filters have been widely studied by UNC and Samaritan's Purse, an international NGO. Studies of bio-sand filters in the field have shown use after 8 years with 85% still using the filter. Also minimal breakage of the system was seen. Additionally the bio-sand filter is a onetime up-front cost which does not require continuous purchase of the disinfectant, such as with chlorine (Sobsey et al 2008).

However, since bio-sand filters are housed in a concrete container, they are often difficult to transport because of their large weight. Bio-sand filters also often show less than 100% removal of bacteria and lower rates of virus inactivation (Lantagne et al 2007). Maintenance of the filters can be tedious because the biofilm layer has to be removed and cleaned when the filter clogs. After the filter is cleaned an initial period has to be observed before use of the filter while the biofilm layer forms again (Sobsey 2002). Additional problems can arise when initially procuring clean sand. Dirty sand often has to be hand cleaned which can be a very labor intensive process.

1.2.4 Ceramic Filters

The traditional ceramic filter is made from clay and some other combustible material, such as sawdust. When fired the sawdust will burn away to create micro-pores within the structure, that is usually shaped similarly to a flower pot. The pot is then impregnated with colloidal silver by painting or dipping the pot in the silver. The clay pot is then inserted into a 5 gallon plastic bucket with a spigot so that water can be stored. Most of the materials needed to make a ceramic filter are available locally anywhere in the world with the exception of the silver (Lantagne et al 2007).

While there are several mechanisms for how ceramic filters work, the main mechanisms are size exclusion by the small pores and inactivation of organisms by the colloidal silver. However the size exclusion is usually only effective down to bacteria sized microorganisms (Lantagne et al 2007). Smaller microorganisms such as viruses can be inactivated by the silver, but the silver will often leach out of the filter within less than a year and needs to be reapplied. Rates of reapplication in the field have been low, with most long-term users never reapplying the silver, and therefore reducing the effectiveness of their filters. Additionally low flow rates of 1 to 3 liters per hour will continue to decrease if the filter is not properly cleaned and maintained (Sobsey et al 2008).

Ceramic filtration has been one of the most successful household treatment interventions. In a comparison of several POU treatment options, ceramic filtration was the only technology that could be rated as clearly effective (Hunter 2009). Local ceramic filter factories have been set up throughout Central America and other parts of the world since 1986. A typical filter will cost $15-$25 with replacement parts at $4-$6 (Potters for Peace 2006).

1.2.5 Solar Disinfection (SODIS)

While solar disinfection has been used for centuries, it began in the developing world as a way to provide the water needed for oral rehydration solutions, which helps treat diarrheal diseases (Reed 2004). Recently, EAWAG, has done extensive research on the SODIS method, including its effectiveness at killing various pathogenic microorganisms, health studies to determine the effect of SODIS programs, and strategies for implementing the SODIS method (SODIS 2010).

The SODIS method works by filling a clear plastic bottle with contaminated water and placing it in the sun for 6 hours to several days, depending on the available sunlight. Additionally it is often necessary to filter the water, if it is very turbid, before placing the water in the sunlight (SODIS 2010). There are several mechanisms by which SODIS works. Optical inactivation is considered the main mechanism, where UV and visible light are absorbed by molecules, raising them to an excited state, where they become reactive oxygen species. Another mechanism is thermal inactivation where the water becomes hot enough to be pasteurized (Reed 2004).

SODIS can be effective because of its low cost and therefore availability to almost anyone in the world, as well as, the small chance of recontamination because the user will most likely drink directly from the bottle (Lantagne et al 2007). However, there are many drawbacks to SODIS including small volumes of water treated, long treatment time, and generally its unavailability during several times of year and in several parts of the world because of lack of sunlight (Sobsey 2002).

1.2.6 Combined Coagulation/Disinfection Systems

One of the more widely distributed combined coagulation/disinfection systems is the PUR water purification packets, developed by Proctor and Gamble (P&G). The packet includes both a coagulant, ferrous sulfate, and a disinfectant, sodium hypochlorite, that are added to a 10 liter bucket of water. The water is stirred, allowed to settle, filtered through cloth and then left for 20 minutes for disinfection. The system has shown to be effective in the reduction of diarrheal disease in both developing world applications and disaster relief applications (Lantagne et al 2007).

The PUR system is effective because it can easily treat a variety of water qualities including highly turbid waters and water containing heavy metals. The system provides the benefits of both a coagulation/flocculation process as well as a chlorine disinfection process. Additionally, the PUR system has been highly marketed by P&G and therefore has shown success in distribution across the world. The system can be difficult to implement though because of the complexity of the treatment process and the use of a consumable product that needs to be purchased again and again (Lantagne et al 2007, Sobsey 2002).

1.3 Policy – The Network

The International Network to Promote Household Water Treatment and Safe Storage (The Network) was established in the early 2000s, through WHO, to provide solutions to difficulties in implementing and scaling up of household water treatment technologies. The Network is comprised of NGOs, health agencies, product suppliers, government agencies, academic organizations, as well as others, with the goal of helping to achieve Target 10 of Millennium Development Goal (MDG) 7. Target 10 of MDG 7 aims to half the proportion of people without a sustainable access to safe drinking water by 2015. The Network meets periodically to collaborate and discuss lessons learned as well as create standards for microbiological effectiveness of treatment technologies and field techniques. The Network is split up into four main components; advocacy, communication, research and implementation. As of 2006, The Network consists of over 100 organizations and has made gains in pilot programs to implement household water treatment around the world (WHO 2007). The Network will soon release a rating system for POU systems based on the log reduction they achieve of bacteria, viruses and protozoa. A summary of the rating system is shown below in Table 1 (Sobsey and Brown 2010):

	Log Reduction		
	Bacteria	Viruses	Protozoa
Highly Protective	>4	>5	>4
Intermediately Protective	>2	>3	>2
Minimally Protective	>1	>1	>1

Table 1. The Network rating system for POU technologies (Sobsey and Brown 2010).

1.4 UV Systems in Developing Communities

Until recently, UV systems with developing community applications have not been studied or implemented. However, over the past decade, several systems have been developed. While they are still uncommon and not yet extensively studied, lessons can be learned from previous UV technologies in both the technical design of these systems and considerations, both social and economic, that need to be taken into account when designing the next generation UV system for a developing community.

1.4.1 Bring Your Own Water System/Manna Energy Limited System

The Bring Your Own Water (BYOW) treatment system was developed by the Engineers Without Borders chapters at the University of Colorado (EWB-CU) and Johnson Space Center (EWB-JSC). The system was designed to treat water at the community scale with the capacity to provide 5000 liters per day of potable water. The BYOW system is placed in a central location where a community member who has collected water can pour their bucket of contaminated water into the top of the system and receive treated water at the bottom of the system. The main disinfection mechanism is a 17 or 25 watt UV low pressure mercury vapor bulb. The system also includes pretreatment through a roughing filter and sand filter and is powered by photovoltaic cells (Gold et al 2007).

Laboratory scale testing of the system showed pretreatment effectively bringing the turbidity down to less than 1 NTU with influent turbidity of up to 100 NTU. *E. coli* concentrations were consistently reduced by 3 to 4 log but without complete removal of E. coli (Gold et al 2007).

Three BYOW systems have been implemented in small communities in rural Rwanda and Mexico. The systems have shown varying levels of success with two systems currently operational and working properly and one system not being used by the community. A field study of one of the systems showed turbidity reduction to around 2 NTU and 2 to 3 log reduction of total coliforms (Gold et al 2007). The system that is currently not in operation can be attributed to operational and social factors. The system was most likely not the appropriate water treatment technology for the specific community and was therefore not well maintained or used. A poor assessment as well as communication barriers between EWB and the community additionally added to the failure of the system (Thomas and Amadei 2009).

The poor use of this system may highlight some of the difficulties with community scale systems and the overall benefits of POU systems. While the UV technology itself was successfully implemented and working, the community did not feel ownership of the system and therefore did not maintain or use it. However, the two successful implementations of the system show that the system does work and can be beneficial to a community.

In response to many of these issues and building on the successes, Manna Energy Limited (Manna) was developed. Manna has developed a system similar to the BYOW system but with in-line filters and other modifications for larger community applications in Rwanda. The Manna system is installed at the end of a major pipeline, where it is accessible to an entire community. This system does not rely on community members to maintain the system. It is operated by Manna through a remote monitoring system and Rwandan staff. Additionally the Manna system has a unique funding mechanism, where the cost of the systems as well as operation and maintenance are funded through offset carbon emissions. While the funding mechanism is still in its approval phase, Manna estimates that hundreds of thousands of people will benefit when their system has been fully rolled out (Manna 2010).

1.4.2 UV Waterworks

UV Waterworks (UVWw) was developed at Lawrence Berkeley National Laboratory (LBNL) in the early 1990s. UVWw is a community scale system that has been implemented in India, South Africa, Bangladesh, Mexico and the Philippines. The current model uses a 40 watt low pressure UV bulb that is housed in aluminum and stainless steel to provide reflective surfaces. The lamp is suspended above the water with the water running in a chamber below the lamp. Since the lamp is not in contact with the water, fouling and therefore maintenance of the system are reduced. The system is lightweight, weighing approximately 15 pounds, making it easy to transport to remote communities. The system is also inexpensive, with a cost of about $900. Additionally, maintenance is only required about twice per year, with the system lasting about 15 years. (Gadgil et al 1998).

UVWw has been tested extensively at LBNL and at field sites in India and South Africa. Lab tests and field tests showed up to a 6 log removal of coliforms and a dose up to 160 mJ/cm^2 (Gadgil et al 1998).

The UVWw system employs a unique funding mechanism. Public-private partnerships are utilized for the expenses of the system. In the Philippines, local Rotary clubs provide funding for the capital costs through a revolving loan program. The systems are then run by local entrepreneurs that charge a small fee for the water. The local entrepreneurs own the system and perform all maintenance. 175 systems have been implemented using this funding mechanism in both the Philippines and Mexico. (Gadgil et al 2009).

1.4.3 UV Tube

The UV Tube was developed at the University of California at Berkeley (UC-Berkeley). The development spun off of the UV Waterworks technology, when it was recognized that a point-of-use UV system may be a better option for many communities (Cohn 2002). The UV Tube was designed through field testing, where feedback from potential users in Mexico was used to design and redesign the system (Brownell et al 2008).

The UV Tube utilizes an 8 watt low pressure UV bulb which sits above the water similar to the UVWw design. The chamber the water sits in is a 4" PVC pipe covered in stainless steel with an additional 3" PVC pipe which houses the ballast. The system can be manufactured for under $50, not including any necessary power needs. All materials with the exception of the bulb itself can be found locally almost anywhere in the world at an inexpensive price (Brownell et al 2008).

Flow characterization and MS2 bacteriophage challenge testing were conducted on the UV Tube. Flow characterization revealed a plug flow with dispersion behavior and no observed dead space. Challenge testing showed an average dose of 90 mJ/cm^2 but was only run with a very high UV transmittance (>97%) (Brownell et al 2008).

Field testing was conducted in Mexico. *E. coli* tests were conducted on water entering the UV tube, leaving the UV tube and water that was stored after treatment. No *E. coli* was detected in most of the samples leaving the UV tube where there was detectable *E. coli* entering the system. *E. coli* was detected in about 20% of the storage samples indicating recontamination after UV exposure (Brownell et al 2008).

1.4.4 UVeta

The UVeta system (also known as the UV Bucket) is also a POU UV system. It was developed through Niparaja Organization and funded mostly through a World Bank grant. The system consists of 3 chambers, made out of plastic buckets, stacked on top of another. Water is poured into the first chamber where it collects before moving to the second chamber. The second chamber consists of the UV bulb and a baffling scheme before the water moves to the third chamber, where the water can be stored. The system is designed with local materials and can be fabricated for approximately $30. The system can produce 20 liters of disinfected water in 10 minutes, if run continuously. Little maintenance is needed, with just the replacement of the bulb every year and cleaning of the storage bucket periodically (Niparaja 2007).

Many parts of the system must be manufactured. This includes the electronic circuit and the injection mold for the middle chamber (Niparaja 2007). While the local manufacturing is beneficial to the local economy, the injection molding machine and electronics fabrication are very expensive products.

A field study of 500 UVeta systems was conducted in Mexico to evaluate several water factors as well as social factors. The elimination of total coliforms was measured in 38% of the systems and elimination of fecal coliforms was measured in 71% of the systems. Additional studies were conducted into use and perception of the UVeta. Of the 500 systems, 57% were no longer in use. Some of the reasons given for not using the system were that they did not like the taste of the water, there was no electricity in the house, and that they didn't know how to use it. Additionally, during the surveying of users, regular maintenance was not being performed on the system and recontamination of the water was occurring (Niparaja 2007).

1.4.5 Lessons Learned

The feasibility of UV based technologies in the developing world has been established with the successful implementations outlined above. However, these systems have revealed many considerations and design challenges that need to be taken into account. On the technical design side, the UV system must be made primarily of local materials and with skills that are available anywhere in the world. To keep cost down, the system must be optimized, as much as possible, with respect to the hydraulic properties and UV bulb sizing while keeping maintenance to a minimum. Water must be available on demand to prevent recontamination and therefore a reasonable flow rate is needed so water will not be stored. Pre-treatment of water needs to be taken into account as UV disinfection is only effective for water with reasonably high UVTs. A power source must be readily available in the area, so the system should come with a simple power supply that can be easily retrofitted to the device but still keeps the system affordable. Additionally the system must be well understood by the user. This can be accomplished through education campaigns or a general willingness of the user to actually use the system. A major challenge of all POU devices is to make sure the user feels ownership of the product. This can be achieved by the user actually purchasing the product, making it again essential to keep the cost down. However, several market based techniques can be explored in order to provide a quality product at an affordable price. These criteria were used to design the household UV system.

1.5 Fundamentals of UV Disinfection

Ultraviolet (UV) disinfection has been around for over a century but had not been used widely in the United States until the 1970s. In the electromagnetic spectrum, UV light can be found between 100-400 nm, with the germicidal wavelengths existing in the UVC range, which are between 200-280 nm.

The energy from UV light can be explained by Planck's law of radiation:

$$u = \frac{h \times c}{\lambda}$$

where u is the energy of one photon (J), h is Planck's constant (6.6261 x 10^{-34} J s), c is the speed of light (2.9979 x 108 m/s) and λ is the wavelength (m).

However, in order for the energy from UV light to be useful, it must meet the first law of photochemistry, which says that only photons absorbed by molecules can produce chemical change. As the UV light passes through water it will be attenuated. This relationship is described by the Beer-Lambert law,

$$A = \log\frac{I_o}{I} = \alpha \times z \times c$$

where A is the absorbance, I_o is the intensity of light entering the water, I is the intensity of light leaving the water, α the the molar absorption coefficient (L/mole-cm), z is the path length of the water (usually the depth) and c is the molar concentration of the dissolved constituents in the water (mol/L).

UV Transmittance (UVT) describes the percentage of light passing through the water over a given path length (typically 1 cm) and is related to the absorbance by,

$$UVT = 100 \times 10^{-A}$$

When UV light is absorbed by an organism, the DNA is damaged. The main mechanism of damage is through dimer formations on adjacent pyrimidine dimers which inhibit replication of the organism, therefore making it so the organism cannot infect.

The UV light is absorbed based on the relative absorbance spectrum of DNA, shown in Figure 1. The absorption spectrum peaks around 260 nm making light emitted around this wavelength more effective at inactivating organisms. Low pressure mercury vapor UV bulbs, which are used commonly for water treatment, emit light at 253.7 nm, which is highly absorbing by an organism's DNA.

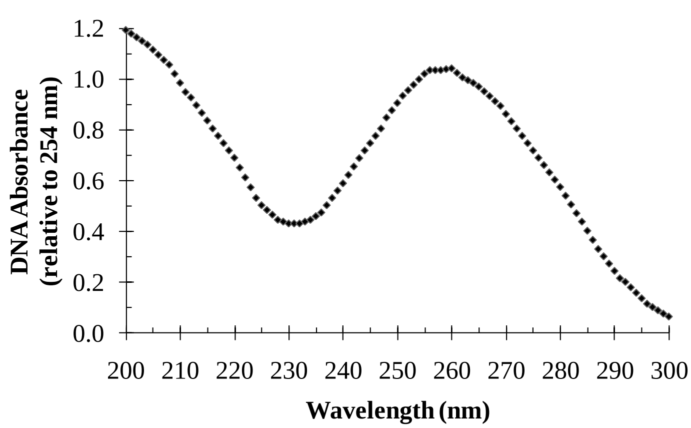

Figure 1. DNA absorbance spectrum relative to 254 nm.

2. Materials and Methods

2.1 Tracer Study

2.1.1 Theory (Lawler and Benjamin 2009)

Tracer studies are used to determine the hydraulic properties of a reactor. A tracer study can reveal the behavior of a reactor to determine its process efficiency in disinfection and also to diagnose possible hydraulic problems with the reactor such as dead space or short circuiting.

In this study, a step-input tracer was used. A step-input tracer study involves inputting a tracer into a system starting at a specified time and continuously adding the tracer to the system at a constant concentration. The tracer can then be measured based on a time interval. An exit age distribution [E(t)] and cumulative age distribution [F(t)] can be developed based on the tracer data. The exit age distribution describes the normalized rate of molecules leaving the system, and the cumulative age distribution describes the fraction of molecules less than or equal to the residence time of the system.

Two ideal reactors are used to first characterize the system. The first is a continuous flow stirred tank reactor (CFSTR). In a CFSTR the system is assumed to be completely mixed at all times and everywhere in the reactor. The second is a plug flow reactor (PFR). A PFR is the opposite of a CFSTR in which there is no mixing. Most reactors are not ideal and will fall somewhere between a CFSTR and a PFR. Figures 2 and 3 describe the exit age distribution and cumulative distribution for an ideal CFSTR and ideal PFR.

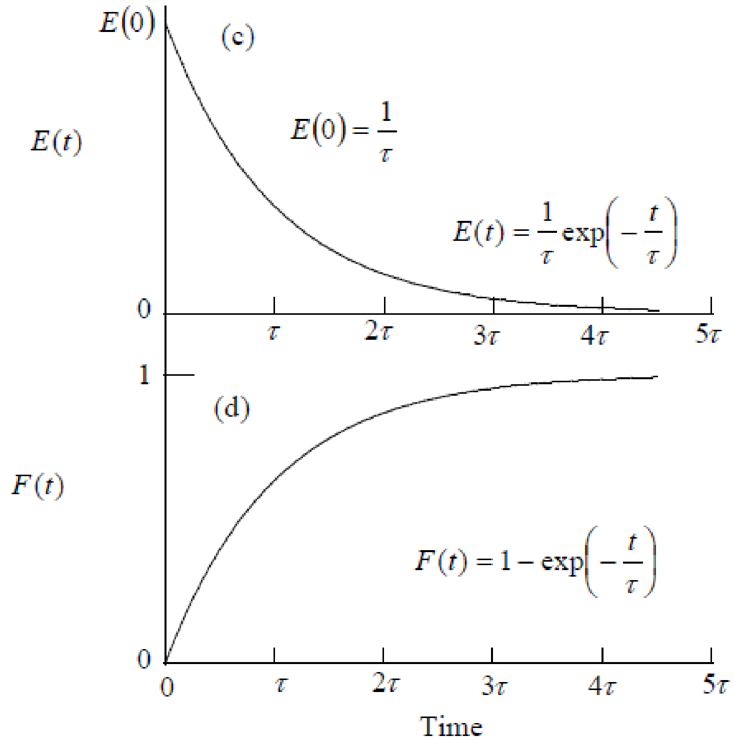

Figure 2. Exit age distribution and cumulative age distribution for an ideal CFSTR (Lawler and Benjamin 2009).

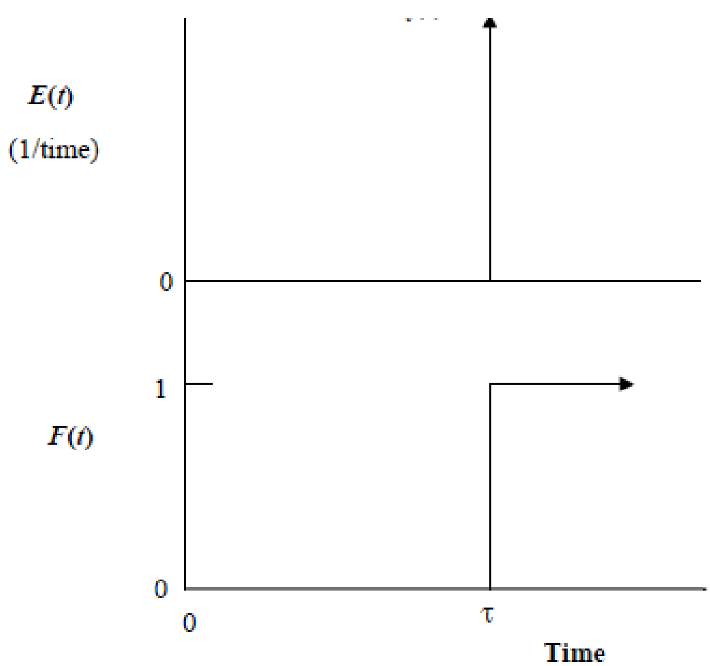

Figure 3. Exit age distribution and cumulative age distribution for an ideal PFR (Lawler and Benjamin 2009).

2.1.2 Experimental Setup

In this experiment, the tracer used was lignin sulfonic acid (LSA), and it was tracked measuring the absorbance at 254 nm (UVA_{254}). A 5-gallon bucket was filled with water and spiked with a small amount (approximately 1 mL) of LSA. With a hydraulic pump, the spiked water was mixed completely and more water or LSA was added until the mixed substance had a UVA_{254} above 0.5. During the mixing process, three holes were drilled into the reactor's source bucket in a low, medium, and high position, and plumbing fittings were inserted into each hole. A large tube was placed on one fitting, corresponding to the low, medium, or high flow rate, and the other holes plugged. The water was then allowed to overflow through the hole that was not plugged based on the flow rate being tested and recycled back into the source bucket. Once the LSA solution was released to the reactor, 5 mL of reactor effluent was collected in borosilicate glass tubes and the UVA_{254} was measured by a Cary 100 spectrophotometer, at 10 second intervals. This setup is shown in Figure 4.

Figure 4. Tracer study experimental setup.

2.2 Collimated Beam Testing (Bolton and Linden 2003)

Collimated beam testing was performed to determine the dose response of the bacteriophage being used for the challenge testing of the system. A collimated beam apparatus has a few essential components including a shutter, window, power supply, collimating tube, platform, stirring device, and the UV lamp. A schematic of a typical collimated beam system is shown in Figure 5.

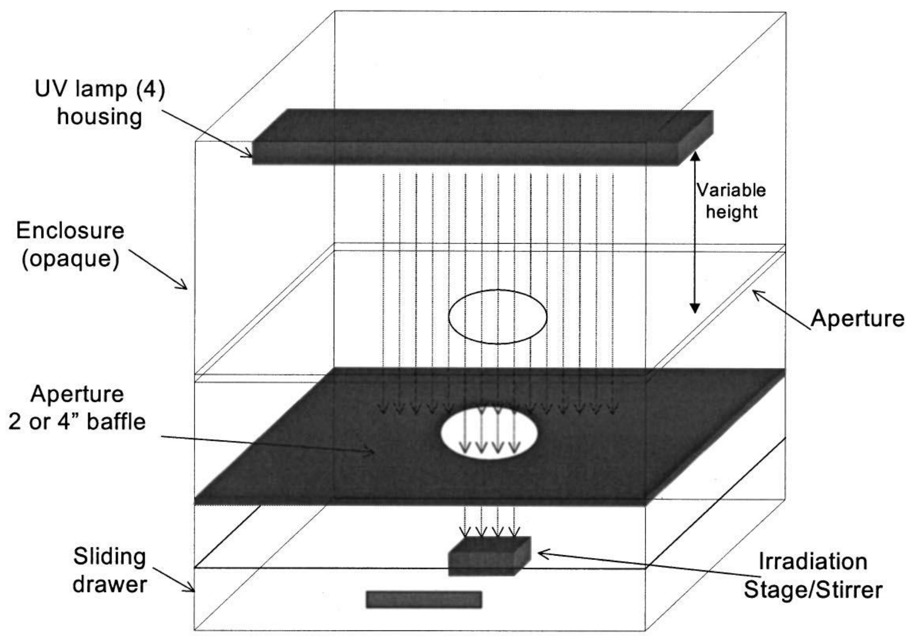

Figure 5. Schematic of a collimated beam system (Bolton and Linden 2003).

Dose was calculated based on Bolton and Linden 2003. In order to calculate the dose the average germicidal fluence rate (E'_{avg}) must first be calculated. E'_{avg} is described by,

$$E'_{avg} = E_o \times Petri\ Factor \times Reflection\ Factor \times Water\ Factor \times Divergence\ Factor$$

where E_o is the incident irradiance measured by a radiometer and the factors explain corrections that are needed. The Petri Factor is used to correct the incident irradiance over the entirety of the dish. It is likely that the irradiance will not be the same throughout the surface area of the entire dish, so the ratio of the average incident irradiance over the area of the dish to the irradiance at the center of the dish, must be calculated. The reflection factor accounts for the small fraction of light that will reflect off of the surface area of the water. The fraction reflected is 2.5% for air and water, resulting in a reflection factor of 0.975. The water factor accounts for the absorption of the water itself. It is described by,

$$Water\ Factor = \frac{1 - 10^{-A \times l}}{A \times l \times \ln(10)}$$

where A is the absorbance of the water and l is the path length. The divergence factor accounts for the light not being perfectly collimated. The light will diverge based on the distance from the lamp. The divergence factor can be calculated by,

$$Divergence\ Factor = \frac{L}{L + l}$$

where L is the distance from the aperture to the sample. Once all of the factors have been calculated and therefore the average irradiance has been calculated, an exposure time can be determined based on the following equation,

$$Exposure\ Time = \frac{Dose}{Average\ Germicidal\ Fluence\ Rate}$$

where the target dose is measured in mJ/cm^2 and the average germicidal fluence rate is measured in mW/cm^2, resulting in an exposure time in seconds.

For this experiment, irradiance was measured with a radiometer (International Light IL 1700) calibrated at 254 nm and absorbance was measured with a Cary 100 spectrophotometer.

2.3 Microbial Challenge Testing

In order to calculate the UV dose applied by the reactor, biodosimetry was performed. Biodosimetry involves challenging the reactor with a non-pathogenic organism to determine the log inactivation. The log inactivation is then related back to the collimated beam testing to determine the dose of the reactor. For this experiment the reactor was challenged with either T1 or MS2 bacteriophage at different flow rates and different UVTs.

The T1 bacteriophage testing was performed first with modifications made based on EPA method 1601.

2.3.1 T1 Bacteriophage Procedure

T1 bacteriophage and the host bacteria, *E. coli* CN13, were obtained from GAP EnviroMicrobial Services Ltd. Bacteriophage and host bacteria were kept in a -80^{o}C freezer until use.

The night before the experiment, 10 µL of the *E. coli* CN13 was spiked into 30 mL of nutrient broth (Difco #234000) and placed stirring into a 37^{o}C incubator. On the morning of the experiment 2 mL of the overnight solution was spiked into 30 mL nutrient broth and placed stirring back into the incubator for 4 to 6 hours, to ensure the *E. coli* CN13 was in log phase growth for the experiment.

Approximately 1.1 mL of bacteriophage was cooled on ice and spiked into 20 L sterile phosphate buffered saline (PBS) water to obtain a starting a concentration of approximately 10^6 plaque forming units (PFU) per mL. To obtain lower UVT solutions, LSA was added to sterile PBS. This solution was stirred for approximately 10 minutes. Two samples were taken at three different flow rates.

1 L of Bacto agar (Difco #214010) was made the morning of the experiment and placed in a 55^{o}C water bath until right before testing. Sterilized 6 mL borosilicate glass vials were placed in a 37^{o}C-39^{o}C water bath and filled with 5 mL of Bacto Agar approximately 15 minutes before plating.

E. coli CN13 was removed from the incubator right before testing and was kept stirring during the duration of the experiment. Three borosilicate vials were removed from the water bath and spiked first with 0.1 mL of the *E. coli* CN13 and then 0.1 mL of the bacteriophage sample. The sample was gently stirred by hand. This solution was immediately poured onto premade nutrient agar (Difco #213000) plates. In addition to the doses, a negative control (only PBS), and a positive control (solution with no UV exposure) were also plated. All samples were plated in triplicate.

After completion of the experiment, all plates were moved to a 37^{o}C incubator. After 18-24 hours, plates were removed from the incubator and plaques counted.

2.3.2 MS2 Bacteriophage Procedure

The MS2 testing was essentially the same as the T1 procedure but with a few changes as outlined below. Changes were made based on the procedure outlined in EPA Method 1601.

- The host used was *E. coli* Famp.
- Tryptic soy broth (Difco #211825) and tryptic soy agar (Difco #236950) were used. The bottom layer was 1.5% tryptic soy agar, while the top layer was 0.7% tryptic soy agar. Both the broth and agar included the addition of ampicillin and streptomycin antibiotics at a concentration of 10 mL of the antibiotic solution to 1 liter of the broth or agar.
- After log phase of the E. coli was reached, it was placed immediately in a 4^{o} C refrigerator to stop the growth.

2.4 Reactor Prototypes

Several prototypes of a POU UV disinfection system were designed and tested in the laboratory. Based on the literature review, it was decided that the materials would be mostly aluminum and plastic, bonded with a common epoxy or cold weld. Design choices were made with the goal of optimizing the hydraulic properties to use a UV bulb with the low energy consumption. Additional study was conducted on a simple photovoltaic power supply for the system.

2.4.1 Prototype 1

The unit uses a Ushio GTL3 3-watt low pressure UV bulb (Figure 6). The bulb has a small footprint (2.5 inches by 0.75 inches), minimal energy requirements and low commercial cost ($6). The reactor is made entirely of a reused aluminum can and simple plumbing parts available at any hardware store. The chamber is sealed with epoxy. A picture and model of the reactor are shown in Figures 7 and 8.

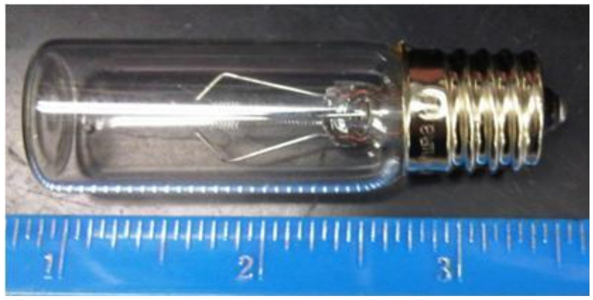

Figure 6. 3-watt low pressure UV bulb (Ushio GTL3).

Figure 7. UV POU system prototype 1.

Figure 8. 3-dimensional computer rendered model of prototype 1.

The cost of Prototype 1 is described in Table 2.

System Component	Cost
Ushio GTL3 Bulb	$6.00
2 – 1/8" barb x 1/4"	$3.24
2 – 1/4" washers	$0.40
2 –1/4" gaskets	$0.30
Gorilla Glue Epoxy	$1.00
Total	$10.94

Table 2. Cost of reactor prototype 1.

2.4.2 Prototype 2

Building on tracer results from prototype 1, prototype 2 was created with baffling. The same UV bulb was used but the reactor contains four round Plexiglas baffles with two Plexiglass circles for the ends. The baffles are separated by thin rectangular pieces of Plexiglass, which also aid in guiding the fluid between baffles, and adhered together with cold weld. The Plexiglas array has an outer covering of pieces of aluminum cans and is also sealed completely with cold weld. A model and picture of the prototype are shown in Figures 9 and 10.

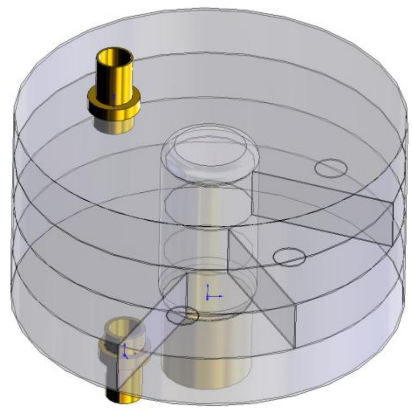

Figure 9. 3-dimensional computer rendered drawing of inside of prototype 2.

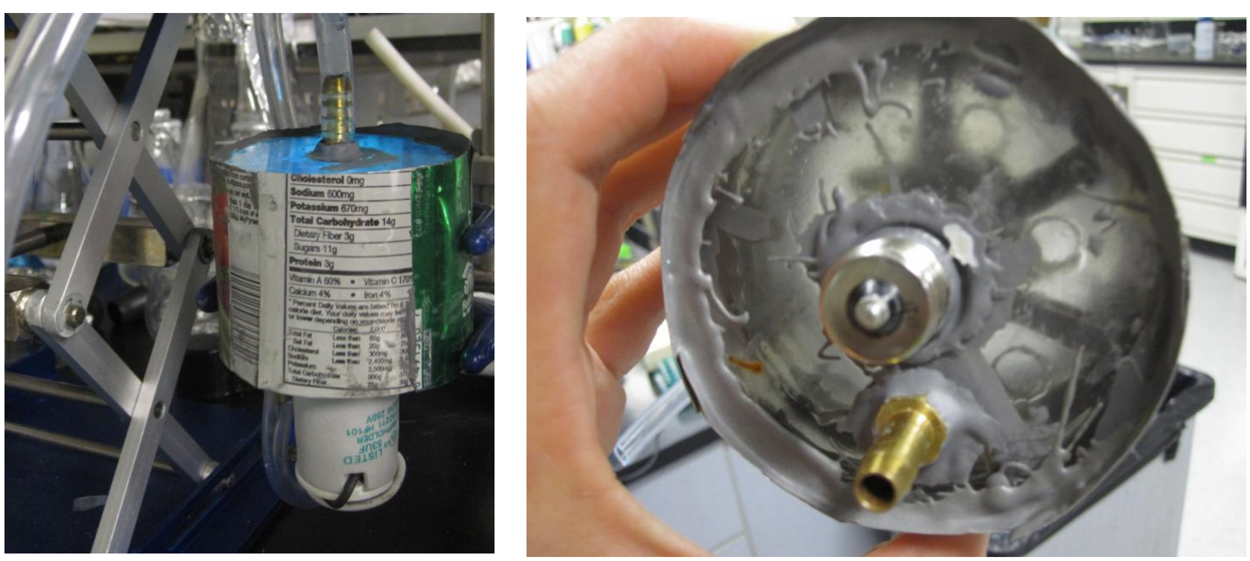

Figure 10. UV POU reactor with UV bulb on (left). Bottom of UV reactor with baffles shown (right).

The cost of Prototype 2 is described in Table 3.

System Component	Cost
Ushio GTL3 Bulb	$6.00
2 – 1/8" barb x 1/4" adaptor	$3.24
2 – 1/4" washers	$0.40
2 –1/4" gaskets	$0.30
Plexiglass	$1.66
JB Weld	$1.50
Total	$13.10

Table 3. Cost of reactor prototype 2.

2.4.3 Prototype 3

Based on tracer and bacteriophage challenge testing from prototype 2, prototype 3 was constructed. The same baffling scheme as prototype 2 was used but with entirely aluminum parts. The reactor was made in octagonal shape with the entire reactor being made of an aluminum sheet and sealed with epoxy and cold weld. Additionally the UV bulb was changed to a higher wattage bulb, a 9-watt Philips PL-S9W/TUV bulb (Figure 11). Pictures of prototype 3 are shown in Figure 12.

Figure 11. Philips PL-S9W/TUV bulb (1000bulbs.com).

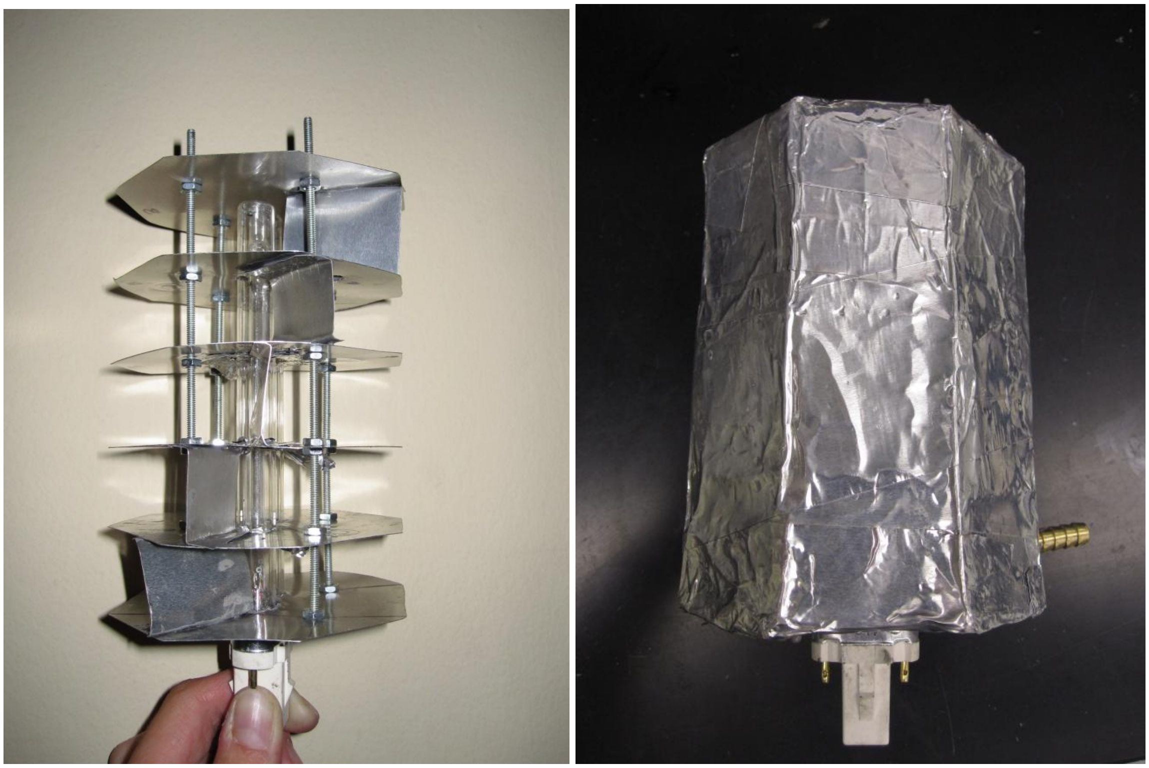

Figure 12. Pictures of the interior (left) and exterior (right) of prototype 3.

The cost of Prototype 3 is described in Table 4.

System Component	Cost
Philips PL-S9W/TUV Bulb	$13.50
2 – 1/8" barb x 1/4" adaptor	$3.24
2 – 1/4" washers	$0.40
1/8" threaded rod	$2.40
24 – 1/8" nuts	$2.59
Aluminum Sheet	$2.49
Gorilla Glue Epoxy	$4.20
Total	$28.82

Table 4. Cost of reactor prototype 3.

2.5 Power Supply – Photovoltaic Design

Two designs were created to power the 3-watt reactor prototypes (Prototypes 2 and 3).

2.5.1 Design 1

The first design is a small-scale conventional stand-alone PV system. All together, it is comprised of a 10W mono-crystalline solar panel, a moveable mounting system including wheels, a 12-volt/5-amp charge controller, a 12-volt/8 amp-hour battery, a 12V-DC/120V-AC inverter, an electrical ballast, and a 3W-AC UV light bulb. The extra components for the solar panel, known as the 'balance-of-systems,' are all enclosed in a portable plastic box. The solar panel mounting system was designed to be compact, moveable, and lightweight. It consists of a Plexiglass base with wheels attached to the bottom, a baking sheet to attach the panel directly to, and a sheet of aluminum to obtain the correct angle. All of these parts of the mounting 'triangle' are attached to each other with hinges so it can be folded upon itself. Design 1 is shown in Figure 13 (Kunik et al 2010).

Figure 13. Solar panel and mounting system (left), and balance of systems (right) of design 1.

The cost of design 1 is summarized in Table 5.

System Component	Cost
Solar Panel	$30.00
Charge Controller	$18.99
12 V Sealed Lead-Acid Battery	$15.09
12 VDC/120 VAC Sine Wave Inverter	$19.99
Adaptor Cords/Wires	$10.00
Mounting Component	$38.00
Ballast	$16.49
Total	$148.56

Table 5. Cost of power supply design 1.

2.5.2 Design 2

The second design is a more compact version of the first prototype. It contains a 10W mono-crystalline solar panel, an easily movable mounting system, a battery charger/pack with 4 D-size batteries and one 9-V battery, a 12V-DC/120V-AC inverter, electrical ballast, and a 3W-AC UV light bulb. The balance-of-systems are also contained in a portable plastic box similar to the first design. It also has a mounting system that is more minimalistic than the first design. It is comprised of a baking sheet to attach to the panel, a sheet of metal, and a hinge to connect the two pieces. This mounting system design uses the ground as a base, eliminating approximately $15 in supplies. Design 2 is shown in Figure 14 (Kunik et al 2010).

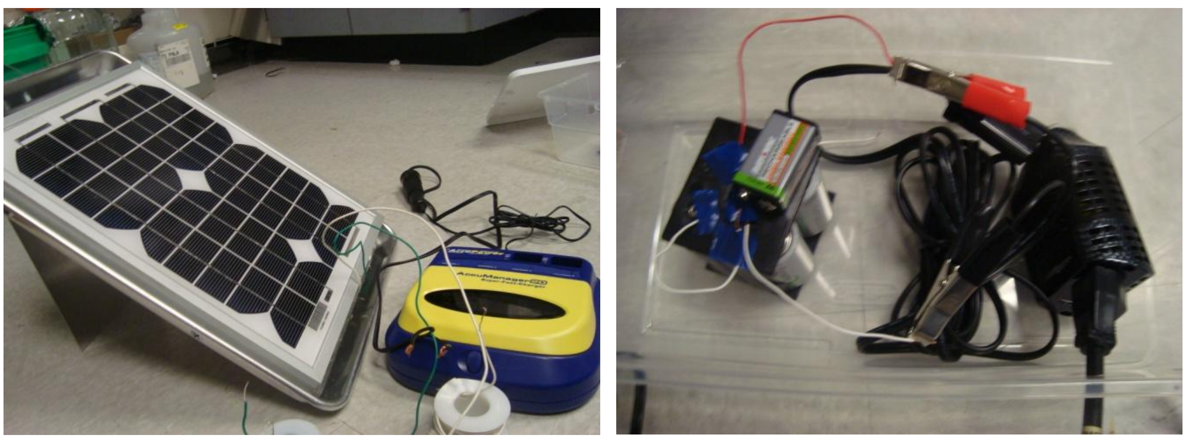

Figure 14. Solar panel and mounting system (left), and balance of systems (right) of design 2.

The cost of design 2 is summarized in Table 6.

System Component	Cost
Solar Panel	$30.00
Battery Charger/Pack	$78.34
Rechargeable D-Size and 9V Batteries	$30.00
12 VDC/120 VAC Sine Wave Inverter	$19.99
Adaptor Cords/Wires	$5.00
Mounting Component	$25.00
Ballast	$16.49
Total	$204.82

Table 6. Cost of power supply design 2.

2.6 Power Supply Experimental Testing

To evaluate the effectiveness of each design, they were both tested under real sun conditions. Both prototypes were tested simultaneously with fewer than optimal testing days due to time constraints. As the testing occurred in Boulder, CO, at latitude 40.02^{o} N, the solar panels were tested at angles of 40^{o} and 45^{o}. Boulder also has approximately 4.5 hours of peak sunlight every summer day, therefore the panels were tested for five hours, from 10am to 3pm.

Before the start of testing, cloud conditions were recorded, so only trials with similar cloud cover would be compared. During the testing process, current and voltage from the solar panel and after the power inverter were observed with a multimeter and recorded at half hour intervals. Also tested was the ability of the system to illuminate the UV lamp (Kunik et al 2010).

3. Results and Discussion

3.1 Tracer Study

3.1.1 Prototype 1

The hydraulic properties of prototype 1 are in Table 7. Normalized exit age distribution and cumulative age distribution curves for prototype 1 are shown in Figure 15 and 16.

Flow Rate (mL/min)	Theoretical residence time/mean hydraulic detention time	Non-dimensional variance
60	1.03	0.201
125	0.79	0.254
270	0.80	0.439

Table 7. Hydraulic properties of prototype 1.

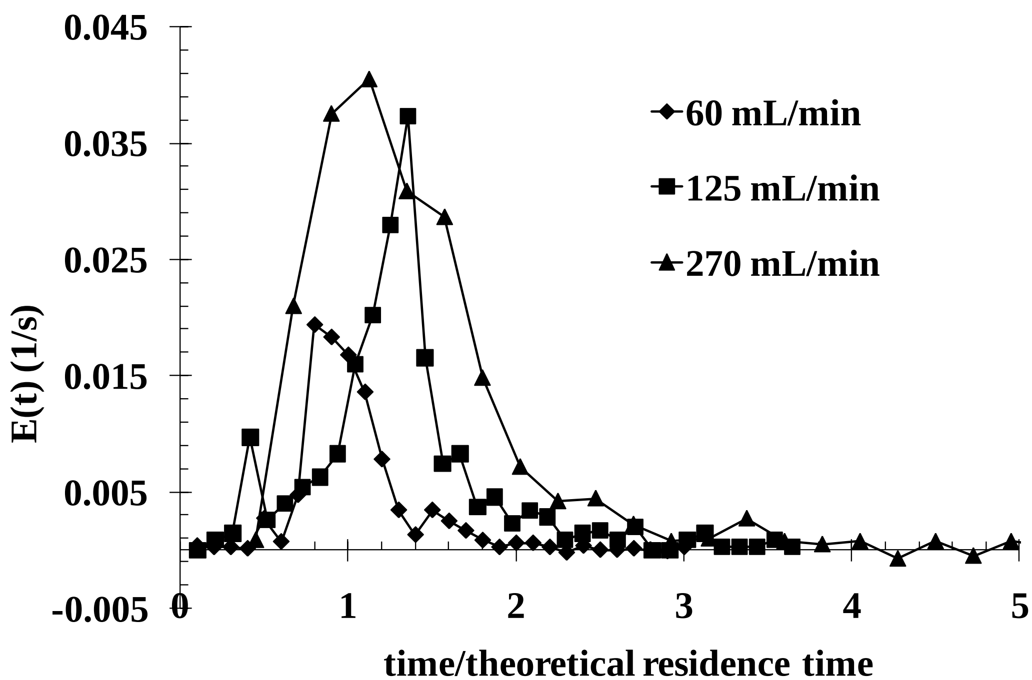

Figure 15. Normalized exit age distribution curves for prototype 1 at 3 different flow rates.

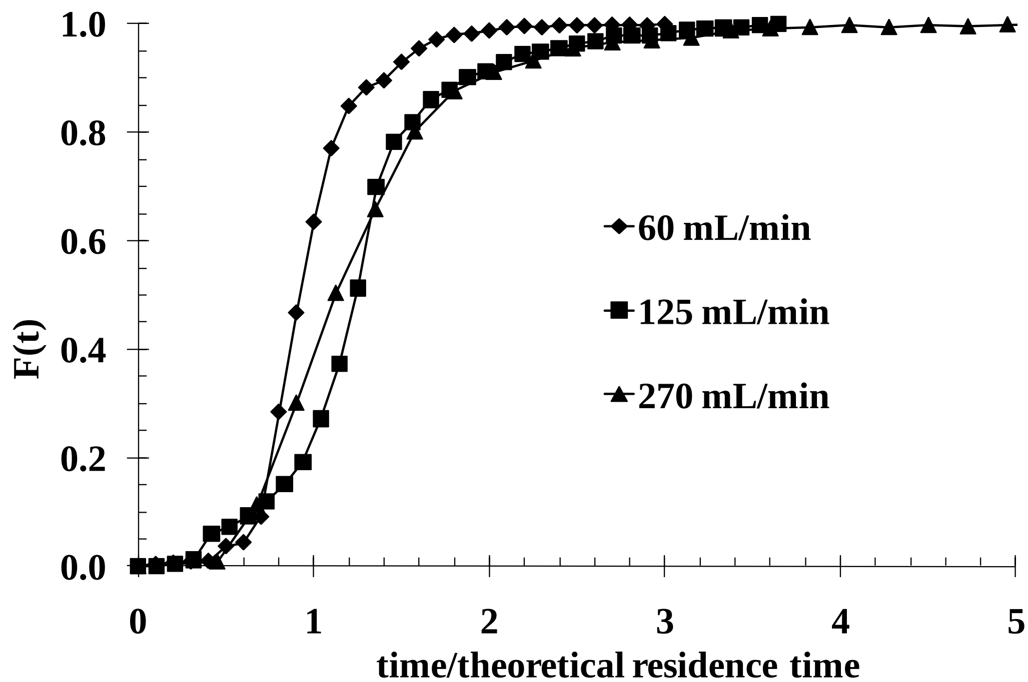

Figure 16. Normalized cumulative age distribution curves for prototype 1 at 3 different flow rates.

The tracer study revealed that the reactor properties changed at different flow rates. This was expected as different flow rates will create different amounts of dispersion therefore changing the hydraulic behavior of the reactor. The tracer study provided insight into many of the hydrodynamic properties of the reactor. At all three flow rates there was an indication of dead space. This was seen through long tails at all flow rates and a higher mean hydraulic detention time over theoretical residence time in the medium and high flow rate studies. There was also indication of short-circuiting observed as multiple peaks in the tracer study. All studies also showed a time lag but this could be from the excess tubing located at the front end of the reactor from the pump.

Non-ideal modeling was conducted on prototype 1. The non-ideal models were corrected to account for the time lag seen from tubing at the front end of the reactor. The non-ideal models for prototype 1 were similar to the experimental data with the hydraulic behavior most similar to a plug flow reactor with dispersion. The 270 mL/min exit age distribution and cumulative age distribution are shown in Figures 17 and 18. Non-ideal modeling of the remaining flow rates are shown in Appendix A.

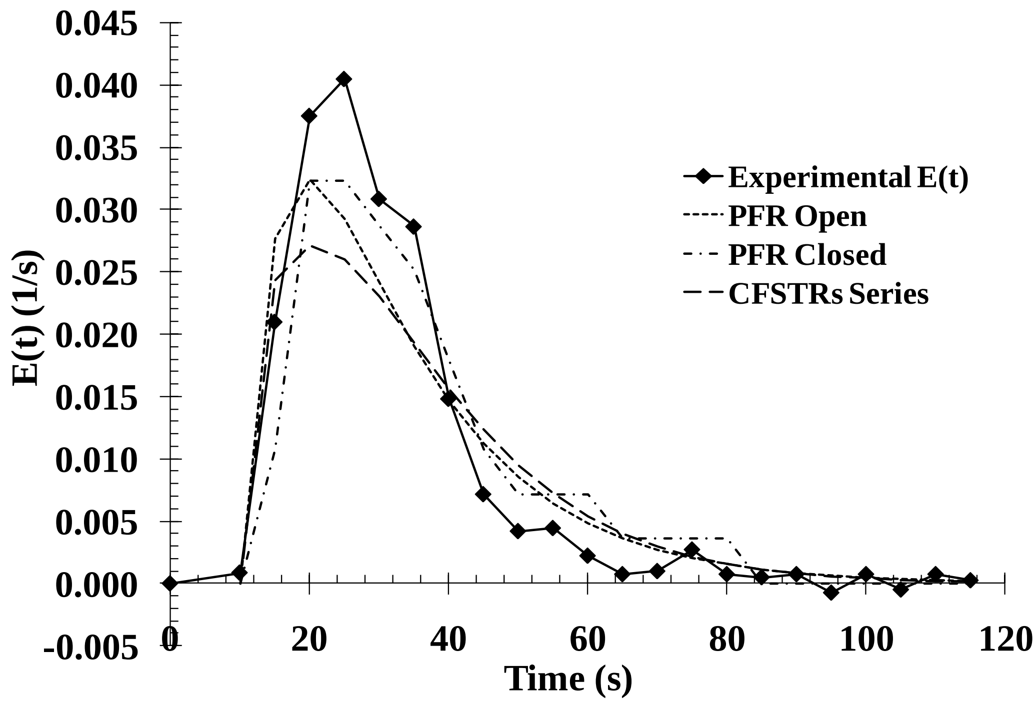

Figure 17. Exit age distribution comparison of experimental data and non-ideal models at 270 mL/min for prototype 1.

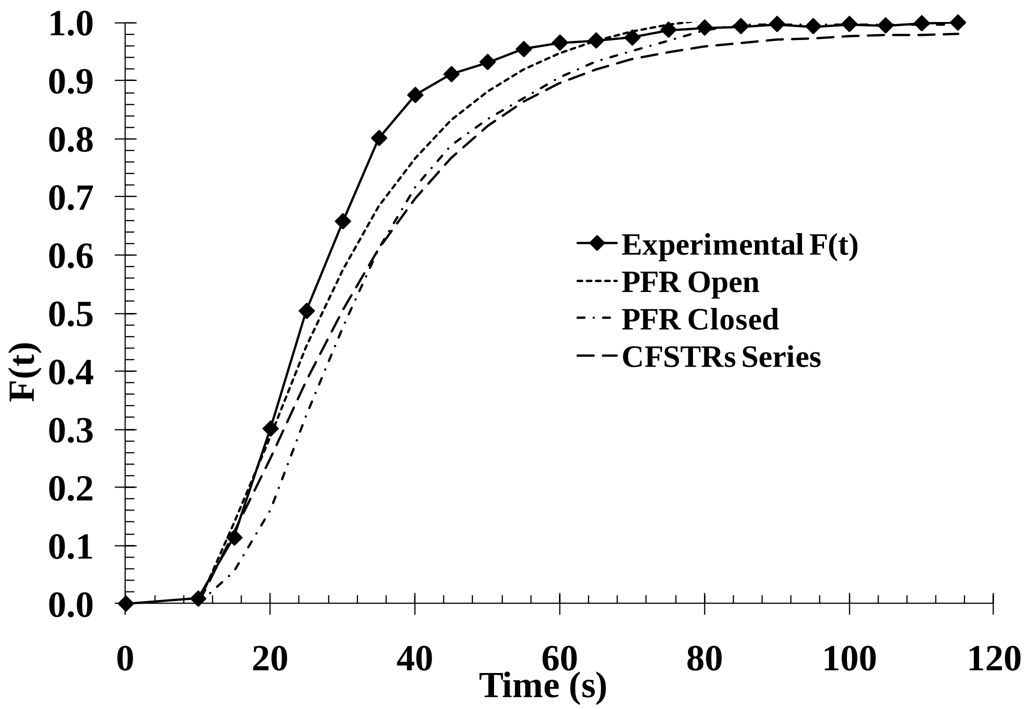

Figure 18. Cumulative age distribution comparison of experimental data and non-ideal models at 270 mL/min for prototype 1.

3.1.2 Prototype 2

The hydraulic properties of prototype 2 are in Table 8. Normalized exit age distribution and cumulative age distribution curves for prototype 1 are shown in Figure 19 and 20.

Flow Rate (L/min)	Theoretical residence time/mean hydraulic detention time	Non-dimensional variance
0.58	1.06	0.533
0.63	1.14	0.626
0.78	1.15	0.533

Table 8. Hydraulic properties of prototype 2.

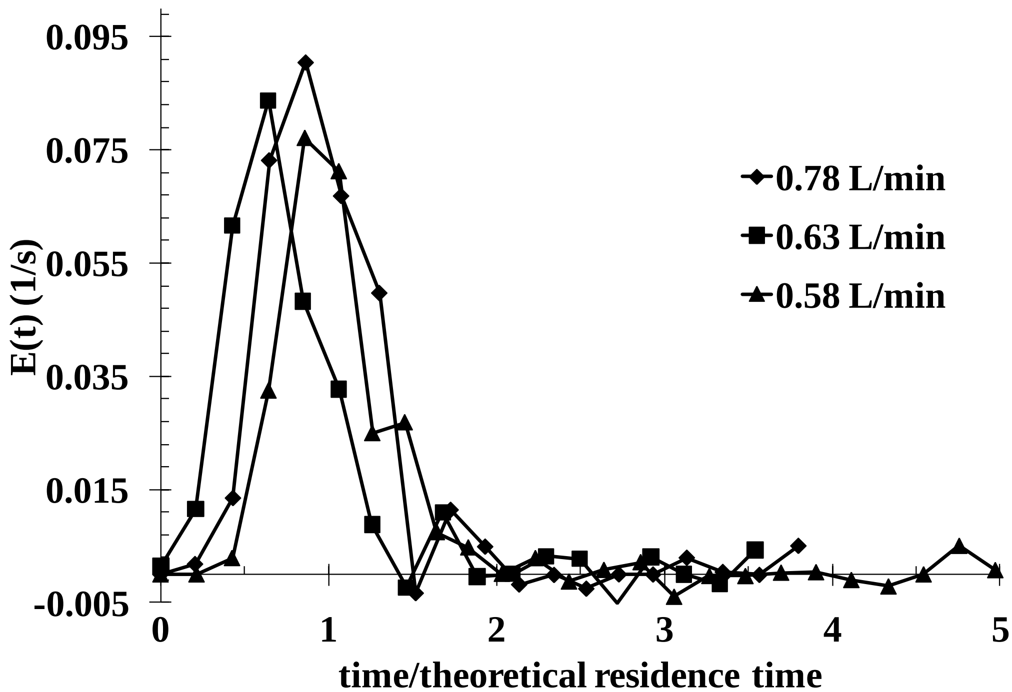

Figure 19. Normalized exit age distribution curves for prototype 2 at 3 different flow rates.

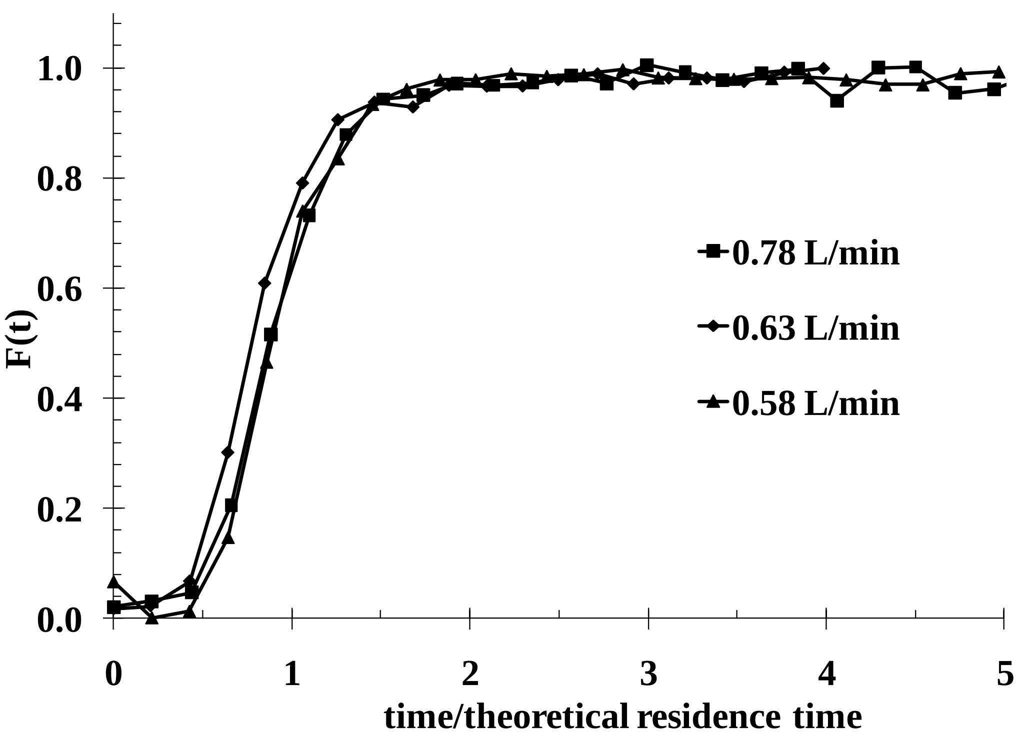

Figure 20. Normalized cumulative age distribution curves for prototype 2 at 3 different flow rates.

While ideal plug flow behavior was not seen, prototype 2 behaved much more like a plug flow reactor than prototype 1. This can be seen through the sharp peaks in the exit age distribution and steep slope of the cumulative age distribution. Additionally, compared to prototype 1, prototype 2 exhibited similar behavior between all 3 flow rates. The ratio of theoretical residence time to mean hydraulic detention time and non-dimensional variance were similar for all 3 flow rates. The reactor showed indications of short circuiting through the ratio of residence to hydraulic detention time being greater than 1. This short circuiting is most likely through the middle of the reactor where the bulb is located or around the edges of the reactor baffles.

Modeling of prototype 2 was also conducted. The plug flow reactor with dispersion model again was most similar to the experimental results. Figures 21 and 22 show the exit age distribution and cumulative age distribution of the 0.78 L/min flow rate, with additional flow rates shown in Appendix A.

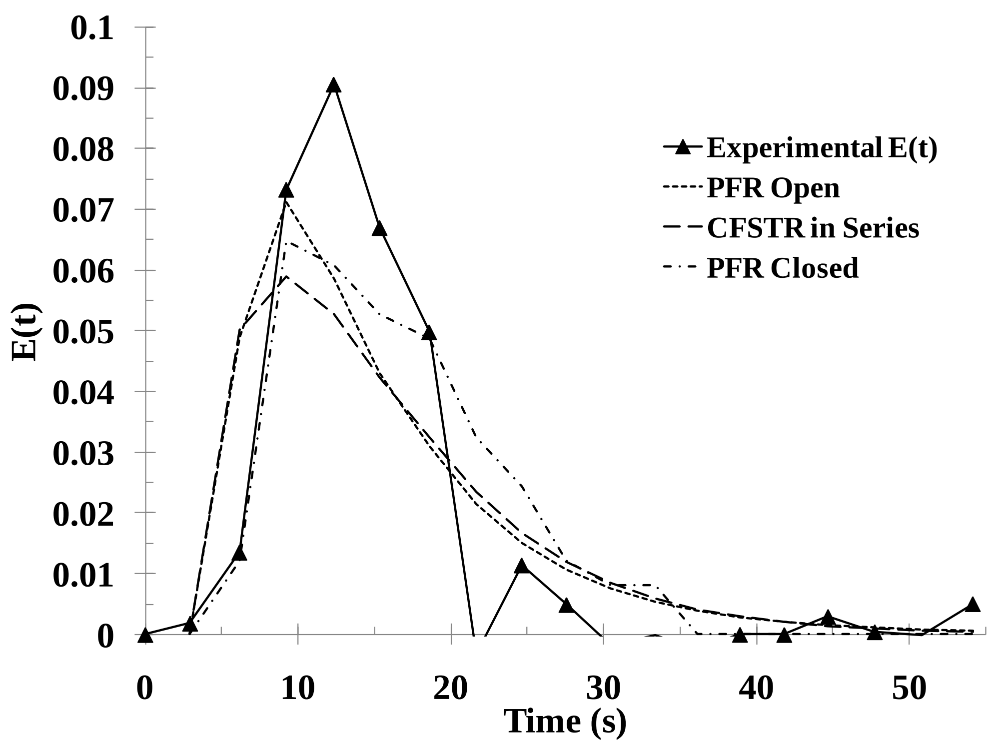

Figure 21. Exit age distribution comparison of experimental data and non-ideal models at 0.78 L/min for prototype 2.

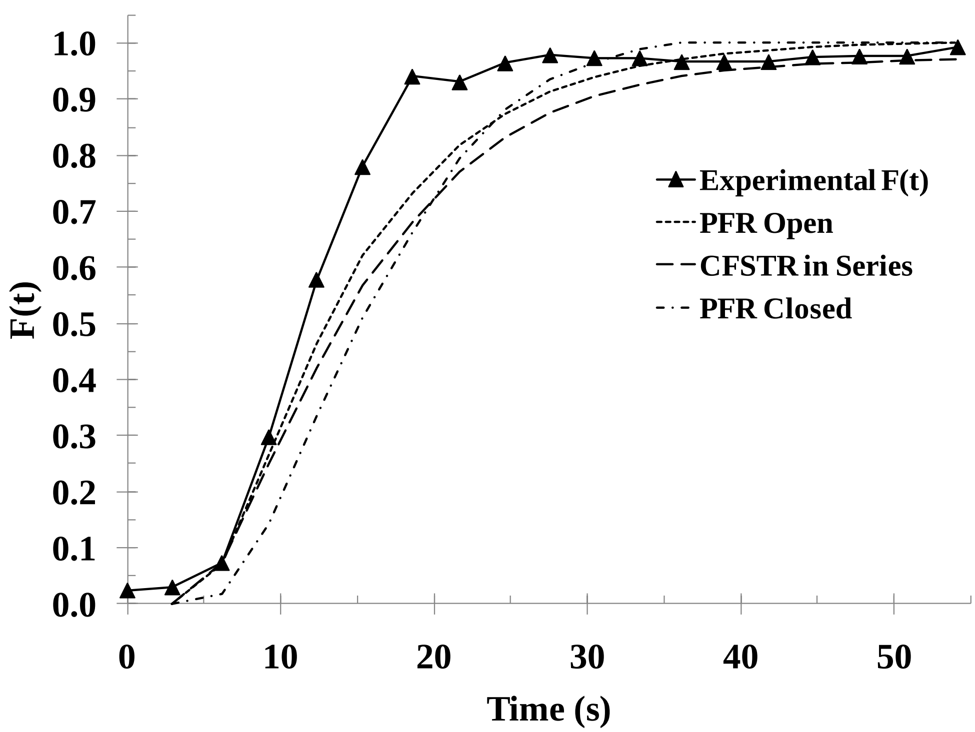

Figure 22. Cumulative age distribution comparison of experimental data and non-ideal models at 0.78 L/min for prototype 2.

3.1.3 Prototype 3

The hydraulic properties of prototype 3 are described in Table 9. Normalized exit age distribution and cumulative age distribution curves for prototype 3 are shown in Figure 23 and 24.

Flow Rate (L/min)	Theoretical residence time/mean hydraulic detention time	Non-dimensional variance
0.766	1.09	0.615
1.07	1.22	0.711
1.21	1.28	1.45

Table 9. Hydraulic properties of prototype 3.

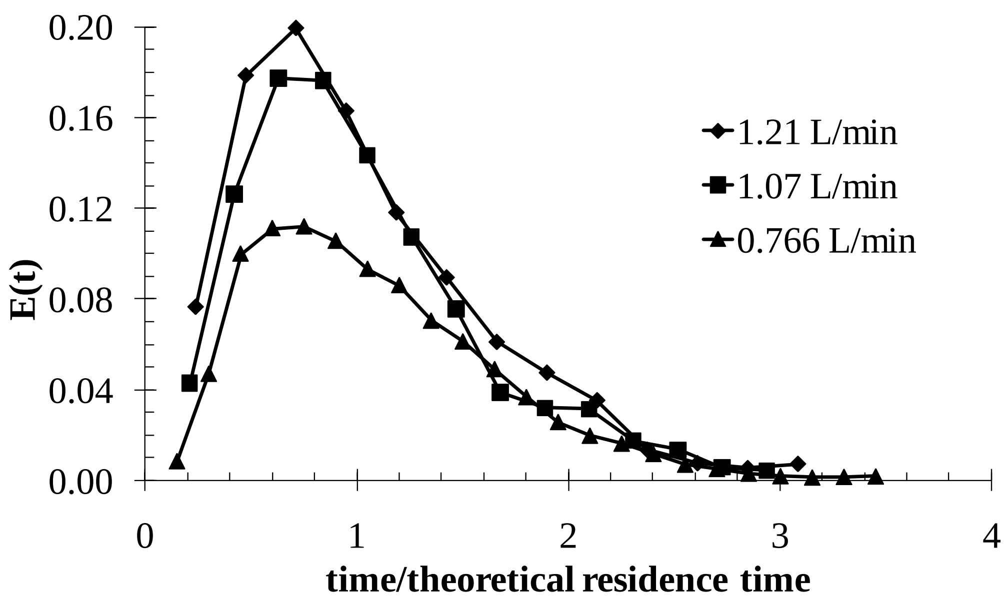

Figure 23. Normalized exit age distribution curves for prototype 3 at 3 different flow rates.

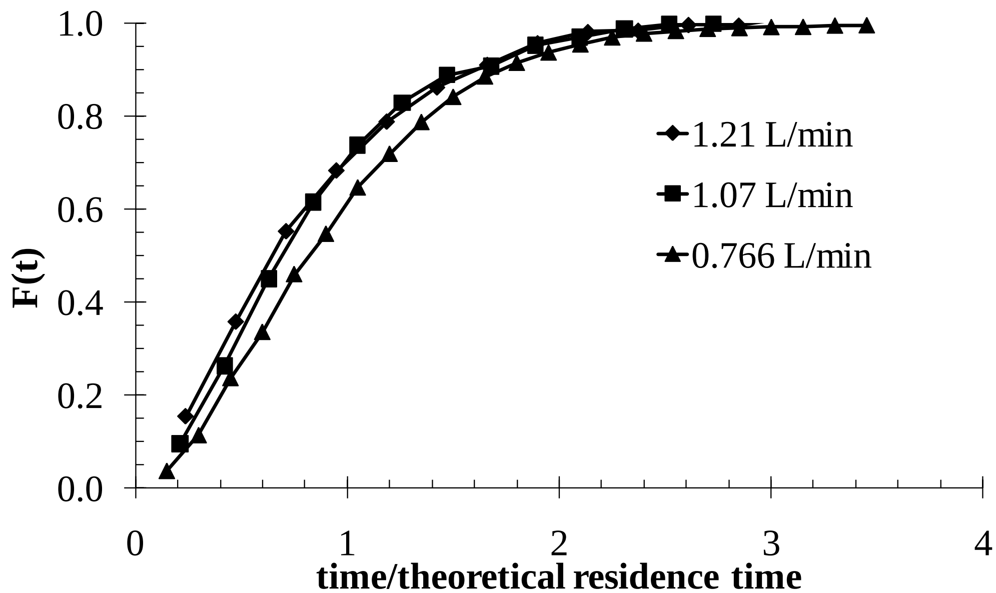

Figure 24. Normalized cumulative age distribution curves for prototype 3 at 3 different flow rates.

Prototype 3 did not exhibit ideal behavior with multiple signs of short circuiting and all three flow rates performing differently. The tracer studies exhibited curves closer to a continuously stirred tank reactor, than a plug flow reactor. While prototype 3 was modeled after prototype 2, its main design change was to increase the reflectivity of the reactor. However, due to the construction limitations of working with an aluminum sheet, the reactor had much more potential for short circuiting as many obvious physical gaps were seen in the system. Additionally, a new bulb was used that is two pronged allowing for water to travel down the middle of the two prongs. Hydraulically this is a problem, in that each parcel of water will not receive the same dose, but it is assumed the intensity of UV light in between the two prongs is highest and so therefore should not negatively affect the overall disinfection efficiency of the system.

Modeling conducted on prototype 3 showed similarities to non-ideal models. The exit age distribution comparison of the experimental data and the non-ideal models showed the dispersion numbers for both open and closed boundaries were overestimated and resembled the behavior of a CFSTR in series. The cumulative age distribution comparison more closely resembled a PFR with closed boundary model. Figures 25 and 26 show the exit age and cumulative age distribution for the tracer study run at 1.21 L/min flow rate. Non-ideal modeling of additional flow rates is shown in Appendix A.

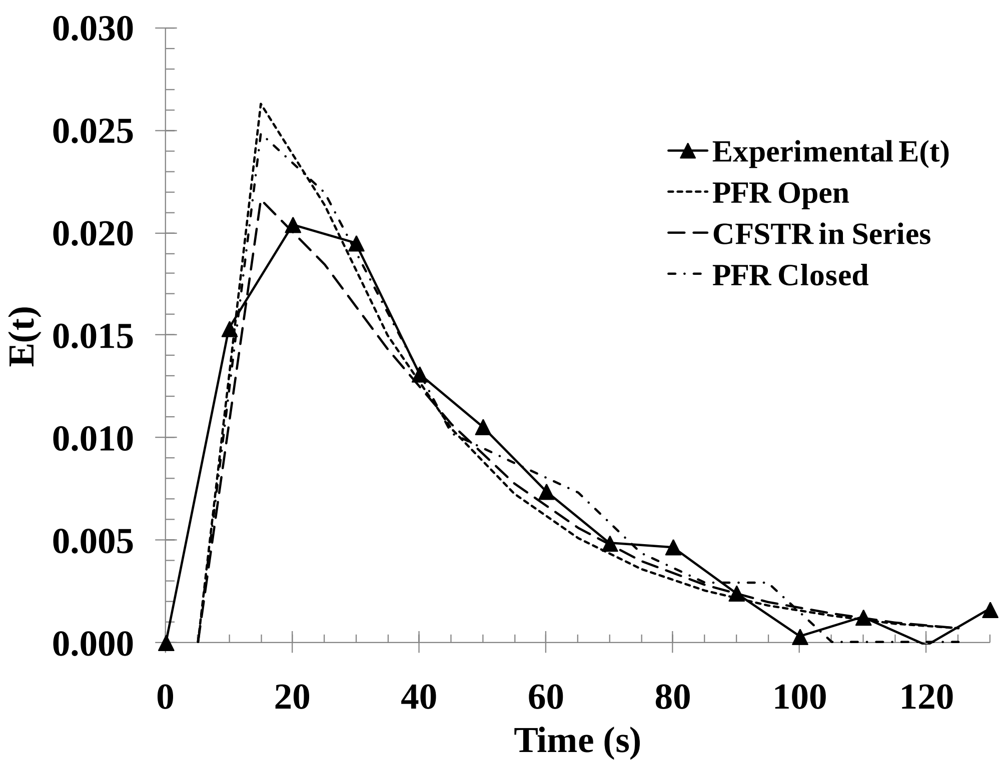

Figure 25. Exit age distribution comparison of experimental data and non-ideal models at 1.21 L/min for prototype 3.

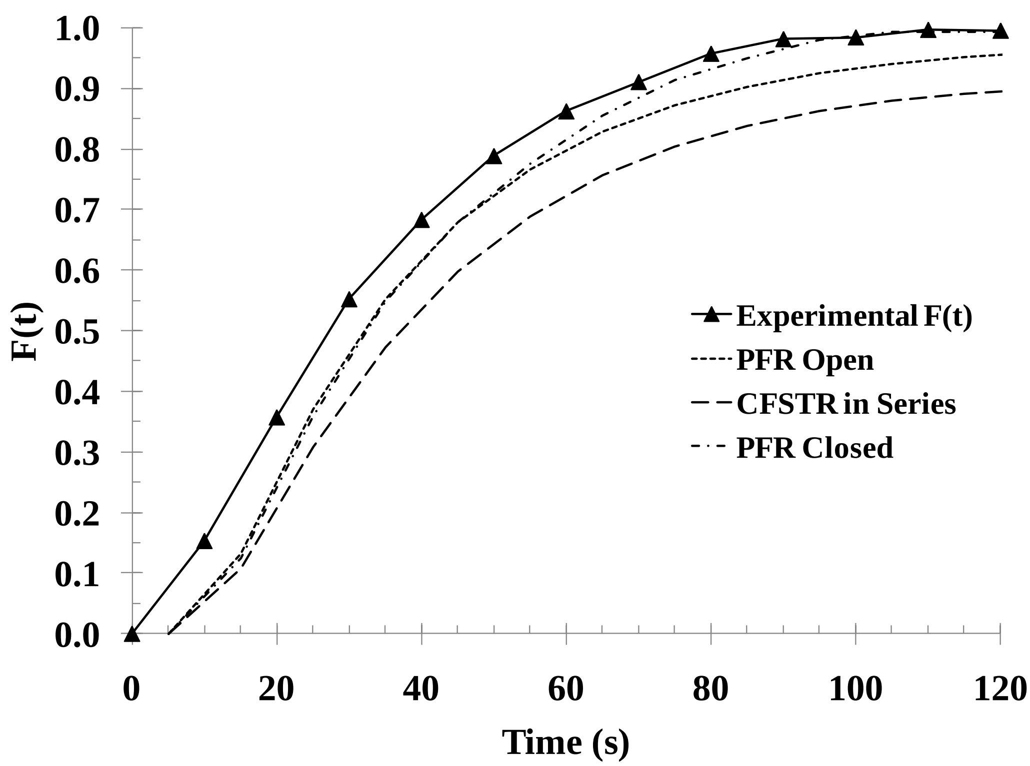

Figure 26. Cumulative age distribution comparison of experimental data and non-ideal models at 1.21 L/min for prototype 3.

3.2 Collimated Beam Testing

3.2.1 T1 Bacteriophage

Figure 27 shows the dose response curve for T1 bacteriophage based on the collimated beam testing performed.

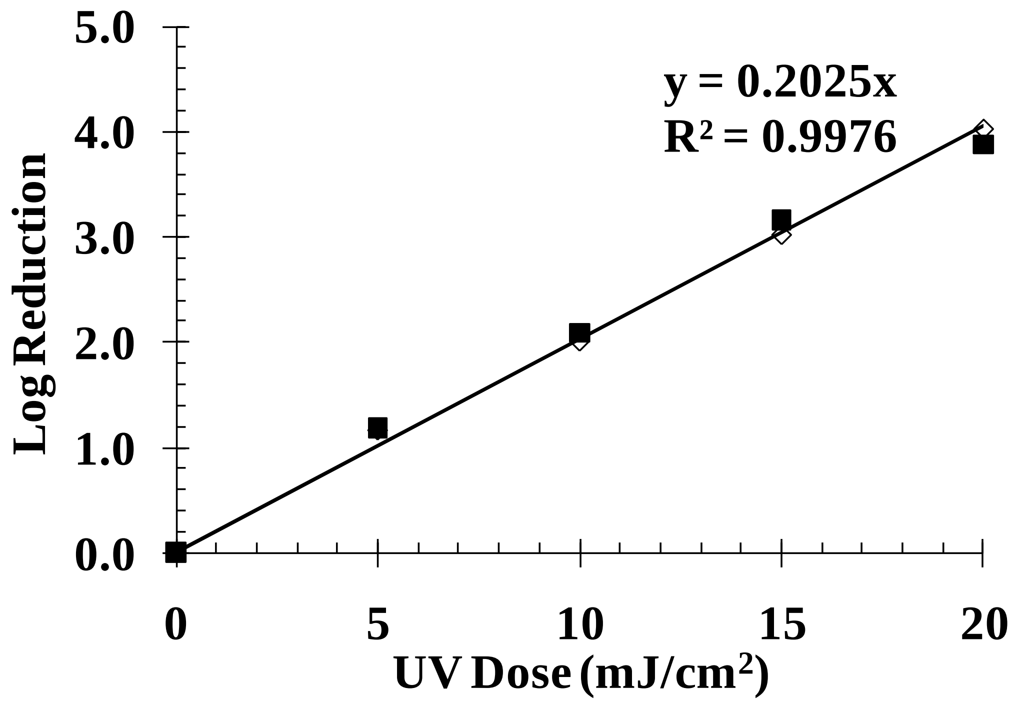

Figure 27. Dose response of T1 bacteriophage.

The dose response of the experimental data was similar to the dose response of T1 seen in Bircher and Wright, 2007 but showed a lower dose per log inactivation than Hargy et al 2008. Figure 28 shows the comparison of the experimental data plotted with these two studies.

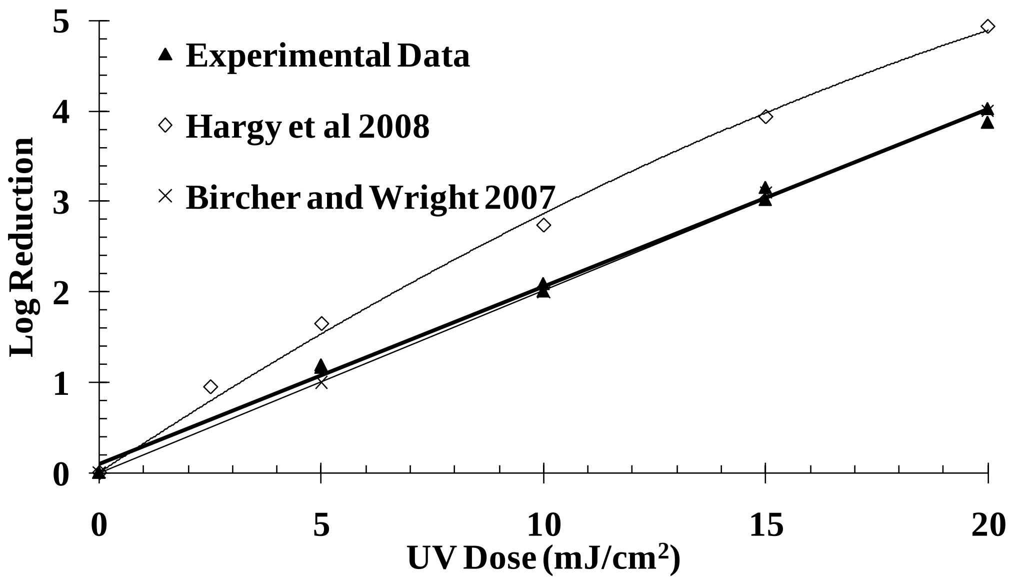

Figure 28. Comparison of the dose response of T1 bacteriophage experimental data and literature studies.

3.2.2 MS2 Bacteriophage

Figure 29 shows the dose response curve for MS2 bacteriophage based on the collimated beam testing performed.

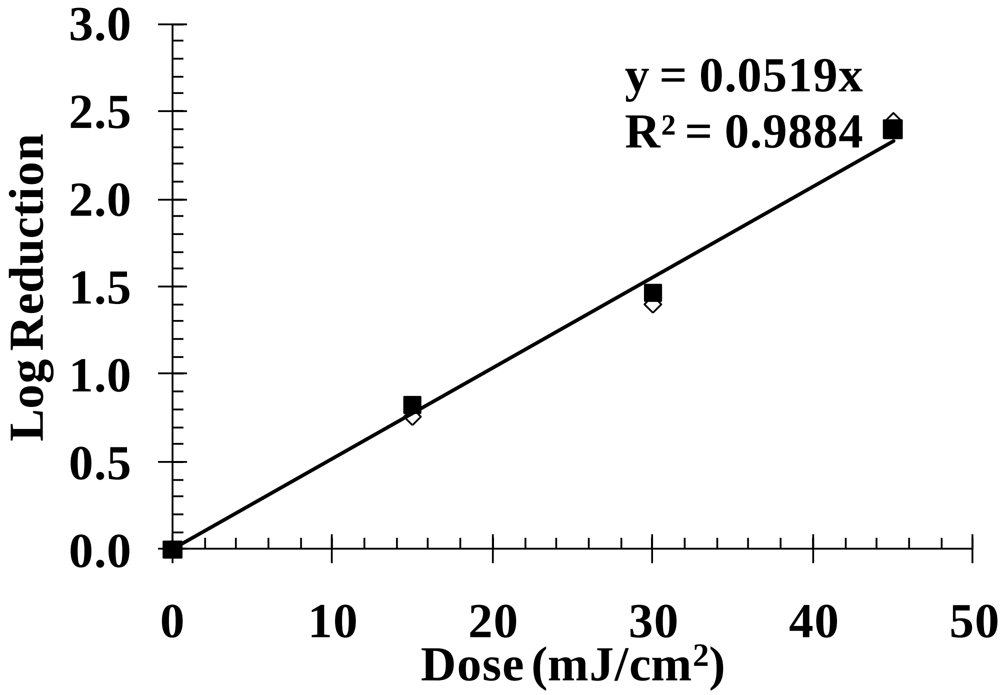

Figure 29. Dose response of MS2 bacteriophage.

The experimental dose response for MS2 relates well to those seen in the literature. The experimental data shows a dose per log reduction of 19.3 while experimental data shows a dose per log reduction of 15.5 to 24.8. Figure 30 shows the comparison between experimental data and literature values.

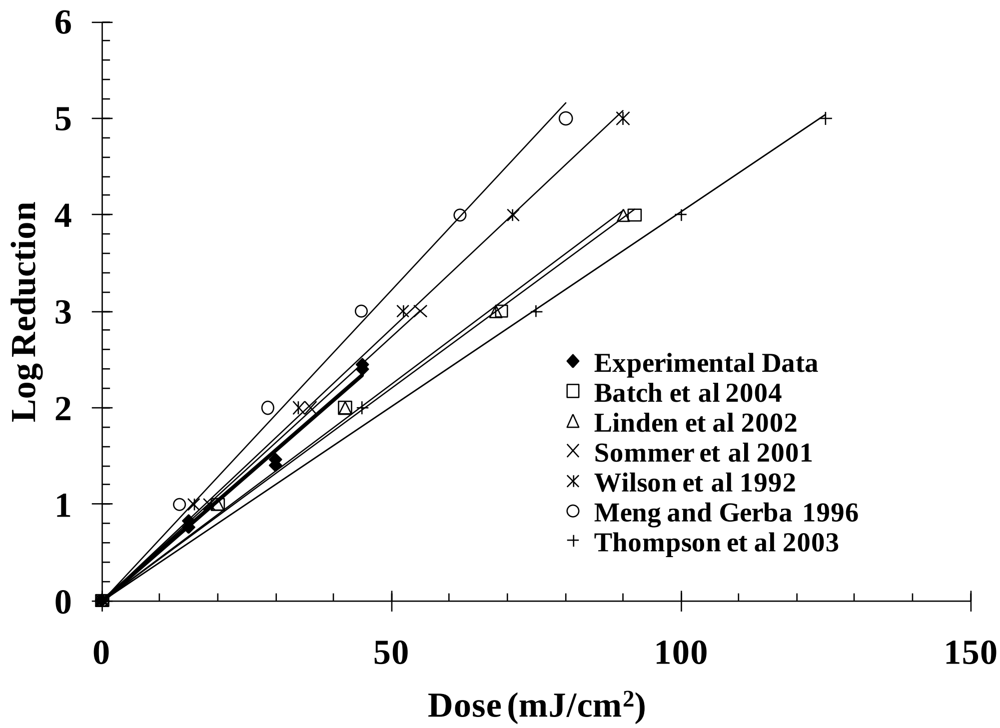

Figure 30. Comparison of the dose response of MS2 bacteriophage experimental data and literature studies.

3.3 Biodosemetry

3.3.1 Prototype 2 – T1 Challenge Testing

Figure 31 shows results of prototype 2 testing with T1 bacteriophage as the challenge organism.

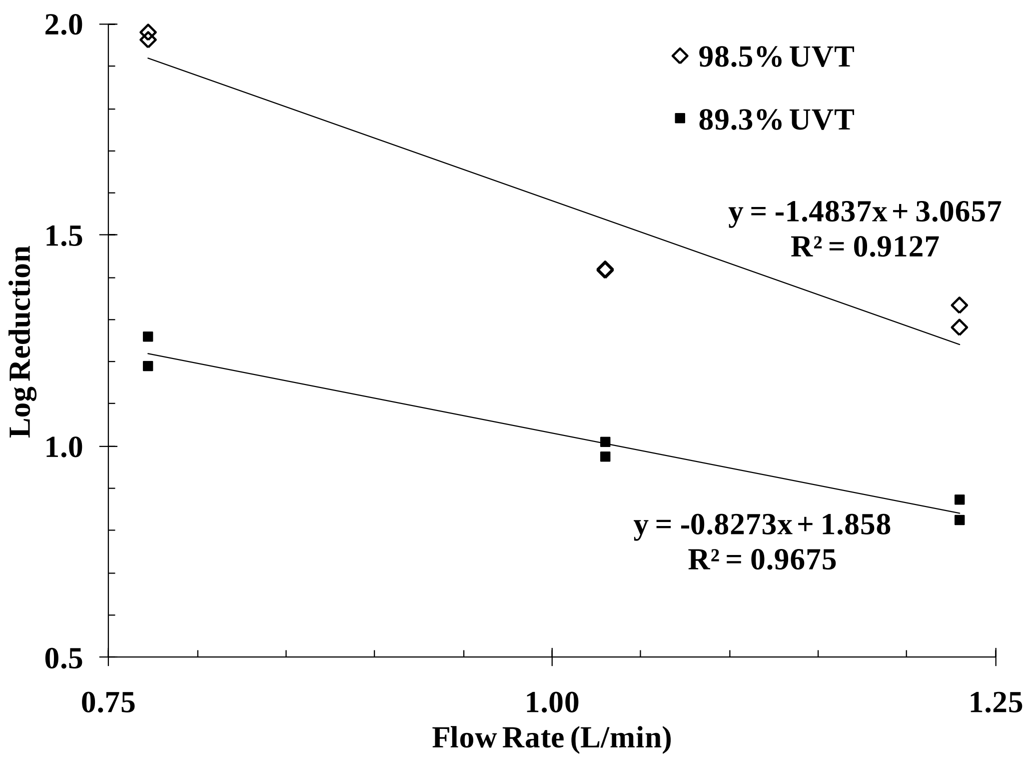

Figure 31. Prototype 2 flow rate response to T1 bacteriophage.

The dose was then calculated based on the T1 collimated beam results. The T1 collimated beam showed a linear response with respect to the log inactivation with a slope of 0.2025. The log inactivation of the prototype was divided by the slope of the collimated beam test to determine the dose at each flow rate. Figure 32 shows the calculated dose at each flow rate.

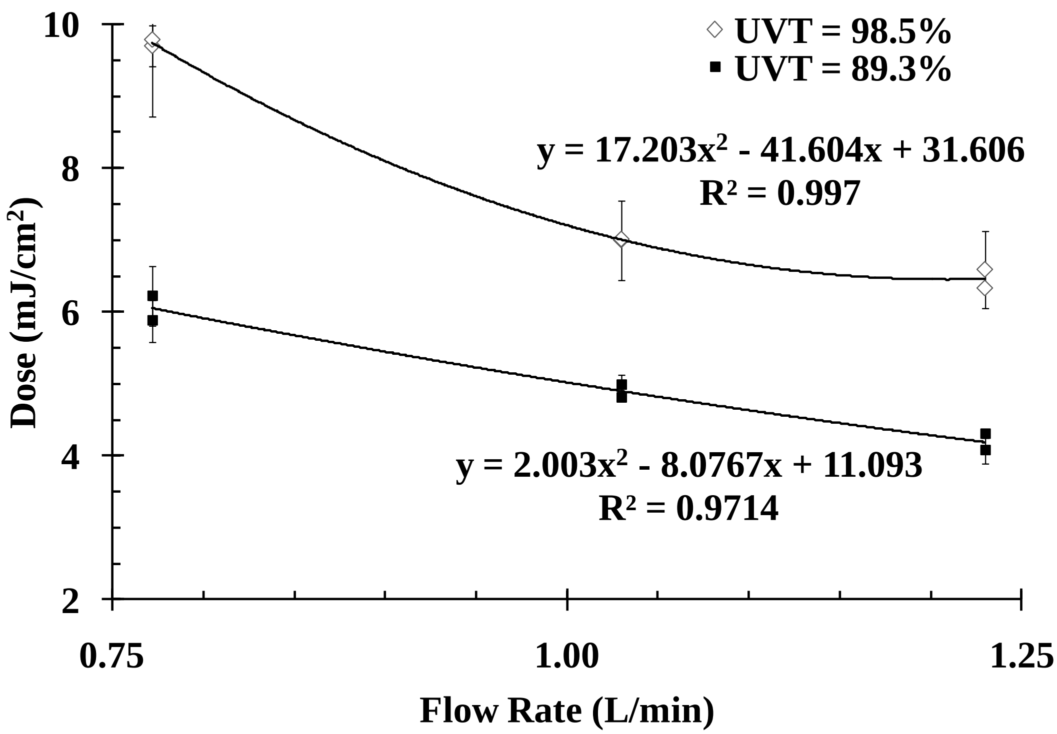

Figure 32. Dose response of prototype 2. Error bars represent a 90% confidence based on the Student's t-test.

Prototype 2 produced doses between 4 and 10 mJ/cm^2. As expected, the high UVT water yielded a higher dose than the lower UVT water. A second order polynomial line was fit to the data and is shown on Figure 32. The dose which can be used for validation purposes is shown in Table 10. The doses outlined are the lower limit of the 90% confidence interval.

	Dose (mJ/cm²)		
UVT	**0.772 L/min**	**1.03 L/min**	**1.23 L/min**
98.5%	8.48	6.18	5.53
89.3%	5.11	3.71	3.46

Table 10. UV dose for prototype 2. Doses are based on lower limit of 90% confidence interval.

The higher doses (5-8 mJ/cm^2) for prototype 2 will achieve a 1 to 2 log reduction in most *E. coli* and 1 to 2 log reduction in *Giardia* and *Cryptosporidium* while the lower doses (3-5 mJ/cm^2) will achieve only 1 log reduction of most bacteria and protozoa (Hijnen et al 2006). Additionally, following the Long Term 2 Enhanced Surface Water Treatment Rule (LT2ESWTR), the reactor would be given "credit" for a 2 log reduction in *Giardia* and *Cryptosporidium* at the higher doses and a 1.5 log reduction "credit" for the lower doses (USEPA 2006). Note that the doses calculated do not include the RED bias factor which would be needed to validate the dose based on the UV Disinfection Guidance Manual.

3.3.2 Prototype 3 – MS2 Challenge Testing

Based on design goals, a higher UV dose was desired. So the bulb size was increased from a 3-watt to a 9-watt low pressure UV bulb. Because MS2 is much more resistant to UV than T1, and the expected dose was much higher based on the increased wattage of the UV bulb, MS2 was used as the challenge organism for prototype 3.

Figure 33 shows results of prototype 3 testing with MS2 bacteriophage.

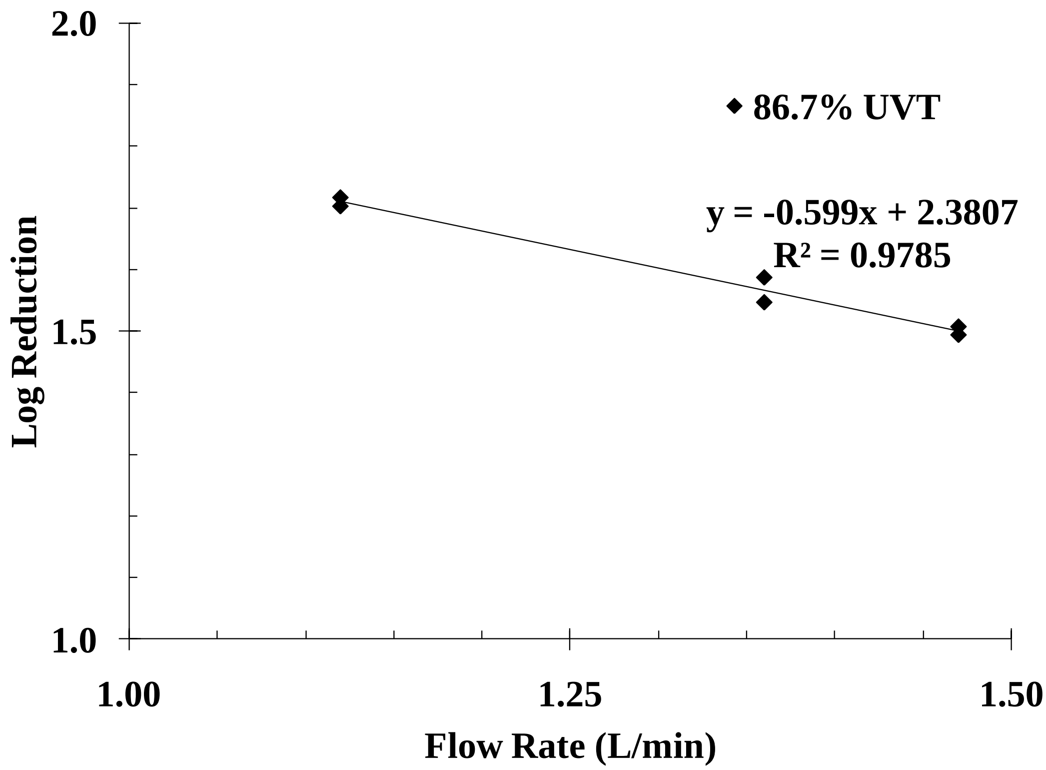

Figure 33. Prototype 3 flow rate response to MS2 bacteriophage.

The dose was then calculated based on the MS2 collimated beam results. The MS2 collimated beam showed a linear response with respect to the log inactivation with a slope of 0.0519. The log inactivation of the prototype was divided by the slope of the collimated beam test to determine the dose at each flow rate. Figure 34 shows the calculated dose at each flow rate.

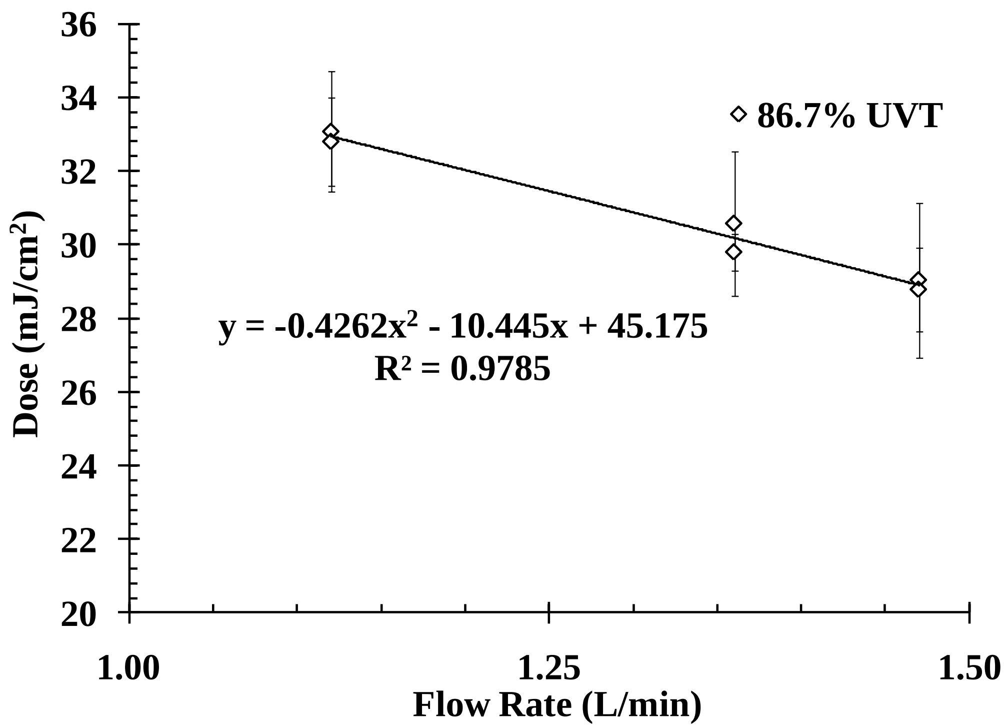

Figure 34. Dose response of prototype 3. Error bars represent a 90% confidence based on the Student's t-test.

Prototype 3 produced doses between 28 and 34 mJ/cm^2. These doses are about five to seven times larger than prototype 2. Greater disinfection is likely from the higher wattage bulb used. A second order polynomial line was fit to the data and is shown on Figure 34. The dose which can be used for validation purposes is shown in Table 11. The doses outlined are the lower limit of the 90% confidence interval.

	Dose (mJ/cm^2)		
UVT	1.12 L/min	1.36 L/min	1.47 L/min
85.7%	31.43	28.60	26.92

Table 11. UV dose for prototype 3. Doses are based on lower limit of 90% confidence interval.

At the doses seen in prototype 3, >4 log reduction in *E. coli*, >3 log reduction in *Giardia* and *Cryptosporidium*, and 3 to 4 log reduction in Poliovirus and Rotavirus are expected (Hijnen et al 2006). These doses are much more reasonable for the reactor design than prototype 2. There will be high levels of inactivation of most bacteria and protozoa, and viruses are also being targeted. Additionally the LT2ESWTR would "credit" this system with 4 log *Cryptosporidium* and *Giardia* reduction without the inclusion of the RED bias (USEPA 2006). The Network's rating system would rate this system as intermediately effective (Sobsey and Brown 2010).

3.4 First Order Kinetic Modeling

Additional modeling was conducted based on first order kinetics of a plug flow reactor with dispersion. Collimated beam testing results with first order hydraulic modeling can be used to predict the log inactivation of a particular reactor.

3.4.1 Reactor 2 with T1 Bacteriophage

The collimated beam test for T1 bacteriophage (Figure 27) was changed to a time based response based on the exposure time used, which can be seen in Figure 35.

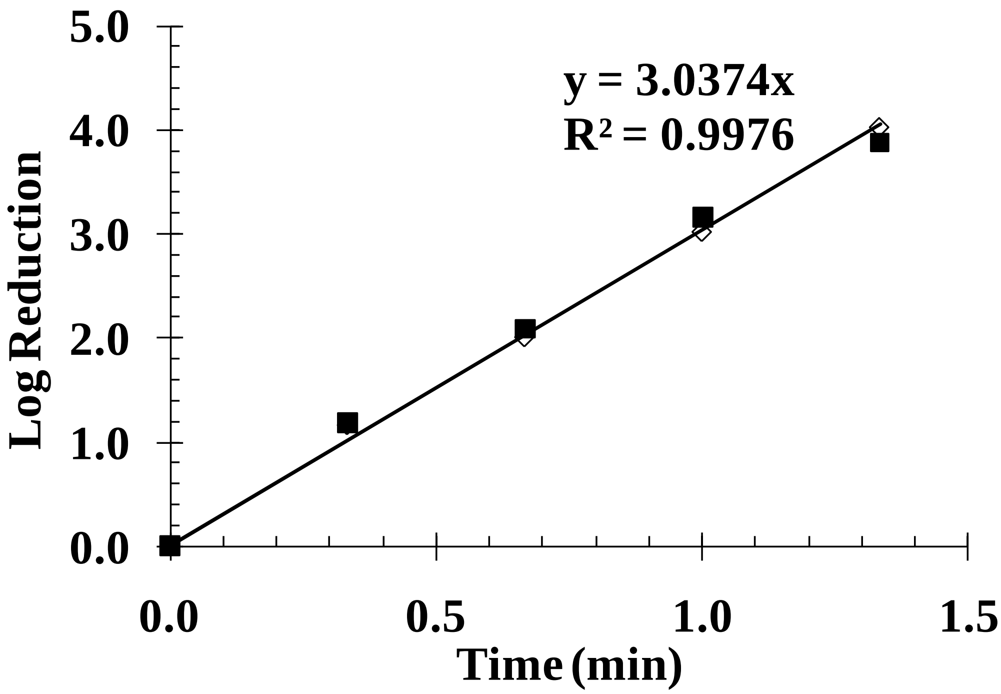

Figure 35. Collimated beam testing of T1 based on a time response at 0.315 mW/cm^2.

It is important to note that when using Figure 35 for future log reduction predictions of reactor 2, the intensity must be the same as the one used in the collimated beam experiment (0.315 mW/cm^2 in Figure 35). Additionally, other factors are not included in the calculation such as those used in the collimated beam test (water factor, divergence factor, etc.). Figure 35 was used to determine the first order reaction coefficient (k_1) by fitting a first order linear model to the data. In the case of the T1 bacteriophage as seen in Figure 35, the first order reaction coefficient was 3.0374. The reactor was assumed to behave similar to an open boundary plug flow reactor with dispersion model. The reaction coefficient, open boundary dispersion number (N_d, open) and the residence time or T_{10} value (the time associated with value of 0.10 on the cumulative exit age distribution), were then used to model the log inactivation based on time. Table 12 summarizes the calculated values with Figure 36 comparing the modeling results using the residence time and T_{10} value. Appendix D shows first order modeling calculations.

Flow Rate (L/min)	N_d,open	Residence Time (min)	T_{10} (min)
0.772	.313	.240	.167
1.03	.386	.180	.133
1.23	.313	.150	.117

Table 12. Values used for first order kinetic modeling as an open boundary plug flow reactor with dispersion for T1 bacteriophage.

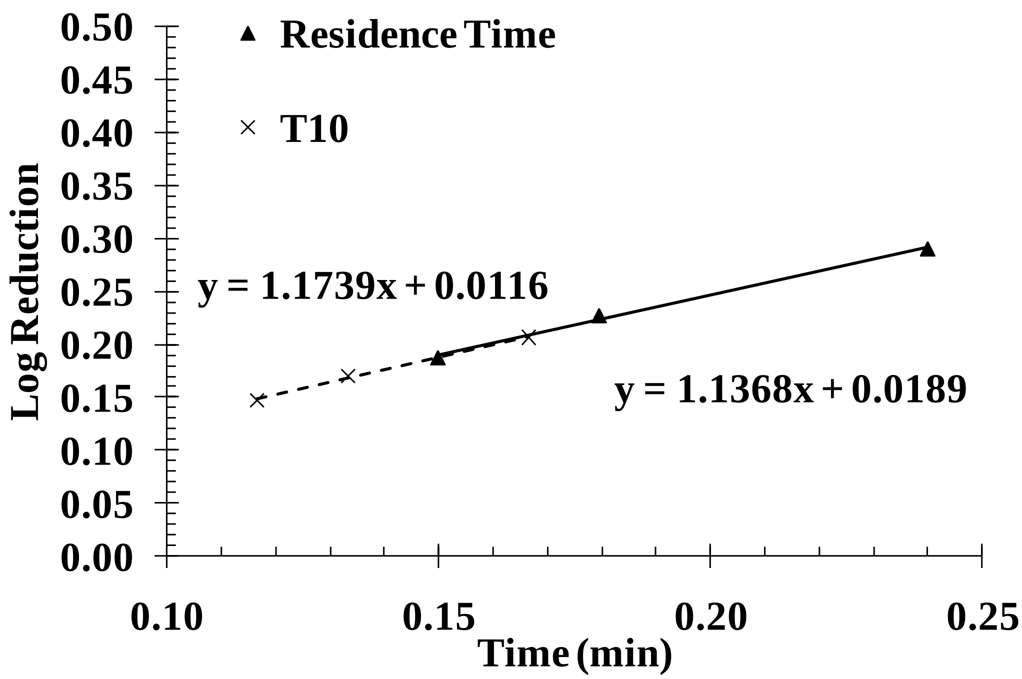

Figure 36. Predicted T1 bacteriophage time rate response based on first order modeling of an open boundary plug flow reactor with dispersion.

When predicting a reactor's log reduction it is likely that the T_{10} value would be used to incorporate a safety factor into the predictions. However, both equations above could be used to estimate the log reduction of a particular reactor based on the time the water parcels spend in the reactor. However, the above formulas would only be realistic for a bulb that has an intensity of 0.315 mW/cm^2. Equations would need to be developed at the particular intensity of the UV bulb being used in order to predict the log reduction of the reactor.

3.4.2 Reactor 3 with MS2 Bacteriophage

The collimated beam test for MS2 bacteriophage (Figure 29) was changed to a time based response based on the exposure time used, which can be seen in Figure 37.

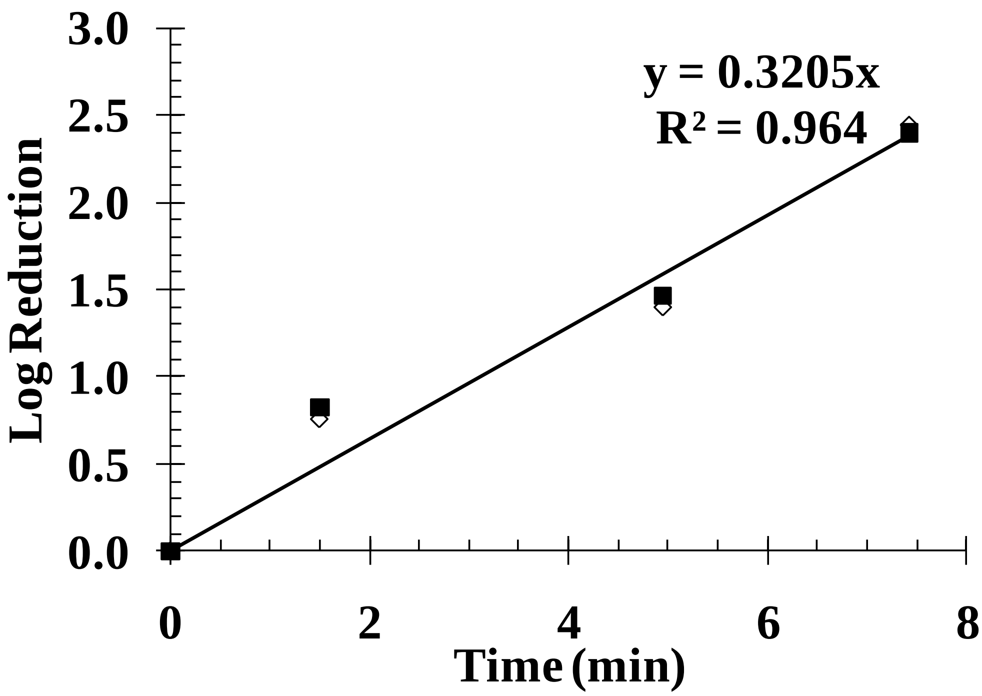

Figure 37. Collimated beam testing of MS2 based on a time response at 0.206 mW/cm^2.

The first order coefficient, open boundary plug flow reactor with dispersion number and residence time or T_{10} value were then used to model the log inactivation based on time for MS2 bacteriophage. Table 13 summarizes the calculated values with Figure 38 comparing the modeling results for the residence time and T_{10} value. Appendix D shows first order modeling calculations.

Flow Rate (L/min)	N_d,open	Residence Time (min)	T_{10} (min)
1.12	.377	.804	.333
1.36	.461	.662	.167
1.47	.487	.612	.117

Table 13. Values used for first order kinetic modeling as an open boundary plug flow reactor with dispersion for MS2 bacteriophage.

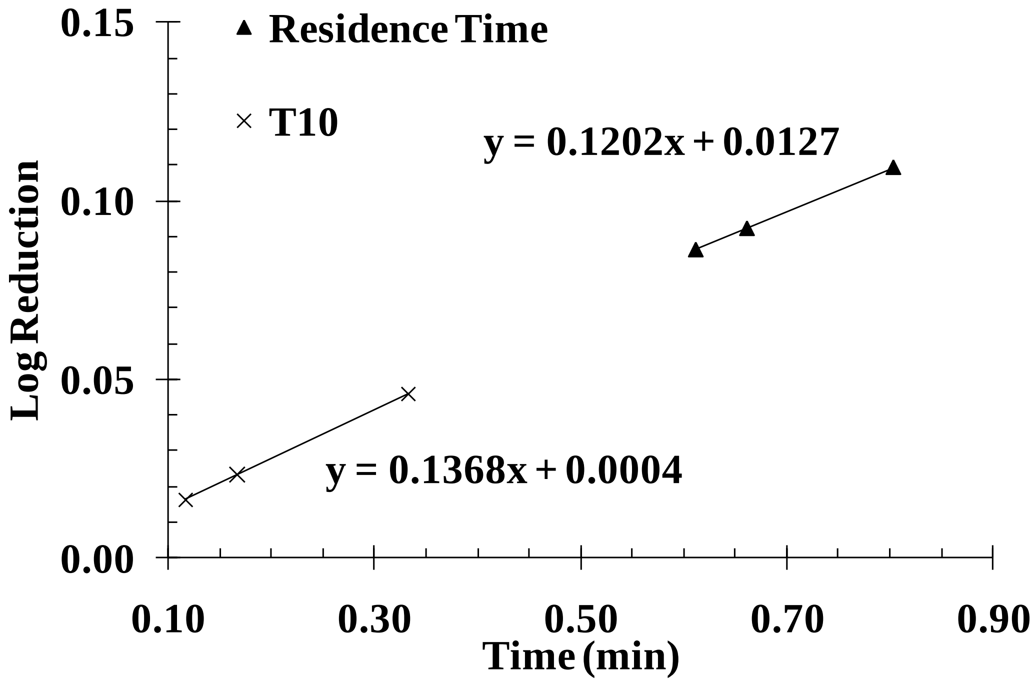

Figure 38. Predicted MS2 bacteriophage time rate response based on first order modeling of an open boundary plug flow reactor with dispersion.

In reactor 3, the T_{10} values were much smaller than the residence times, likely from the short circuiting occurring in the system. The log reduction prediction equations are much further apart than those in reactor 2. If the T_{10} values were used for log reduction prediction it would result in much lower values than those seen with the residence time of the reactor.

The first order kinetic modeling is a useful tool to predict log reduction without conducting challenge testing. However, it is limited to certain conditions such as the intensity of the bulb where a dose response curve accounts for many of these variations.

3.5 Preliminary Power Source Design

Both power source designs yielded only a few results because of the limited success of the designs. Both designs showed a voltage around 21 V as an initial power surge from the solar panel and then a constant voltage around 19 V. While prototype 1 did illuminate the UV bulb, the light was flashing on and off due to the modified sine wave inverter used over a continuous sine wave inverter. Prototype 2 failed to illuminate the UV bulb all together because the inverter was not working properly. However, the reason the inverter wasn't working is still unknown. The batteries were fully charged and outputting enough power to run the inverter, so the inverter should have been running properly (Kunik et al 2010).

4. Conclusion

A UV POU device constructed using simple techniques with readily available materials can be produced at a low cost. Aluminum cans specifically, which can be found almost anywhere in the world, are an effective material to build inexpensive UV reactors out of. Optimization of a UV POU system includes a balance of hydraulic properties and the output (wattage) of the UV bulb. Adding a minimal amount of simple baffling can drastically increase the hydraulic efficiency of the system. However challenges did arise in the construction of the system. To ensure dead space and short circuiting don't occur an easily replicable construction procedure must be developed. A 3-watt bulb will reduce the protozoa and bacteria by 1 to 2 log, but will be ineffective at reducing viruses. Increasing the bulb to 9-watts produces high enough doses to reduce protozoa, bacteria and viruses by 3 to 4 log at flow rates over 1 liter per minute, if the UVT is above approximately 85%. Low UVT waters will not be effective based on cost, so pretreatment will likely be needed. A photovoltaic power supply is likely not the best option for the UV POU device as it drastically raises the cost of the system and in its current state does not provide a reliable source of UV light.

A UV POU device has many advantages and disadvantages over commonly used POU technologies. Advantages include on-demand flow rates, no taste and odor issues, effectiveness at inactivating a variety of pathogens and low maintenance cost. Disadvantages include no residual disinfectant, high capital cost and the need for a power supply. Table 14 compares a UV POU device to common POU devices.

	Boiling	Chlorine	Bio-Sand Filter	Ceramic Filter	SODIS	Combined Coagulation/ Disinfection	UV Treatment
On Demand Flow Rates	✓	✓	✓✓	✓	✓	✓	✓✓✓
Bacteria Reduction	✓✓✓	✓✓✓	✓✓	✓✓✓	✓✓✓	✓✓✓	✓✓✓
Virus Reduction	✓✓✓	✓✓	✓	✓	✓✓✓	✓✓✓	✓✓
Protozoa Reduction	✓✓✓	✓	✓✓✓	✓✓✓	✓✓	✓✓✓	✓✓✓
Taste and Odor	✓✓✓	✓	✓✓✓	✓✓✓	✓✓✓	✓	✓✓✓
Residual Disinfectant	None	✓✓✓	None	None	None	✓✓✓	None
User Power Consumption	✓	✓✓✓	✓✓✓	✓✓✓	✓✓✓	✓✓✓	✓✓
User Acceptability	✓✓✓	✓✓	✓✓✓	✓✓	✓✓	✓✓	Unknown
Capital Cost	✓	✓✓✓	✓	✓✓	✓✓✓	✓✓	✓
Recurring or Maintenance Cost	✓	✓✓	✓✓✓	✓✓✓	✓✓✓	✓✓	✓✓✓

Table 14. Comparison of POU technologies, where one check mark corresponds to a poor rating and three check marks correspond to a favorable rating. Adapted from Lantagne et al 2007, Sobsey 2002, and Sobsey et al 2008.

4.1 Future Work

4.1.1 Reactor Development

Further optimization of the hydraulic properties and the UV bulb is needed to create the most effective solution. Likely, a slightly smaller bulb with a cleaner baffling scheme will be able to effectively reduce bacteria, protozoa and viruses to waters with at least an 85% UVT. Additionally the construction procedure must be simplified to eliminate gaps and produce systems quickly with high quality. One possibility to simply the construction procedure is to produce the design as a single sheet of aluminum that can be folded together and glued. The single aluminum sheet itself can be made out of a mold that is stamped out, therefore not requiring measuring or tweaking. An example of this design is shown in Figure 39.

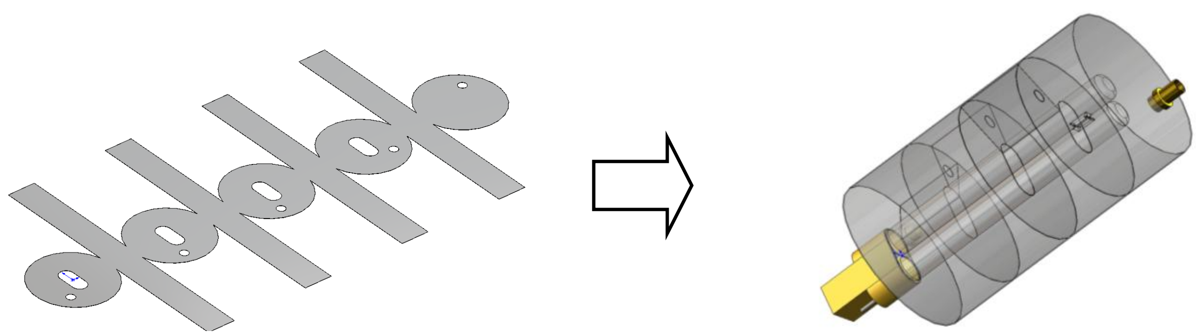

Figure 39. 3-dimensional model of unfolded and folded reactor design.

4.1.2 Power Supply

Other methods of providing power in remote areas needs to be explored. A photovoltaic design could likely be further optimized but will likely still drastically increase the cost of the system. Another option may be the use of a hand crank. Additionally, the cost of the power supply could be greatly reduced by switching to a direct current UV bulb over an alternate current UV bulb. The inverter would then be eliminated reducing the cost of the system.

4.1.3 Field Testing

The UV POU system will need to be field tested in order to address many of the social issues that may occur while using the system. As with many POU devices, unexpected behavioral barriers may occur making the user uninterested in the product. These may not be easily recognizable until the system is in someone's home. Education tools, which have been introduced with many other POU devices, may be useful in implementing this system. Additionally the technical aspect of the system can be accessed to ensure the field based prototypes are performing as predicted in the laboratory.

4.1.4 Business Potential

As mentioned earlier, adoption rates of many POU systems are often low. However, if a user actually purchases a POU system, it is often more sustainable because the user has invested their own money into the system. The UV POU system has tremendous potential in providing a product that users can invest in but also create local business opportunities by manufacturing the product. A market based strategy will have a larger impact, because it doesn't rely on the implementation of one system at a time but the users themselves to generate the demand. Additionally, unique funding mechanisms, such as those used by Manna Energy Limited and the UV Waterworks system may be useful for adoption of the UV POU system.

5. References

Batch, L., Schulz, C., and Linden, K. (2004). “Evaluating Water Quality Effects on UV Disinfection of MS2 Coliphage”. *Journal of American Water Works Association*, 96(7), 75-87.

Bircher, K. and Wright, H. (2007). “Who Needs RED? An Empirical Method for Validating the Log-Inactivation of a UV Reactor Thereby Eliminating the Need for RED and RED Bias”. American Water Works Association, WQTC Conference.

Bolton, J and Linden, K. (2003). “Standardization of Methods for Fluence (UV Dose) Determination in Bench-Scale UV Experiments”. *Journal of Environmental Engineering.*

Brownell, S., Chakrabarti, A., Kaser, F., Connelly, L., Peletz, R., Reygadas, F., Lang, M., Kammen, D., and Nelson, K. (2008). Assessment of a Low-Cost, Point-of-Use, Ultraviolet Water Disinfection Technology”. *Journal of Water and Health*.

Clasen, T. and Bastable, A. (2003). “Faecal Contamination of Drinking Water During Collection and Household Storage: The Need to Extend Protection to the Point of Use”. *Journal of Water and Health,* 109-115.

Clasen, T., Schmidt, W., Rabie, T., Roberts, I., and Cairncross, S. (2007). “Interventions to Improve Water Quality for Preventing Diarrhoea: Systemic Review and Meta-Analysis”. *British Medical Journal*, Vol. 334, No. 7597.

Cohn, A. (2002). “The UV-Tube as an Appropriate Water Disinfection Technology: An Assessment of Technical Performance and Potential for Dissemination”. Master’s Report. University of California at Berkeley.

Environmental Protection Agency (2001). “Method 1601: Male-Specific (F+) and Somatic Coliphage in Water by Two-Step Enrichment Procedure”.

Fewtrell, L., Kaufmann, R., Kay, D., Enanoria, L., and Calford, J. (2005). “Water, Sanitation, and Hygiene Interventions to Reduce Diarrhoea in Less Developed Countries: A Systematic Review and Meta-Analysis”. *Lancet Infectious Disease*, Vol 5, 42-52.

Gadgil, A., Greene, D., and Drescher, A. (1998). “Low Cost UV Disinfection System for Developing Countries: Field Tests in South Africa”. First International Symposium on Safe Drinking Water in Small Systems, Washington, D.C.

Gadgil, A., Lim, M., and Ruggeberg, E. (2009). “Ultraviolet (UV) Waterworks: Mexico and the Philippines”. Energy and Water for Sustainable Living. Obtained from www.pi.energy.gov/ documents/EWSLmexicoPhilippinesUVW.pdf.

Gold, M., Thomas, E., Byyny, R., and Habanabakize, J. (2007). “Development and Implementation of the Bring Your Own Water Treatment System in Dense, Rural, and Mountainous Rwandan Communities”. *Journal of Engineering for Sustainable Development*, Vol 2, No 1.

Hargy, T., Lawal, O., Bemus, R., Townsend, B., and Sobrinho, J. (2008). “Coliphage T1 as a Bioassay Surrogate for Cryptosporidium in Validations of UV Reactors for Drinking Water and Wastewater”. American Water Works Association, WQTC Conference.

Hijnen, W., Beerendonk, E., and Medema, G. (2006). “Inactivation Credit of UV Radiation for Viruses, Bacteria, and Protozoan Cysts in Water”. *Water Research*, 40, 3-22.

Hunter, P. (2009). “Household Water Treatment in Developing Communities: Comparing Different Intervention Types Using Meta-Regression”. *Environment Science and Technology*.

Kunik, E., Barstow, C., and Linden, K. (2010). “Development of Solar Power Supply and Investigation of Reactor Fluid Flow in UV-Can Point-of-Use Water Treatment System”. Final report submission for National Science Foundation Research Experience for Undergraduate Program at University of Colorado.

Lantagne, D., Quick, R., and Mintz, E. (2007). “Household Water Treatment and Safe Storage Options in Developing Countries: A Review of Current Implementation Practices”. Woodrow Wilson International Center for Scholars, Environmental Change and Security Program. P. 17-38

Linden, K., Batch, L., and Schulz, C. (2002). “UV Disinfection of Filtered Water Supplies: Water Quality Impacts on MS2 Dose-Response Curves”. Proceedings from American Water Works Association Annual Conference, Denver, CO.

Lawler and Benjamin. (2009). The McGraw Hill Companies.

Manna Energy Limited. (2010). “Case Study: Manna in Rwanda”. www.mannaenergy.com/projects-rwanda.php.

Meng, Q. and Gerba, C. (1996). “Comparative Inactivation by Enteric Adenoviruses, Poliovirus and Coliphages by Ultraviolet Radiation”, *Water Research*, 30(11), 2665-2668.

Mintz, E., Bartram, J., Lochery, P., and Wegelin, M. (2001). “Not Just a Drop in the Bucket: Expanding Access to Point-of-Use Water Treatment Systems”. *American Journal of Public Health*, Vol 9, No. 10.

Murcott, S. (2006). “Implementation, Critical Factors and Challenges to Scale-Up of Household Drinking Water Treatment and Safe Storage Systems”. Background Paper on Household Water Treatment and Safe Storage for the Electronic Conference on HWTS. Available online at http://ocw.mit.edu /courses/urban-studies-and-planning/11-479j-water-and-sanitation-infrastructure-in-developing-countries-spring-2007/readings/hwts_paper.pdf.

Niparaja (2007). “Final Report: Evaluation of UV Buckets in Rural Communities of Baja California Sur”. Obtained from http://www.niparaja.org/uveta/proyecto/inov/main.htm.

Potters for Peace (2006). Obtained from www.pottersforpeace.org.

Quick, R., Venczel L., Mintz, E., Soleto, L., Aparicio, J., Gironaz, M., Hutwagner, L., Greene, K., Bopp, C., Maloney, K., Chavez, D., Sobsey, M., and Tauxe R. (1999). "Diarrhoea Prevention in Bolivia Through Point-of-Use Water Treatment and Safe Storage: A Promising New Strategy". *Epidemiol. Infect.,* 122, 83-90.

Reed, R. (2004). "The Inactivation of Microbes by Sunlight: Solar Disinfection as a Water Treatment Process". *Advances in Applied Microbiology*, 54, 333-365.

Rosa, G. and Clasen, T. (2010). "Estimating the Scope of Household Water Treatment in Low- and Medium-Income Countries". *American Journal of Tropical Medicine and Hygiene*, 82(2), 289-300.

Semenza, J., Henderson, R., Bogan, J., and Rubin, C. (1998). "Water Distribution System and Diarrheal Disease Transmission: A Case Study in Uzbekistan". *American Journal of Tropical Medicine and Hygiene*, 59(6), 941-946.

Sobsey, M. (2002). "Managing Water in the Home: Accelerated Health Gains From Improved Water Supply". Geneva: World Health Organization. Available online at http://www.who.int/water_ sanitation_ health/dwq/wsh0207/en/.

Sobsey, M., Stauber, C., Casanova, L., Brown, J., and Elliott, M. (2008). "Point of Use Household Drinking Water Filtration: A Practical, Effective Solution for Providing Sustained Access to Safe Drinking Water in the Developing World". *Environment Science and Technology*, 42, 4261-5267.

Sobsey, M. and Brown, J. (2010). "Evaluating Household Water Treatment Options: Health-Based Targets and Performance Specifications". Water and Health: Where Science Meets Policy Conference, University of North Carolina.

SODIS (2010). EAWAG. Obtained from http://www.sodis.ch/methode/forschung/index_EN.

Sommer, R., Pribil, W., Appelt, S., Gehringer, P., Eschweiler, H., Leth, H., Cabaj, A., and Haider, T. (2001). "Inactivation of Bacteriophages in Water By Means of Non-Ionizing (UV-253.7 nm) and Ionizing (Gamma) Radiation: A Comparative Approach". *Water Research*, 35(13), 3109-3116.

Stockman, L., Fischer, T., Deming, M., Ngwira, B., Bowie, C., Cunliffe, N., Bresee, J., and Quick, R. (2007). "Point-of-Use Water Treatment and Use Among Mothers in Malawi". *Emerging Infectious Diseases,* Vol. 13, No. 7.

Thomas, E., and Amadei, B. (2009). "Accounting for Human Behavior, Local Conditions, and Organizational Constraints in Humanitarian Development Models". *Journal of Environment, Development and Sustainability,* Vol 12, 313-327.

Thompson, S., Jackson, J., Suva-Castillo, M., Yanko, W., Jack, Z., Kuo, J., Chen, C., Williams, F., and Schnurr, D. (2003). "Detection of Infectious Human Adenoviruses in Tertiary-Treated and Ultraviolet-Disinfected Wastewater". *Water Environment Research*, 75(2), 163-170.

United States Environmental Protection Agency (2006). Ultraviolet Disinfection Guidance Manual. EPA 815-R-06-007, Office of Water, Washington, DC.

Wilson, B., Roessler, P., Van Dellen, E., Abbaszadegan, M., and Gerba, C. (1992). "Coliphage MS-2 as a UV Water Disinfection Efficacy Test Surrogate for Bacterial and Viral Pathogens". Proceedings from American Water Works Association Water Quality Technology Conference, Denver, CO.

World Health Organization (WHO) and United Nations Children's Fund Joint Monitoring Programme for Water Supply and Sanitation (2010). "Progress on Drinking Water and Sanitation". UNICEF; Geneva; WHO.

World Health Organization (2007). "Combating Waterborne Diseases at the Household Level". WHO Press.

Wright, J., Gundry, S., and Conroy, R. (2004). "Household Drinking Water in Developing Countries: A Systematic Review of Micobiological Contamination Between Source and Point-Of-Use". *Tropical Medicine and International Health*, Vol 9, 106-117.

Yung, K. (2003). "Biosand Filtration: Application in the Developing World". University of Waterloo. Available online at http://ase.tufts.edu/ewb/workshops/ssf/UniversityOfWaterloo-BioSandFiltration.pdf.

APPENDIX A: TRACER STUDY DATA AND NON-IDEAL REACTOR MODELING

Prototype 1 – 60 mL/min Tracer Data

Volume	100	mL	**Time (s)**	**dimensionless time**	**delta t**	**t/tau**	**A_{254} (1/cm)**	**F(t)**	**E(t)**	**tavg**	**delta F(t)**	**tavg delta F(t)**	**Eave(t) delta t**	**Variance Calc**
Input A_{254}	0.847	1/cm	0	0.00		0.0	0.000	0.000						
Flow Rate	60	mL/min	10	0.10	10	0.1	0.003	0.004	0.000	5	0.004	0.018	0.002	0.044
Theoretical Residence Time	100	s	20	0.21	10	0.2	0.005	0.006	0.000	15	0.002	0.035	0.003	0.665
Mean Hydraulic Detention Time	97.35	s	30	0.31	10	0.3	0.007	0.008	0.000	25	0.002	0.059	0.002	1.478
Variance	1903	s^2	40	0.41	10	0.4	0.008	0.009	0.000	35	0.001	0.041	0.002	2.172
Non-dimensional Variance	0.201		50	0.51	10	0.5	0.031	0.037	0.003	45	0.027	1.222	0.014	28.723
Nd-cb	0.113	0.201	60	0.62	10	0.6	0.037	0.044	0.001	55	0.007	0.390	0.017	51.847
Nd-ob	0.104	0.201	70	0.72	10	0.7	0.077	0.091	0.005	65	0.047	3.070	0.027	114.864
tau-cb	97.35		80	0.82	10	0.8	0.241	0.285	0.019	75	0.194	14.522	0.120	678.191
tau-ob	80.65		90	0.92	10	0.9	0.396	0.468	0.018	85	0.183	15.555	0.188	1362.160
N	4.98		100	1.03	10	1.0	0.538	0.635	0.017	95	0.168	15.927	0.175	1584.176
Gamma Function (4.98)	23.29		110	1.13	10	1.1	0.653	0.771	0.014	105	0.136	14.256	0.152	1674.601
			120	1.23	10	1.2	0.719	0.849	0.008	115	0.078	8.961	0.107	1414.731
			130	1.34	10	1.3	0.748	0.883	0.003	125	0.034	4.280	0.056	877.290
			140	1.44	10	1.4	0.759	0.896	0.001	135	0.013	1.753	0.024	430.851
			150	1.54	10	1.5	0.788	0.930	0.003	145	0.034	4.965	0.024	497.045
			160	1.64	10	1.6	0.809	0.955	0.002	155	0.025	3.843	0.030	709.959
			170	1.75	10	1.7	0.823	0.972	0.002	165	0.017	2.727	0.021	563.165
			180	1.85	10	1.8	0.830	0.980	0.001	175	0.008	1.446	0.012	380.098
			190	1.95	10	1.9	0.832	0.982	0.000	185	0.002	0.437	0.005	182.048
			200	2.05	10	2.0	0.837	0.988	0.001	195	0.006	1.151	0.004	157.314
			210	2.16	10	2.1	0.842	0.994	0.001	205	0.006	1.210	0.006	248.375
			220	2.26	10	2.2	0.844	0.996	0.000	215	0.002	0.508	0.004	191.238
			230	2.36	10	2.3	0.842	0.994	0.000	225	-0.002	-0.531	0.000	0.000
			240	2.47	10	2.4	0.845	0.998	0.000	235	0.004	0.832	0.001	32.639
			250	2.57	10	2.5	0.845	0.998	0.000	245	0.000	0.000	0.002	106.427
			260	2.67	10	2.6	0.845	0.998	0.000	255	0.000	0.000	0.000	0.000
			270	2.77	10	2.7	0.846	0.999	0.000	265	0.001	0.313	0.001	41.504
			280	2.88	10	2.8	0.846	0.999	0.000	275	0.000	0.000	0.001	44.696
			290	2.98	10	2.9	0.845	0.998	0.000	285	-0.001	-0.336	-0.001	-48.005
			300	3.08	10	3.0	0.847	1.000	0.000	295	0.002	0.697	0.001	51.433
									0.100			97.349	0.999	11379.728

Prototype 1 – 60 mL/min Modeling Data

PFR Open E(t) (2-71)	E avg delta t	CFSTR E(t) (2-87)	E avg delta t	PFR closed (figure 2-16)	PFR Closed E(t)	E avg delta t	PFR Open F(t)	CFSTR F(t)	PFR Closed F(t)
0.000		0.000		0.000	0.000		0.000	0.000	0.000
0.000	0.000	0.000	0.000	0.000	0.000	0.000	0.000	0.000	0.000
0.000	0.000	0.001	0.005	0.000	0.000	0.000	0.000	0.005	0.000
0.001	0.007	0.003	0.017	0.000	0.000	0.000	0.008	0.023	0.000
0.004	0.029	0.005	0.038	0.200	0.002	0.010	0.037	0.060	0.010
0.008	0.062	0.007	0.060	0.550	0.006	0.039	0.099	0.120	0.049
0.010	0.090	0.009	0.080	0.800	0.008	0.069	0.189	0.201	0.118
0.011	0.107	0.010	0.093	1.050	0.011	0.095	0.296	0.294	0.213
0.011	0.110	0.010	0.099	1.100	0.011	0.110	0.406	0.393	0.324
0.010	0.105	0.010	0.098	1.090	0.011	0.112	0.510	0.491	0.436
0.009	0.094	0.009	0.092	0.850	0.009	0.100	0.604	0.583	0.536
0.007	0.080	0.008	0.082	0.800	0.008	0.085	0.684	0.665	0.620
0.006	0.067	0.006	0.071	0.700	0.007	0.077	0.751	0.736	0.697
0.005	0.055	0.005	0.059	0.600	0.006	0.067	0.806	0.795	0.764
0.004	0.044	0.004	0.048	0.400	0.004	0.051	0.850	0.843	0.816
0.003	0.035	0.003	0.039	0.300	0.003	0.036	0.885	0.882	0.852
0.002	0.027	0.003	0.030	0.250	0.003	0.028	0.912	0.912	0.880
0.002	0.021	0.002	0.023	0.200	0.002	0.023	0.933	0.935	0.903
0.001	0.016	0.002	0.018	0.200	0.002	0.021	0.949	0.953	0.923
0.001	0.012	0.001	0.013	0.200	0.002	0.021	0.962	0.966	0.944
0.001	0.009	0.001	0.010	0.100	0.001	0.015	0.971	0.976	0.959
0.001	0.007	0.001	0.007	0.080	0.001	0.009	0.978	0.983	0.969
0.000	0.005	0.000	0.005	0.070	0.001	0.008	0.984	0.988	0.976
0.000	0.004	0.000	0.004	0.060	0.001	0.007	0.988	0.992	0.983
0.000	0.003	0.000	0.003	0.050	0.001	0.006	0.991	0.995	0.989
0.000	0.002	0.000	0.002	0.040	0.000	0.005	0.993	0.996	0.993
0.000	0.002	0.000	0.001	0.030	0.000	0.004	0.995	0.998	0.997
0.000	0.001	0.000	0.001	0.010	0.000	0.002	0.996	0.999	0.999
0.000	0.001	0.000	0.001	0.000	0.000	0.001	0.997	0.999	0.999
0.000	0.001	0.000	0.000	0.000	0.000	0.000	0.998	1.000	0.999
0.000	0.001	0.000	0.000	0.000	0.000	0.000	0.998	1.000	0.999
	0.998		1.000			0.999			

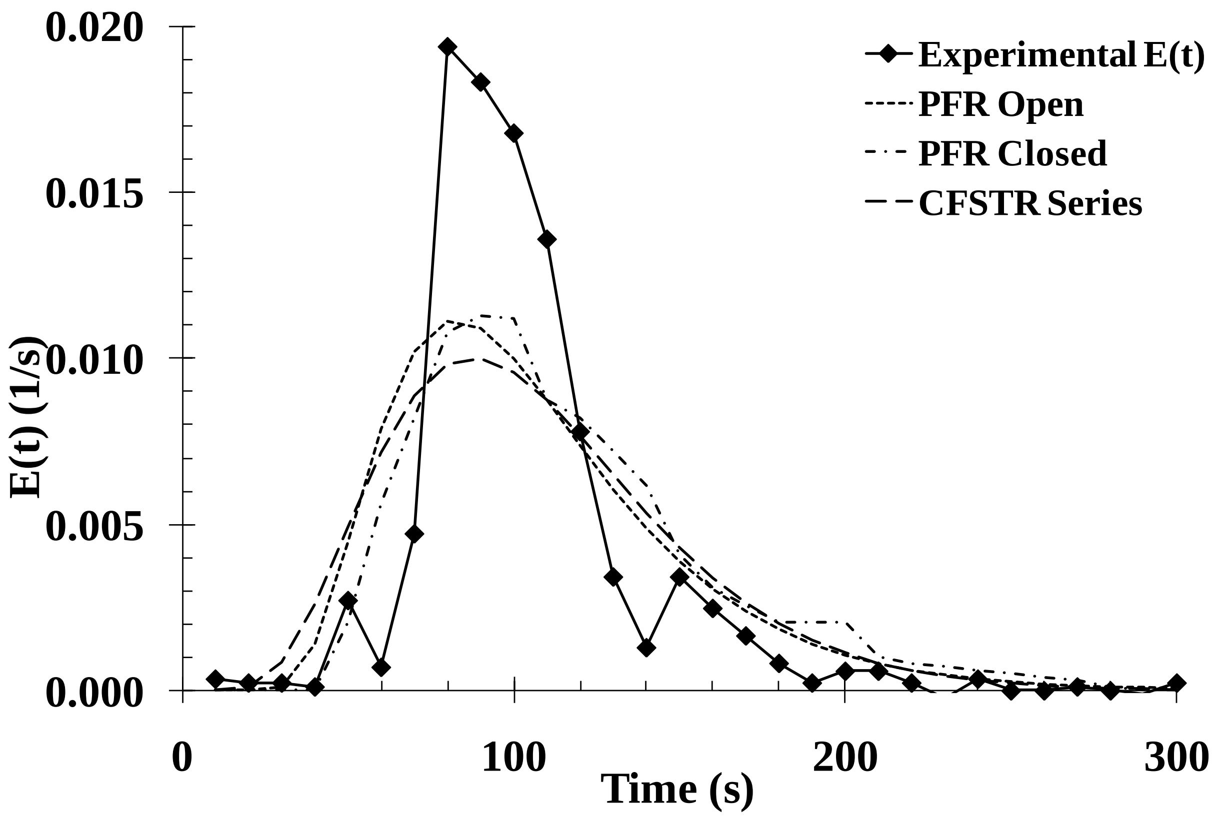
0.020
0.015
0.010
0.005
0.000
E(t) (1/s)
0
100
200
300
Time (s)
Experimental E(t)
PFR Open
PFR Closed
CFSTR Series

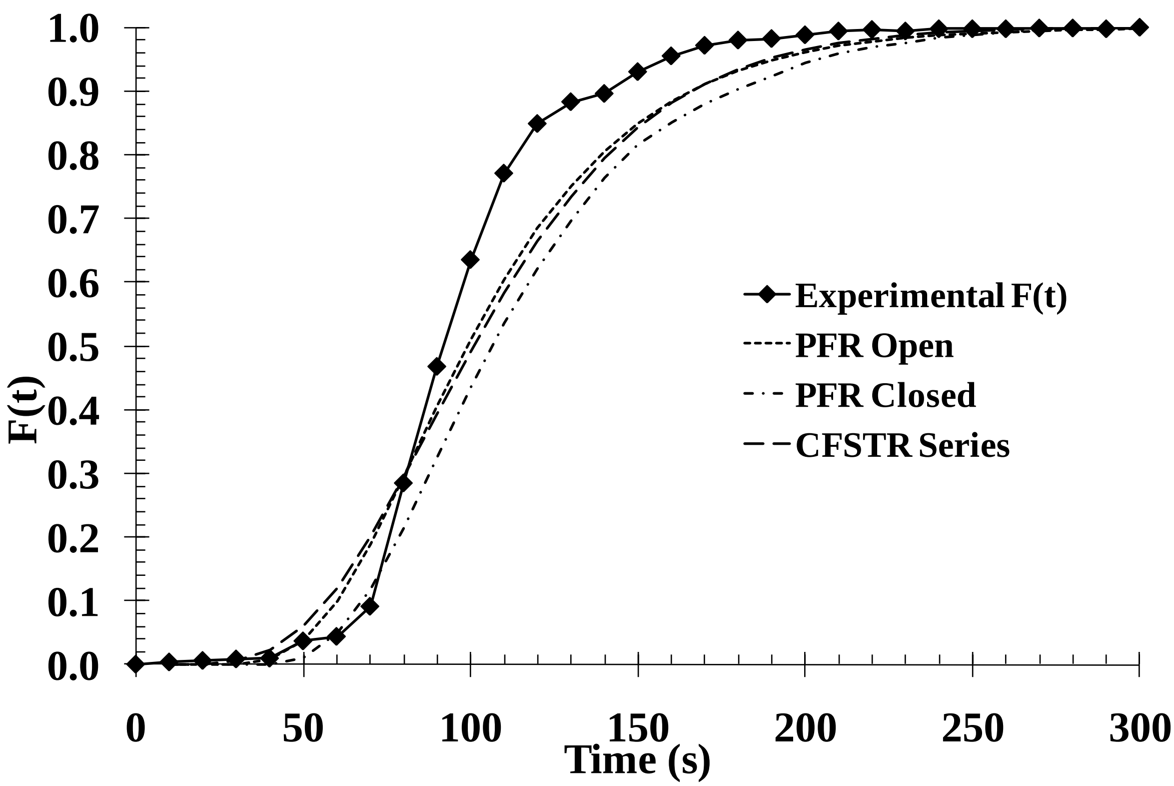
1.0
0.9
0.8
0.7
0.6
0.5
0.4
0.3
0.2
0.1
0.0
F(t)
0
50
100
150
200
250
300
Time (s)
Experimental F(t)
PFR Open
PFR Closed
CFSTR Series

Prototype 1 – 125 mL/min Tracer Data

Volume	100	mL	Time (s)	dimensionless time	delta t	t/tau	A_{254} (1/cm)	F(t)	E(t)	tavg	delta F(t)	tavg delta F(t)	Eave(t) delta t	Variance Calc
Input A_{254}	0.702	1/cm	0	0.00		0.0	0.000	0.000						
Flow Rate	125	mL/min	5	0.08	5	0.1	0.000	0.000	0.000	2.5	0.000	0.000	0.000	0.000
Theoretical Residence Time	48.00	s	10	0.16	5	0.2	0.003	0.004	0.001	7.5	0.004	0.032	0.002	0.120
Mean Hydraulic Detention Time	60.93	s	15	0.25	5	0.3	0.008	0.011	0.001	12.5	0.007	0.089	0.006	0.891
Variance	944	s^2	20	0.33	5	0.4	0.042	0.060	0.010	17.5	0.048	0.848	0.028	8.513
Non-dimensional Variance	0.254		25	0.41	5	0.5	0.051	0.073	0.003	22.5	0.013	0.288	0.031	15.516
Nd-cb	0.149	0.254	30	0.49	5	0.6	0.065	0.093	0.004	27.5	0.020	0.548	0.016	12.398
Nd-ob	0.133	0.254	35	0.57	5	0.7	0.084	0.120	0.005	32.5	0.027	0.880	0.024	24.844
tau-cb	60.93		40	0.66	5	0.8	0.106	0.151	0.006	37.5	0.031	1.175	0.029	41.095
tau-ob	48.14		45	0.74	5	0.9	0.135	0.192	0.008	42.5	0.041	1.756	0.036	65.658
N	3.93		50	0.82	5	1.0	0.191	0.272	0.016	47.5	0.080	3.789	0.061	136.694
Gamma Function (3.93)	5.5		55	0.90	5	1.1	0.262	0.373	0.020	52.5	0.101	5.310	0.090	249.497
			60	0.98	5	1.3	0.360	0.513	0.028	57.5	0.140	8.027	0.120	398.258
			65	1.07	5	1.4	0.491	0.699	0.037	62.5	0.187	11.663	0.163	637.585
			70	1.15	5	1.5	0.549	0.782	0.017	67.5	0.083	5.577	0.135	613.779
			75	1.23	5	1.6	0.575	0.819	0.007	72.5	0.037	2.685	0.060	314.701
			80	1.31	5	1.7	0.604	0.860	0.008	77.5	0.041	3.202	0.039	235.455
			85	1.40	5	1.8	0.617	0.879	0.004	82.5	0.019	1.528	0.030	203.751
			90	1.48	5	1.9	0.633	0.902	0.005	87.5	0.023	1.994	0.021	158.255
			95	1.56	5	2.0	0.641	0.913	0.002	92.5	0.011	1.054	0.017	146.365
			100	1.64	5	2.1	0.653	0.930	0.003	97.5	0.017	1.667	0.014	135.513
			105	1.72	5	2.2	0.663	0.944	0.003	102.5	0.014	1.460	0.016	164.745
			110	1.81	5	2.3	0.666	0.949	0.001	107.5	0.004	0.459	0.009	107.079
			115	1.89	5	2.4	0.671	0.956	0.001	112.5	0.007	0.801	0.006	72.167
			120	1.97	5	2.5	0.677	0.964	0.002	117.5	0.009	1.004	0.008	108.246
			125	2.05	5	2.6	0.680	0.969	0.001	122.5	0.004	0.524	0.006	96.262
			130	2.13	5	2.7	0.687	0.979	0.002	127.5	0.010	1.271	0.007	115.868
			135	2.22	5	2.8	0.687	0.979	0.000	132.5	0.000	0.000	0.005	87.594
			140	2.30	5	2.9	0.687	0.979	0.000	137.5	0.000	0.000	0.000	0.000
			145	2.38	5	3.0	0.690	0.983	0.001	142.5	0.004	0.609	0.002	43.420
			150	2.46	5	3.1	0.695	0.990	0.001	147.5	0.007	1.051	0.006	124.056
			155	2.54	5	3.2	0.696	0.991	0.000	152.5	0.001	0.217	0.004	99.457
			160	2.63	5	3.3	0.697	0.993	0.000	157.5	0.001	0.224	0.001	35.362
			165	2.71	5	3.4	0.698	0.994	0.000	162.5	0.001	0.231	0.001	37.643
			170	2.79	5	3.5	0.701	0.999	0.001	167.5	0.004	0.716	0.003	79.989
			175	2.87	5	3.6	0.702	1.000	0.000	172.5	0.001	0.246	0.003	84.836
												60.926	0.999	4655.609

Prototype 1 – 125 mL/min Modeling Data

PFR Open E(t) (2-71)	E avg delta t	CFSTR E(t) (2-87)	E avg delta t	PFR closed (figure 2-16)	PFR Closed E(t)	E avg delta t	PFR Open F(t)	CFSTR F(t)	PFR Closed F(t)
0.000		0.000		0.000	0.000		0.000	0.000	0.000
0.000	0.000	0.000	0.001	0.000	0.000	0.000	0.000	0.001	0.000
0.000	0.000	0.002	0.005	0.100	0.002	0.004	0.000	0.006	0.004
0.002	0.004	0.004	0.014	0.300	0.005	0.016	0.005	0.020	0.021
0.005	0.017	0.007	0.027	0.600	0.010	0.037	0.022	0.047	0.057
0.010	0.037	0.010	0.041	0.800	0.013	0.057	0.059	0.088	0.115
0.013	0.057	0.012	0.053	1.000	0.016	0.074	0.117	0.142	0.189
0.016	0.072	0.013	0.063	1.050	0.017	0.084	0.189	0.204	0.273
0.017	0.080	0.014	0.069	1.000	0.016	0.084	0.269	0.274	0.357
0.016	0.083	0.015	0.073	1.030	0.017	0.083	0.352	0.346	0.440
0.016	0.081	0.014	0.073	0.850	0.014	0.077	0.432	0.419	0.517
0.015	0.076	0.014	0.071	0.800	0.013	0.068	0.508	0.490	0.585
0.013	0.069	0.013	0.067	0.700	0.011	0.062	0.577	0.557	0.647
0.012	0.062	0.012	0.062	0.600	0.010	0.053	0.639	0.619	0.700
0.010	0.055	0.011	0.056	0.500	0.008	0.045	0.694	0.676	0.745
0.009	0.048	0.009	0.050	0.300	0.005	0.033	0.741	0.726	0.778
0.008	0.041	0.008	0.044	0.250	0.004	0.023	0.783	0.770	0.801
0.006	0.035	0.007	0.039	0.250	0.004	0.021	0.818	0.809	0.821
0.005	0.030	0.006	0.033	0.230	0.004	0.020	0.848	0.842	0.841
0.005	0.025	0.005	0.028	0.200	0.003	0.018	0.873	0.871	0.858
0.004	0.021	0.004	0.024	0.150	0.002	0.014	0.894	0.895	0.873
0.003	0.018	0.004	0.020	0.140	0.002	0.012	0.912	0.915	0.885
0.003	0.015	0.003	0.017	0.130	0.002	0.011	0.927	0.932	0.896
0.002	0.013	0.003	0.014	0.120	0.002	0.010	0.940	0.945	0.906
0.002	0.010	0.002	0.011	0.110	0.002	0.009	0.950	0.957	0.915
0.002	0.009	0.002	0.009	0.150	0.002	0.011	0.959	0.966	0.926
0.001	0.007	0.001	0.008	0.120	0.002	0.011	0.966	0.974	0.937
0.001	0.006	0.001	0.006	0.100	0.002	0.009	0.972	0.980	0.946
0.001	0.005	0.001	0.005	0.090	0.001	0.008	0.977	0.985	0.954
0.001	0.004	0.001	0.004	0.080	0.001	0.007	0.981	0.989	0.961
0.001	0.003	0.001	0.003	0.070	0.001	0.006	0.984	0.992	0.967
0.001	0.003	0.000	0.003	0.060	0.001	0.005	0.987	0.995	0.972
0.000	0.002	0.000	0.002	0.050	0.001	0.005	0.989	0.997	0.977
0.000	0.002	0.000	0.002	0.040	0.001	0.004	0.991	0.998	0.981
0.000	0.002	0.000	0.001	0.030	0.000	0.003	0.993	1.000	0.984
0.000	0.001	0.000	0.001	0.020	0.000	0.002	0.994	1.001	0.986
	0.994		1.001			0.986			

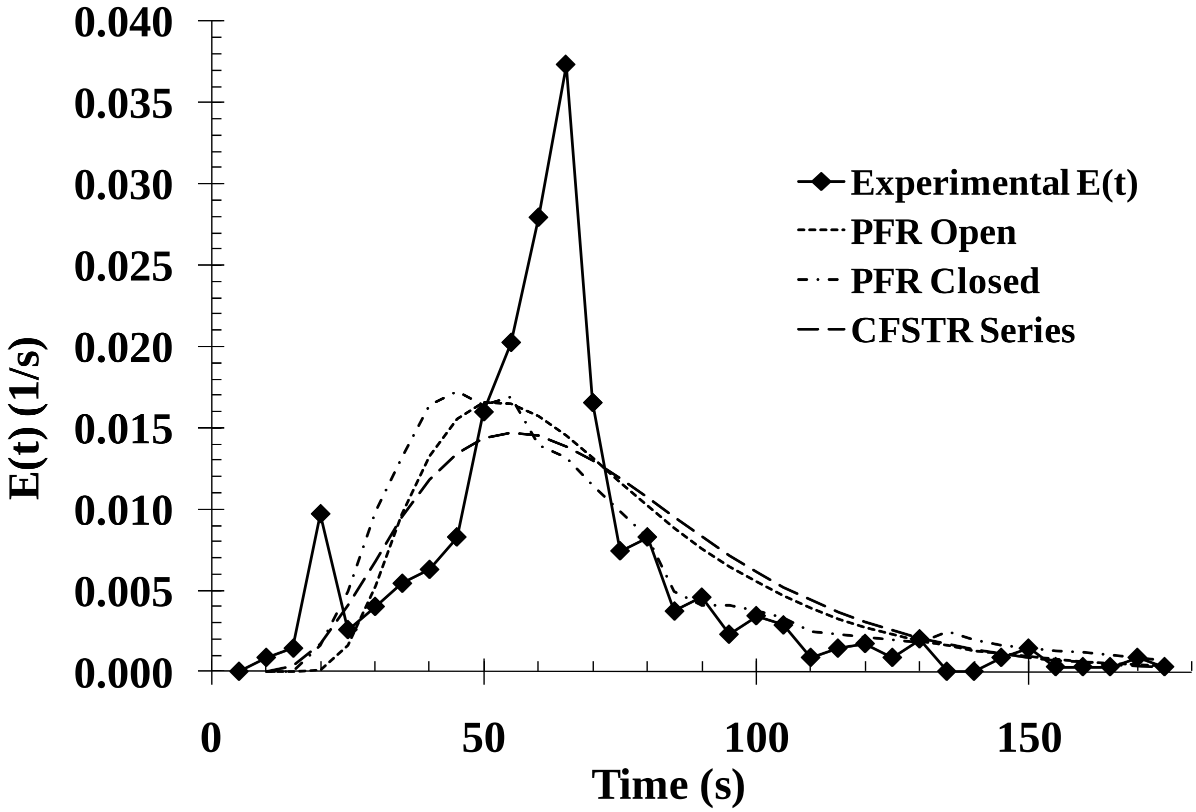
0.040
0.035
0.030
0.025
0.020
0.015
0.010
0.005
0.000
E(t) (1/s)
Experimental E(t)
PFR Open
PFR Closed
CFSTR Series
0
50
100
150
Time (s)

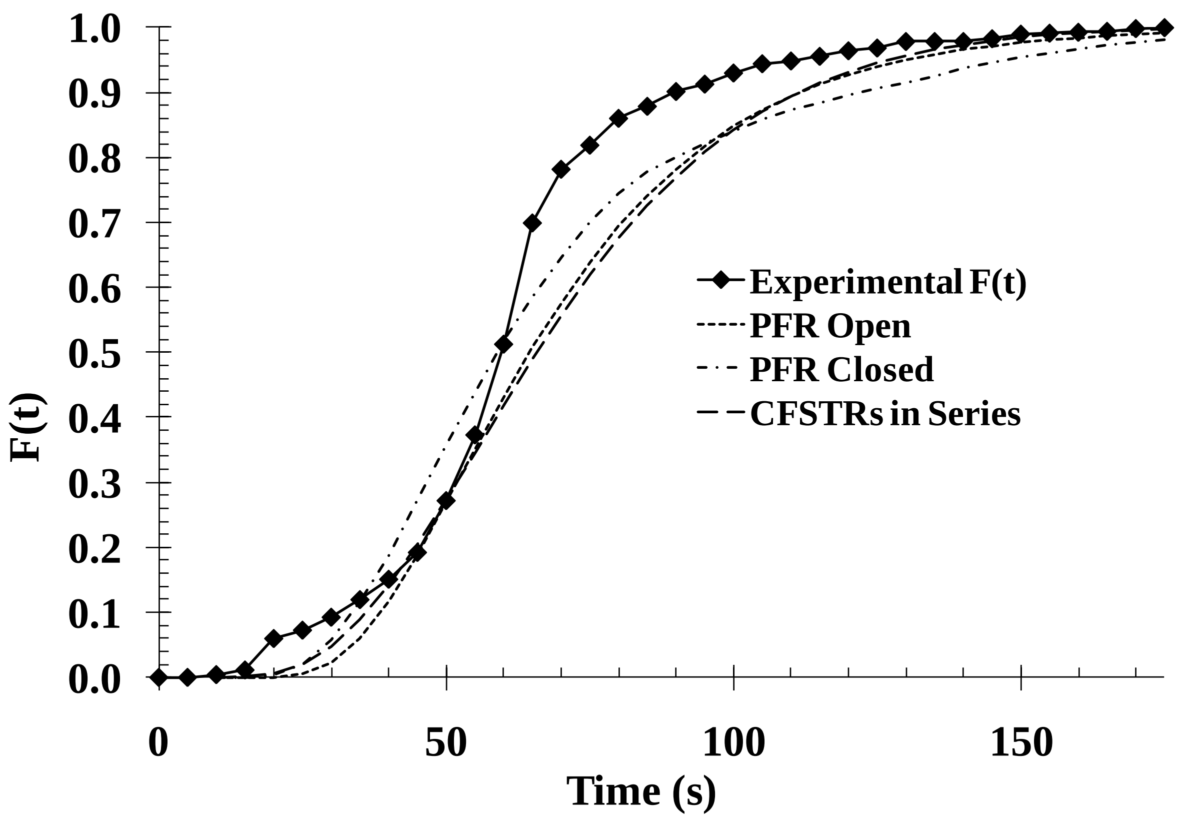
1.0
0.9
0.8
0.7
0.6
0.5
0.4
0.3
0.2
0.1
0.0
F(t)
Experimental F(t)
PFR Open
PFR Closed
CFSTRs in Series
0
50
100
150
Time (s)

Prototype 1 – 270 mL/min Tracer Data

Volume	100	mL	Time (s)	dimensionless time	delta t	t/tau	A_{254} (1/cm)	F(t)	E(t)	tavg	delta F(t)	tavg delta F(t)	Eave(t) delta t	Variance Calc
Input A_{254}	0.81	1/cm	0	0.00		0.00	0.000	0.000	0.000					
Flow Rate	270	mL/min	10	0.36	10	0.45	0.007	0.009	0.001	5	0.009	0.043	0.004	0.108
Theoretical Residence Time	22.22	s	15	0.54	5	0.68	0.092	0.114	0.021	12.5	0.105	1.312	0.055	8.560
Mean Hydraulic Detention Time	27.86	s	20	0.72	5	0.90	0.244	0.301	0.038	17.5	0.188	3.284	0.146	44.928
Variance	341	s^2	25	0.90	5	1.13	0.408	0.504	0.040	22.5	0.202	4.556	0.195	99.025
Non-dimensional Variance	0.439		30	1.08	5	1.35	0.533	0.658	0.031	27.5	0.154	4.244	0.178	135.287
Nd-cb	0.314	0.439	35	1.26	5	1.58	0.649	0.801	0.029	32.5	0.143	4.654	0.149	157.571
Nd-ob	0.246	0.439	40	1.44	5	1.80	0.709	0.875	0.015	37.5	0.074	2.778	0.109	153.203
tau-cb	27.86		45	1.62	5	2.03	0.738	0.911	0.007	42.5	0.036	1.522	0.055	99.509
tau-ob	18.67		50	1.79	5	2.25	0.755	0.932	0.004	47.5	0.021	0.997	0.028	64.245
N	2.28		55	1.97	5	2.48	0.773	0.954	0.004	52.5	0.022	1.167	0.022	59.714
Gamma Function (2.28)	1.15		60	2.15	5	2.70	0.782	0.965	0.002	57.5	0.011	0.639	0.017	55.258
			65	2.33	5	2.93	0.785	0.969	0.001	62.5	0.004	0.231	0.007	29.016
			70	2.51	5	3.15	0.789	0.974	0.001	67.5	0.005	0.333	0.004	19.742
			75	2.69	5	3.38	0.800	0.988	0.003	72.5	0.014	0.985	0.009	48.805
			80	2.87	5	3.60	0.803	0.991	0.001	77.5	0.004	0.287	0.009	52.050
			85	3.05	5	3.83	0.805	0.994	0.000	82.5	0.002	0.204	0.003	21.065
			90	3.23	5	4.05	0.808	0.998	0.001	87.5	0.004	0.324	0.003	23.696
			95	3.41	5	4.28	0.805	0.994	-0.001	92.5	-0.004	-0.343	0.000	0.000
			100	3.59	5	4.50	0.808	0.998	0.001	97.5	0.004	0.361	0.000	0.000
			105	3.77	5	4.73	0.806	0.995	0.000	102.5	-0.002	-0.253	0.001	6.503
			110	3.95	5	4.95	0.809	0.999	0.001	107.5	0.004	0.398	0.001	7.153
			115	4.13	5	5.18	0.810	1.000	0.000	112.5	0.001	0.139	0.002	31.337
												27.861	0.997	1116.777

Prototype 1 – 270 mL/min Modeling Data

PFR Open E(t) (2-71)	E avg delta t	CFSTR E(t) (2-87)	E avg delta t	PFR closed (figure 2-16)	PFR Closed E(t)	E avg delta t	PFR Open F(t)	CFSTR F(t)	PFR Closed F(t)
0.000		0.000		0.000	0.000		0.000	0.000	0.000
0.028	0.138	0.024	0.121	0.300	0.011	0.054	0.138	0.121	0.054
0.032	0.150	0.027	0.128	0.900	0.032	0.108	0.288	0.250	0.162
0.029	0.154	0.026	0.133	0.900	0.032	0.162	0.442	0.383	0.323
0.024	0.134	0.023	0.122	0.800	0.029	0.153	0.576	0.505	0.476
0.019	0.108	0.019	0.106	0.700	0.025	0.135	0.684	0.611	0.610
0.015	0.084	0.016	0.087	0.500	0.018	0.108	0.768	0.698	0.718
0.011	0.065	0.012	0.070	0.300	0.011	0.072	0.833	0.768	0.790
0.008	0.049	0.009	0.054	0.200	0.007	0.045	0.882	0.822	0.834
0.006	0.037	0.007	0.042	0.200	0.007	0.036	0.919	0.864	0.870
0.005	0.028	0.005	0.032	0.200	0.007	0.036	0.947	0.896	0.906
0.004	0.021	0.004	0.024	0.100	0.004	0.027	0.968	0.919	0.933
0.003	0.016	0.003	0.017	0.100	0.004	0.018	0.984	0.937	0.951
0.002	0.012	0.002	0.013	0.100	0.004	0.018	0.996	0.949	0.969
0.002	0.009	0.002	0.009	0.100	0.004	0.018	1.005	0.959	0.987
0.001	0.007	0.001	0.007	0.000	0.000	0.009	1.011	0.965	0.996
0.001	0.005	0.001	0.005	0.000	0.000	0.000	1.016	0.970	0.996
0.001	0.004	0.001	0.003	0.000	0.000	0.000	1.020	0.974	0.996
0.000	0.003	0.000	0.002	0.000	0.000	0.000	1.023	0.976	0.996
0.000	0.002	0.000	0.002	0.000	0.000	0.000	1.025	0.978	0.996
0.000	0.002	0.000	0.001	0.000	0.000	0.000	1.027	0.979	0.996
0.000	0.001	0.000	0.001	0.000	0.000	0.000	1.028	0.980	0.996
0.000	0.001	0.000	0.001	0.000	0.000	0.000	1.029	0.981	0.996
	1.029		0.981			0.996			

Prototype 2 – 0.58 L/min Tracer Data

Flow Rate	0.58	L/min	Initial Mass (g)	Final Mass (g)	Water Mass (g)	Cumulative Mass (g)	Cumulative Volume (L)	A(254) (1/cm)	Normalized absorbance (F(t))	Time (min)	Time (sec)	delta t	t/tau	E(t)	t avg	Δt (s)	Δ F(t)	t avg Δ F(t)	Eavg(t) Δt
Initial Absorbance (RO water)	0.0654	1/cm	0.000	0.000	0.000	0.000	0.000	0.065	0.067	0.000	0.000		0.000	0.000					
Initial Absorbance (LSA Water)	0.98	1/cm	24.380	63.136	39.656	39.656	0.040	0.001	0.001	0.068	4.091	4.091	0.214	0.000	2.045	4.091	-0.065	-0.134	0.000
Theoretical Residence Time	19.08	s	24.325	62.496	39.071	78.727	0.079	0.013	0.013	0.135	8.121	4.030	0.426	0.003	6.106	4.030	0.012	0.071	0.006
Mean Hydraulic Detention Time	18.07	s	24.267	63.483	40.116	118.842	0.119	0.144	0.147	0.204	12.259	4.138	0.642	0.032	10.190	4.138	0.134	1.368	0.073
Variance	174		23.998	63.157	40.059	158.901	0.159	0.456	0.466	0.273	16.391	4.132	0.859	0.077	14.325	4.132	0.318	4.560	0.226
Non-dimensional Variance	0.533	s^2	24.164	60.665	37.401	196.302	0.196	0.725	0.740	0.337	20.248	3.858	1.061	0.071	18.319	3.858	0.275	5.030	0.286
Nd-cb	0.440		24.003	59.987	36.884	233.186	0.233	0.818	0.835	0.401	24.053	3.805	1.260	0.025	22.151	3.805	0.095	2.102	0.183
Nd-ob	0.313		24.118	58.914	35.696	268.882	0.269	0.915	0.934	0.462	27.735	3.682	1.453	0.027	25.894	3.682	0.099	2.560	0.095
tau-cb	18.07		24.340	58.852	35.412	304.294	0.304	0.942	0.961	0.523	31.388	3.653	1.645	0.007	29.561	3.653	0.027	0.805	0.063
tau-ob	11.12		25.566	59.309	34.643	338.937	0.339	0.959	0.978	0.583	34.961	3.573	1.832	0.005	33.174	3.573	0.017	0.565	0.022
N	1.88		24.200	60.316	37.016	375.953	0.376	0.959	0.979	0.646	38.779	3.818	2.032	0.000	36.870	3.818	0.000	0.015	0.009
Gamma Function (1.88)	0.955		24.374	60.361	36.887	412.840	0.413	0.970	0.990	0.710	42.584	3.805	2.232	0.003	40.682	3.805	0.011	0.444	0.006
			24.067	60.168	37.001	449.841	0.450	0.965	0.985	0.773	46.401	3.817	2.432	-0.001	44.492	3.817	-0.005	-0.213	0.003
			24.864	62.427	38.463	488.304	0.488	0.968	0.988	0.839	50.368	3.967	2.639	0.001	48.384	3.967	0.003	0.153	-0.001
			24.162	63.706	40.444	528.747	0.529	0.977	0.997	0.909	54.540	4.172	2.858	0.002	52.454	4.172	0.009	0.471	0.006
			24.216	60.149	36.833	565.580	0.566	0.962	0.982	0.972	58.339	3.799	3.057	-0.004	56.440	3.799	-0.015	-0.847	-0.003
			23.083	61.050	38.867	604.447	0.604	0.961	0.981	1.039	62.348	4.009	3.267	0.000	60.344	4.009	-0.001	-0.068	-0.008
			23.372	62.147	39.675	644.121	0.644	0.960	0.980	1.107	66.441	4.092	3.482	0.000	64.394	4.092	-0.001	-0.079	-0.001
			23.563	61.946	39.283	683.404	0.683	0.961	0.981	1.175	70.493	4.052	3.694	0.000	68.467	4.052	0.001	0.084	0.000
			23.164	60.764	38.500	721.904	0.722	0.963	0.982	1.241	74.464	3.971	3.902	0.000	72.478	3.971	0.002	0.111	0.001

Prototype 2 – 0.58 L/min Modeling Data

PFR Open E(t) (2-71)	E avg delta t	CFSTR E(t) (2-87)	E avg delta t	PFR closed (figure 2-16)	PFR Closed E(t)	E avg delta t	PFR Open F(t)	CFSTR F(t)	PFR Closed F(t)
0.000		0.000		0.000	0.000		0.000	0.000	0.000
0.031	0.064	0.034	0.069	0.500	0.028	0.057	0.064	0.069	0.057
0.049	0.162	0.040	0.149	0.900	0.050	0.156	0.226	0.218	0.213
0.043	0.190	0.038	0.161	0.800	0.044	0.195	0.417	0.379	0.407
0.033	0.157	0.032	0.143	0.650	0.036	0.166	0.573	0.522	0.573
0.025	0.112	0.025	0.110	0.500	0.028	0.123	0.686	0.632	0.696
0.019	0.083	0.020	0.086	0.400	0.022	0.095	0.769	0.718	0.791
0.014	0.060	0.015	0.065	0.300	0.017	0.071	0.829	0.783	0.862
0.011	0.045	0.012	0.050	0.250	0.014	0.056	0.874	0.833	0.918
0.008	0.033	0.009	0.037	0.200	0.011	0.045	0.907	0.870	0.962
0.006	0.026	0.007	0.030	0.180	0.010	0.040	0.933	0.900	1.002
0.004	0.019	0.005	0.022	0.100	0.006	0.029	0.953	0.921	1.032
0.003	0.014	0.003	0.016	0.100	0.006	0.021	0.967	0.937	1.053
0.002	0.011	0.002	0.012	0.000	0.000	0.011	0.978	0.949	1.064
0.002	0.008	0.002	0.009	0.000	0.000	0.000	0.987	0.958	1.064
0.001	0.006	0.001	0.006	0.000	0.000	0.000	0.992	0.963	1.064
0.001	0.004	0.001	0.004	0.000	0.000	0.000	0.997	0.967	1.064
0.001	0.003	0.001	0.003	0.000	0.000	0.000	1.000	0.970	1.064
0.000	0.002	0.000	0.002	0.000	0.000	0.000	1.002	0.972	1.064
0.000	0.002	0.000	0.001	0.000	0.000	0.000	1.004	0.974	1.064

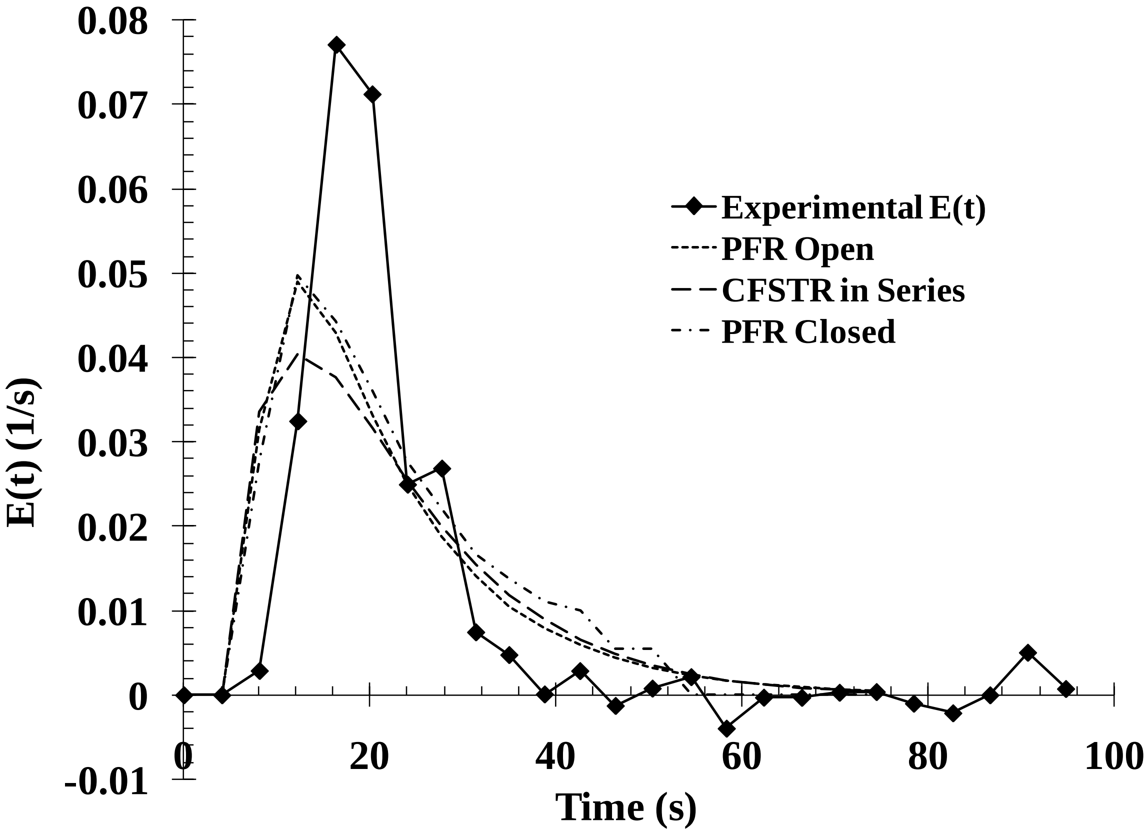
0.08
0.07
0.06
0.05
0.04
0.03
0.02
0.01
0
-0.01
E(t) (1/s)
0
20
40
60
80
100
Time (s)
Experimental E(t)
PFR Open
CFSTR in Series
PFR Closed

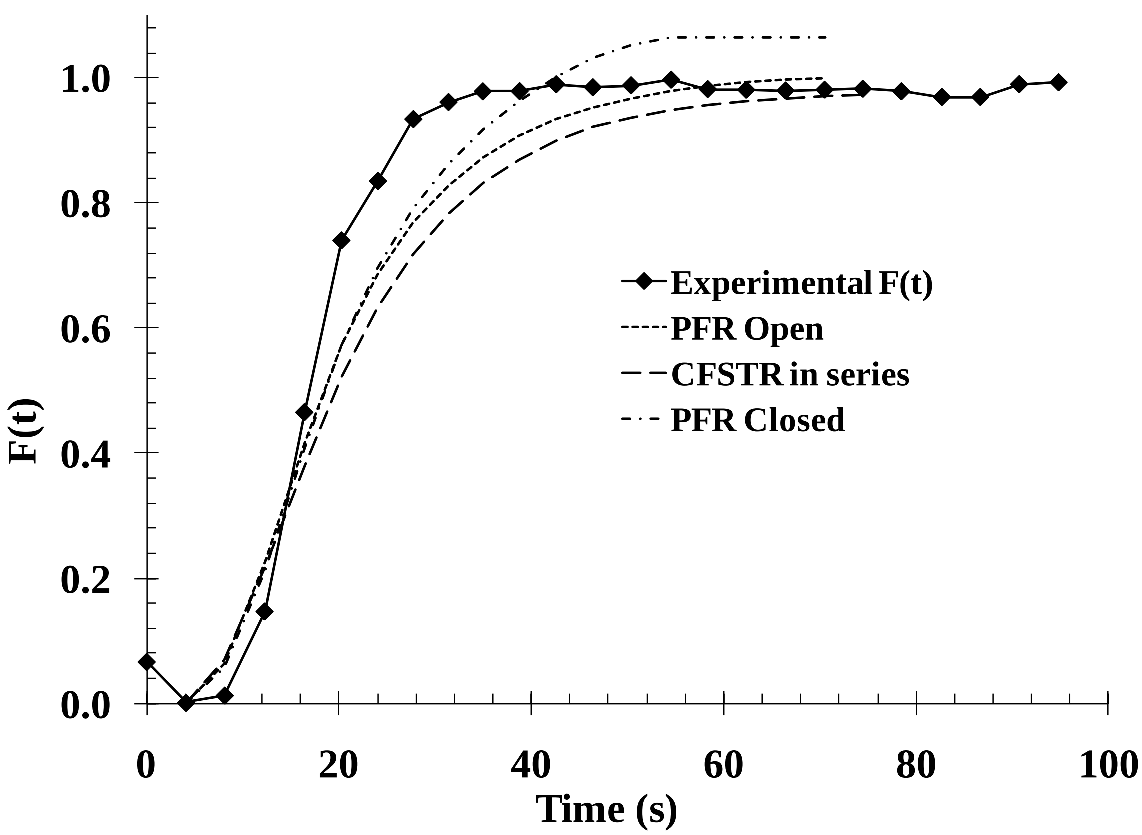
1.0
0.8
0.6
0.4
0.2
0.0
F(t)
0
20
40
60
80
100
Time (s)
Experimental F(t)
PFR Open
CFSTR in series
PFR Closed

Prototype 2 – 0.63 L/min Tracer Data

Flow Rate	0.63	L/min	Initial Mass (g)	Final Mass (g)	Water Mass (g)	Cumulative Mass (g)	Cumulative Volume (L)	A(254) (1/cm)	Normalized absorbance (F(t))	Time (min)	Time (sec)	delta t	t/tau	E(t)	t avg	Δt (s)	Δ F(t)	t avg Δ F(t)	Eavg(t) Δt	Variance Calc
Initial Absorbance (RO water)	0.017	1/cm	0.000	0.000	0.000	0.000	0.000	0.017	0.017	0.000	0.000		0.000	0.000						
Initial Absorbance (LSA Water)	0.91	s	24.380	61.977	38.497	38.497	0.038	0.020	0.022	0.061	3.668	3.668	0.207	0.001	1.834	3.668	0.005	0.010	0.003	0.009
Theoretical Residence Time	17.73	s	24.325	64.279	40.854	79.351	0.079	0.061	0.067	0.126	7.561	3.893	0.427	0.011	5.614	3.893	0.045	0.251	0.025	0.813
Mean Hydraulic Detention Time	15.51	s^2	24.267	63.168	39.801	119.152	0.119	0.274	0.301	0.189	11.353	3.792	0.640	0.062	9.457	3.792	0.234	2.210	0.139	12.696
Variance	151		23.998	61.632	38.534	157.686	0.158	0.554	0.608	0.250	15.025	3.672	0.848	0.084	13.189	3.672	0.308	4.057	0.267	47.540
Non-dimensional Variance	0.626		24.164	62.856	39.592	197.278	0.197	0.719	0.790	0.313	18.797	3.772	1.060	0.048	16.911	3.772	0.182	3.079	0.249	72.923
Nd-cb	0.624		24.003	60.011	36.908	234.185	0.234	0.824	0.905	0.372	22.314	3.517	1.259	0.033	20.556	3.517	0.115	2.365	0.142	61.602
Nd-ob	0.386		24.118	61.394	38.176	272.361	0.272	0.853	0.937	0.433	25.951	3.637	1.464	0.009	24.133	3.637	0.032	0.772	0.075	45.014
tau-cb	15.51		24.340	63.725	40.285	312.646	0.313	0.845	0.929	0.496	29.790	3.838	1.681	-0.002	27.871	3.838	-0.009	-0.245	0.012	9.923
tau-ob	8.75		25.566	62.381	37.715	350.360	0.350	0.881	0.968	0.556	33.383	3.594	1.883	0.011	31.587	3.594	0.039	1.246	0.016	15.946
N	1.60		24.200	62.744	39.444	389.804	0.390	0.880	0.967	0.619	37.142	3.758	2.095	0.000	35.263	3.758	-0.002	-0.054	0.020	25.284
Gamma Function (1.60)	0.894		24.374	60.884	37.410	427.214	0.427	0.880	0.967	0.678	40.706	3.565	2.296	0.000	38.924	3.565	0.000	0.009	-0.001	-0.961
			24.067	60.297	37.130	464.344	0.464	0.890	0.978	0.737	44.244	3.538	2.496	0.003	42.475	3.538	0.011	0.485	0.006	10.757
			24.864	65.169	41.205	505.549	0.506	0.900	0.989	0.803	48.170	3.926	2.717	0.003	46.207	3.926	0.011	0.493	0.012	25.513
			24.162	60.897	37.635	543.184	0.543	0.883	0.971	0.863	51.756	3.586	2.920	-0.005	49.963	3.586	-0.018	-0.911	-0.004	-10.870
			24.216	59.976	36.660	579.844	0.580	0.893	0.981	0.921	55.249	3.493	3.117	0.003	53.503	3.493	0.011	0.570	-0.004	-10.418
			23.083	62.124	39.941	619.785	0.620	0.893	0.981	0.984	59.055	3.806	3.332	0.000	57.152	3.806	0.000	0.000	0.006	19.419
			23.372	61.168	38.696	658.481	0.658	0.887	0.975	1.046	62.742	3.687	3.540	-0.002	60.898	3.687	-0.006	-0.395	-0.003	-12.309
			23.563	64.705	42.042	700.522	0.701	0.903	0.992	1.112	66.748	4.006	3.766	0.004	64.745	4.006	0.017	1.110	0.005	21.671
			23.164	63.292	41.028	741.550	0.742	0.909	0.999	1.178	70.657	3.909	3.986	0.002	68.703	3.909	0.007	0.461	0.012	56.620
																		15.512	0.977	391.170

Prototype 2 – 0.63 L/min Modeling Data

PFR Open E(t) (2-71)	E avg delta t	CFSTR E(t) (2-87)	E avg delta t	PFR closed (figure 2-16)	PFR Closed E(t)	E avg delta t	PFR Open F(t)	CFSTR F(t)	PFR Closed F(t)
0.000		0.000		0.000	0.000		0.000	0.000	0.000
0.048	0.087	0.044	0.081	0.600	0.039	0.071	0.087	0.081	0.071
0.055	0.200	0.046	0.175	0.850	0.055	0.182	0.287	0.255	0.253
0.044	0.187	0.039	0.161	0.800	0.052	0.202	0.474	0.416	0.455
0.033	0.140	0.032	0.131	0.550	0.035	0.160	0.614	0.547	0.614
0.024	0.106	0.025	0.107	0.400	0.026	0.116	0.720	0.653	0.730
0.018	0.073	0.019	0.077	0.250	0.016	0.074	0.793	0.730	0.804
0.013	0.056	0.014	0.061	0.200	0.013	0.053	0.849	0.791	0.856
0.009	0.043	0.010	0.048	0.100	0.006	0.037	0.892	0.839	0.893
0.007	0.029	0.008	0.033	0.100	0.006	0.023	0.921	0.871	0.917
0.005	0.023	0.006	0.025	0.100	0.006	0.024	0.943	0.896	0.941
0.004	0.016	0.004	0.017	0.100	0.006	0.023	0.959	0.914	0.964
0.003	0.012	0.003	0.013	0.100	0.006	0.023	0.971	0.926	0.987
0.002	0.010	0.002	0.010	0.000	0.000	0.013	0.980	0.936	0.999
0.002	0.006	0.002	0.006	0.000	0.000	0.000	0.987	0.943	0.999
0.001	0.005	0.001	0.005	0.000	0.000	0.000	0.991	0.947	0.999
0.001	0.004	0.001	0.004	0.000	0.000	0.000	0.995	0.951	0.999
0.001	0.003	0.001	0.002	0.000	0.000	0.000	0.998	0.953	0.999
0.000	0.002	0.000	0.002	0.000	0.000	0.000	1.000	0.955	0.999
0.000	0.002	0.000	0.001	0.000	0.000	0.000	1.001	0.956	0.999
	1.001		0.956			0.999			

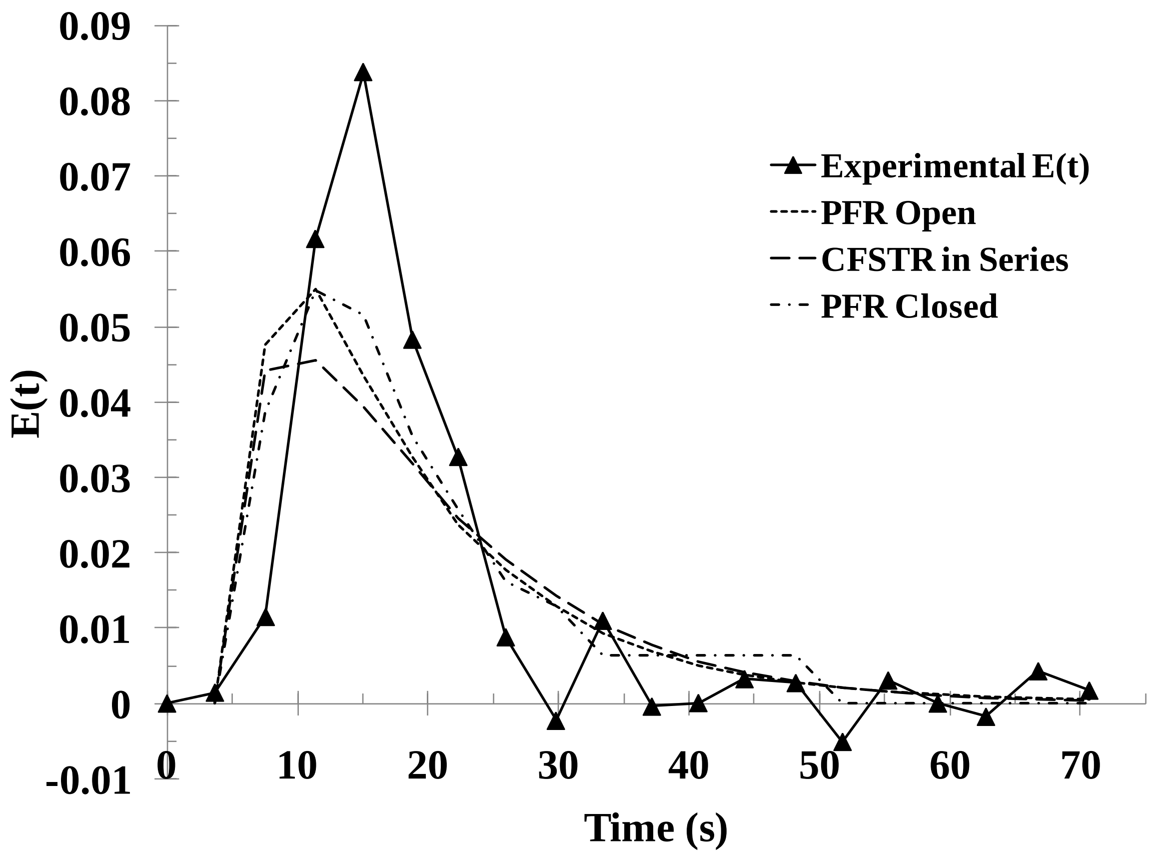
0.09
0.08
0.07
0.06
0.05
0.04
0.03
0.02
0.01
0
-0.01
E(t)
0
10
20
30
40
50
60
70
Time (s)
Experimental E(t)
PFR Open
CFSTR in Series
PFR Closed

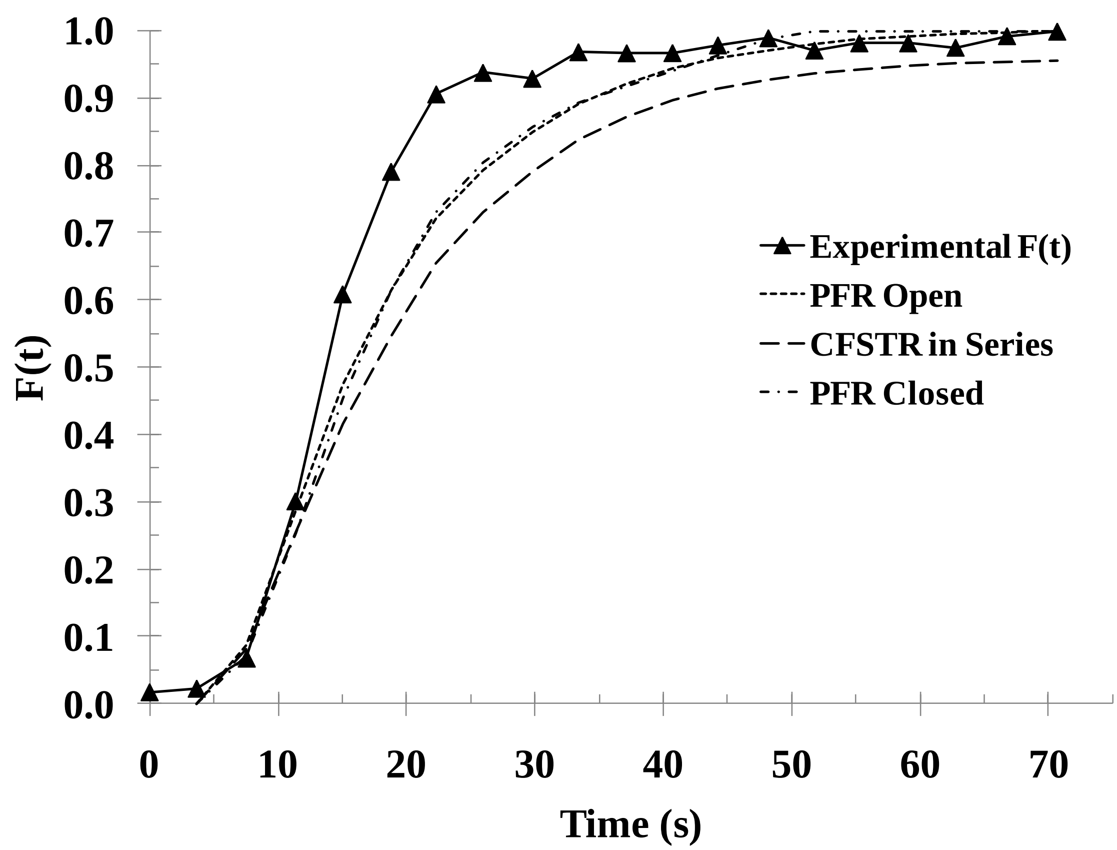
1.0
0.9
0.8
0.7
0.6
0.5
0.4
0.3
0.2
0.1
0.0
F(t)
0
10
20
30
40
50
60
70
Time (s)
Experimental F(t)
PFR Open
CFSTR in Series
PFR Closed

Prototype 2 – 0.78 L/min Tracer Data

Flow Rate	0.78	L/min	Initial Mass (g)	Final Mass (g)	Water Mass (g)	Cumulative Mass (g)	Cumulative Volume (L)	A(254) (1/cm)	Normalized Absorbance (F(t))	Time (min)	Time (sec)	t/tau	E(t)	t avg (s)	Δt (s)	Δ F(t)	t avg Δ F(t)	Eavg(t) Δt	Variance Calc
Initial Absorbance (RO water)	0.022	1/cm				0.000		0.022	0.024	0.000	0.000	0.000	0.000						
Initial Absorbance (LSA Water)	0.941	1/cm	24.380	61.507	38.027	38.027	0.038	0.027	0.029	0.049	2.929	0.206	0.002	1.465	2.929	0.005	0.008	0.003	0.006
Theoretical Residence Time	14.25	s	24.325	65.231	41.806	79.833	0.080	0.068	0.073	0.102	6.150	0.432	0.014	4.539	3.220	0.044	0.198	0.025	0.531
Mean Hydraulic Detention Time	12.34	s	24.267	63.191	39.824	119.657	0.120	0.280	0.297	0.154	9.217	0.647	0.073	7.683	3.068	0.225	1.726	0.133	8.168
Variance	81	s^2	23.998	63.403	40.305	159.962	0.160	0.544	0.578	0.205	12.322	0.865	0.091	10.770	3.105	0.281	3.027	0.254	30.656
Non-dimensional Variance	0.533		24.164	62.277	39.013	198.974	0.199	0.734	0.780	0.255	15.327	1.076	0.067	13.825	3.005	0.201	2.781	0.237	47.017
Nd-cb	0.442	0.534	24.003	65.194	42.091	241.065	0.241	0.978	0.941	0.309	18.570	1.303	0.050	16.948	3.242	0.161	2.736	0.189	56.510
Nd-ob	0.313	0.533	24.118	63.372	40.154	281.219	0.281	0.876	0.931	0.361	21.663	1.520	-0.003	20.116	3.093	-0.010	-0.205	0.072	30.248
tau-cb	12.34		24.340	61.919	38.479	319.698	0.320	0.908	0.965	0.410	24.627	1.728	0.011	23.145	2.964	0.034	0.785	0.012	6.723
tau-ob	7.59		25.566	62.711	38.045	357.744	0.358	0.921	0.979	0.459	27.557	1.934	0.005	26.092	2.931	0.014	0.377	0.024	16.977
N	1.88		24.200	60.789	37.489	395.233	0.395	0.917	0.974	0.507	30.445	2.136	-0.002	29.001	2.888	-0.005	-0.148	0.005	3.996
Gamma Function (1.88)	0.955		24.374	61.913	38.439	433.671	0.434	0.916	0.974	0.557	33.406	2.344	0.000	31.926	2.961	0.000	-0.007	-0.003	-2.884
			24.067	58.719	35.552	469.224	0.469	0.902	0.967	0.602	36.145	2.536	-0.003	34.776	2.739	-0.007	-0.238	-0.004	-4.435
			24.864	59.893	35.929	505.153	0.505	0.910	0.967	0.649	38.913	2.731	0.000	37.529	2.768	0.000	0.002	-0.003	-5.033
			24.162	60.908	37.646	542.799	0.543	0.910	0.967	0.697	41.813	2.934	0.000	40.363	2.900	0.000	0.000	0.000	0.050
			24.216	60.488	37.172	579.971	0.580	0.918	0.976	0.745	44.676	3.135	0.003	43.244	2.863	0.009	0.368	0.004	8.265
			23.083	61.870	39.687	619.658	0.620	0.919	0.977	0.796	47.733	3.350	0.000	46.205	3.057	0.001	0.064	0.005	11.606
			23.372	62.781	40.309	659.966	0.660	0.919	0.977	0.847	50.838	3.567	0.000	49.286	3.105	0.000	-0.010	0.001	1.503
			23.563	65.618	42.955	702.921	0.703	0.935	0.994	0.902	54.147	3.800	0.005	52.493	3.309	0.017	0.881	0.008	23.726
													0.313				12.344	0.962	233.631

Prototype 2 – 0.78 L/min Modeling Data

PFR Open E(t) (2-71)	E avg delta t	CFSTR E(t) (2-87)	E avg delta t	PFR closed (figure 2-16)	PFR Closed E(t)	E avg delta t	PFR Open F(t)	CFSTR F(t)	PFR Closed F(t)
0.000		0.000		0.000	0.000		0.000	0.000	0.000
0.049	0.072	0.050	0.074	0.150	0.012	0.018	0.072	0.074	0.018
0.071	0.194	0.059	0.176	0.800	0.065	0.124	0.265	0.249	0.142
0.058	0.199	0.053	0.171	0.750	0.061	0.193	0.464	0.420	0.334
0.043	0.158	0.042	0.147	0.650	0.053	0.176	0.622	0.568	0.510
0.031	0.111	0.032	0.112	0.600	0.049	0.152	0.733	0.680	0.663
0.021	0.085	0.023	0.091	0.400	0.032	0.131	0.818	0.771	0.794
0.015	0.056	0.017	0.062	0.300	0.024	0.088	0.875	0.833	0.882
0.011	0.038	0.012	0.043	0.150	0.012	0.054	0.913	0.876	0.936
0.008	0.027	0.008	0.030	0.100	0.008	0.030	0.940	0.906	0.965
0.005	0.019	0.006	0.021	0.100	0.008	0.023	0.958	0.927	0.989
0.004	0.014	0.004	0.015	0.000	0.000	0.012	0.972	0.941	1.001
0.003	0.009	0.003	0.010	0.000	0.000	0.000	0.981	0.951	1.001
0.002	0.007	0.002	0.007	0.000	0.000	0.000	0.988	0.958	1.001
0.001	0.005	0.001	0.005	0.000	0.000	0.000	0.993	0.963	1.001
0.001	0.004	0.001	0.003	0.000	0.000	0.000	0.997	0.966	1.001
0.001	0.003	0.001	0.002	0.000	0.000	0.000	1.000	0.969	1.001
0.001	0.002	0.000	0.002	0.000	0.000	0.000	1.002	0.970	1.001
0.000	0.001	0.000	0.001	0.000	0.000	0.000	1.003	0.972	1.001

Prototype 3 – 0.76 L/min Tracer Data

			Time (s)	delta t	t/tau	A_{254} (1/cm)	F(t)	E(t)	tavg	delta F(t)	tavg delta F(t)	Eave(t) delta t	Variance Calc
Volume	900	mL											
Input A_{254}	0.53		0			0.010	0.020	0.000					
Flow Rate	766	mL/min	10	10	0.142	0.019	0.037	0.002	5	0.017	0.085	0.008	0.218
Theoretical Residence Time	70.50		20	10	0.284	0.060	0.114	0.008	15	0.077	1.155	0.047	10.834
Mean Hydraulic Detention Time	60.90		30	10	0.426	0.125	0.236	0.012	25	0.123	3.071	0.100	63.999
Variance	2283		40	10	0.567	0.178	0.336	0.010	35	0.099	3.480	0.111	139.533
Non-dimensional Variance	0.615		50	10	0.709	0.244	0.460	0.012	45	0.124	5.595	0.112	232.223
Nd-cb	0.598	0.615	60	10	0.851	0.290	0.547	0.009	55	0.087	4.774	0.106	327.304
Nd-ob	0.377	0.615	70	10	0.993	0.343	0.647	0.010	65	0.100	6.475	0.093	403.626
tau-cb	60.90		80	10	1.135	0.381	0.719	0.007	75	0.072	5.434	0.086	496.036
tau-ob	34.71		90	10	1.277	0.417	0.787	0.007	85	0.068	5.806	0.070	521.161
N	1.62		100	10	1.419	0.446	0.842	0.005	95	0.054	5.144	0.061	566.353
Gamma Function (1.62)	0.9		110	10	1.560	0.469	0.885	0.004	105	0.044	4.616	0.049	554.342
			120	10	1.702	0.485	0.915	0.003	115	0.029	3.385	0.037	497.440
			130	10	1.844	0.497	0.937	0.002	125	0.022	2.759	0.026	412.456
			140	10	1.986	0.506	0.954	0.002	135	0.017	2.343	0.020	368.306
			150	10	2.128	0.514	0.969	0.002	145	0.015	2.189	0.016	349.671
			160	10	2.270	0.518	0.978	0.001	155	0.008	1.287	0.012	288.058
			170	10	2.411	0.521	0.983	0.001	165	0.006	0.934	0.007	194.803
			180	10	2.553	0.524	0.988	0.000	175	0.005	0.792	0.005	159.906
			190	10	2.695	0.524	0.989	0.000	185	0.002	0.279	0.003	105.898
			200	10	2.837	0.526	0.992	0.000	195	0.002	0.442	0.002	73.535
			210	10	2.979	0.526	0.992	0.000	205	0.000	0.077	0.001	56.889
			220	10	3.121	0.527	0.995	0.000	215	0.003	0.608	0.002	75.984
			230	10	3.263	0.528	0.996	0.000	225	0.001	0.170	0.002	93.007
											60.901	0.976	5991.583

Prototype 3 – 0.76 L/min Modeling Data

PFR Open E(t) (2-71)	E avg delta t	CFSTR E(t) (2-87)	E avg delta t	PFR closed (figure 2-16)	PFR Closed E(t)	E avg delta t	PFR Open F(t)	CFSTR F(t)	PFR Closed F(t)
0.000		0.000		0.000	0.000		0.000	0.000	0.000
0.008	0.038	0.010	0.050	0.300	0.005	0.025	0.038	0.050	0.025
0.014	0.109	0.012	0.108	0.750	0.012	0.086	0.148	0.158	0.111
0.014	0.141	0.012	0.117	0.850	0.014	0.131	0.289	0.275	0.242
0.012	0.131	0.011	0.111	0.800	0.013	0.135	0.420	0.386	0.378
0.010	0.111	0.009	0.100	0.700	0.011	0.123	0.531	0.486	0.501
0.008	0.091	0.008	0.087	0.600	0.010	0.107	0.622	0.573	0.608
0.007	0.074	0.007	0.074	0.400	0.007	0.082	0.697	0.646	0.690
0.005	0.060	0.006	0.062	0.350	0.006	0.062	0.757	0.708	0.751
0.004	0.048	0.005	0.051	0.300	0.005	0.053	0.805	0.760	0.805
0.003	0.039	0.004	0.042	0.200	0.003	0.041	0.844	0.802	0.846
0.003	0.031	0.003	0.034	0.200	0.003	0.033	0.875	0.836	0.878
0.002	0.025	0.002	0.028	0.150	0.002	0.029	0.900	0.864	0.907
0.002	0.020	0.002	0.023	0.130	0.002	0.023	0.920	0.887	0.930
0.001	0.016	0.002	0.018	0.100	0.002	0.019	0.936	0.905	0.949
0.001	0.013	0.001	0.015	0.080	0.001	0.015	0.949	0.920	0.964
0.001	0.011	0.001	0.012	0.050	0.001	0.011	0.960	0.931	0.975
0.001	0.009	0.001	0.009	0.030	0.000	0.007	0.969	0.940	0.981
0.001	0.007	0.001	0.007	0.020	0.000	0.004	0.975	0.948	0.985
0.001	0.006	0.001	0.006	0.010	0.000	0.002	0.981	0.953	0.988
0.000	0.005	0.000	0.005	0.010	0.000	0.002	0.986	0.958	0.989
0.000	0.004	0.000	0.004	0.010	0.000	0.002	0.989	0.962	0.991
0.000	0.003	0.000	0.003	0.010	0.000	0.002	0.992	0.965	0.993
0.000	0.002	0.000	0.002	0.010	0.000	0.002	0.995	0.967	0.994

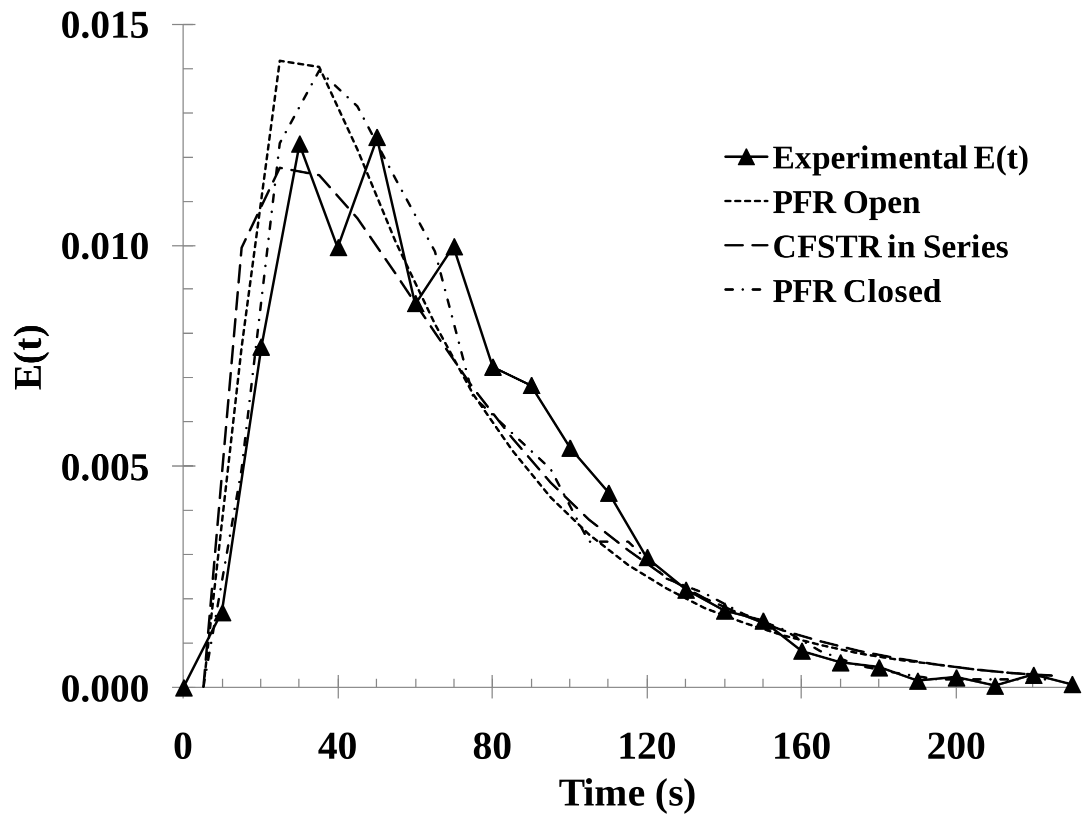
0.015
0.010
0.005
0.000
E(t)
0
40
80
120
160
200
Time (s)
Experimental E(t)
PFR Open
CFSTR in Series
PFR Closed

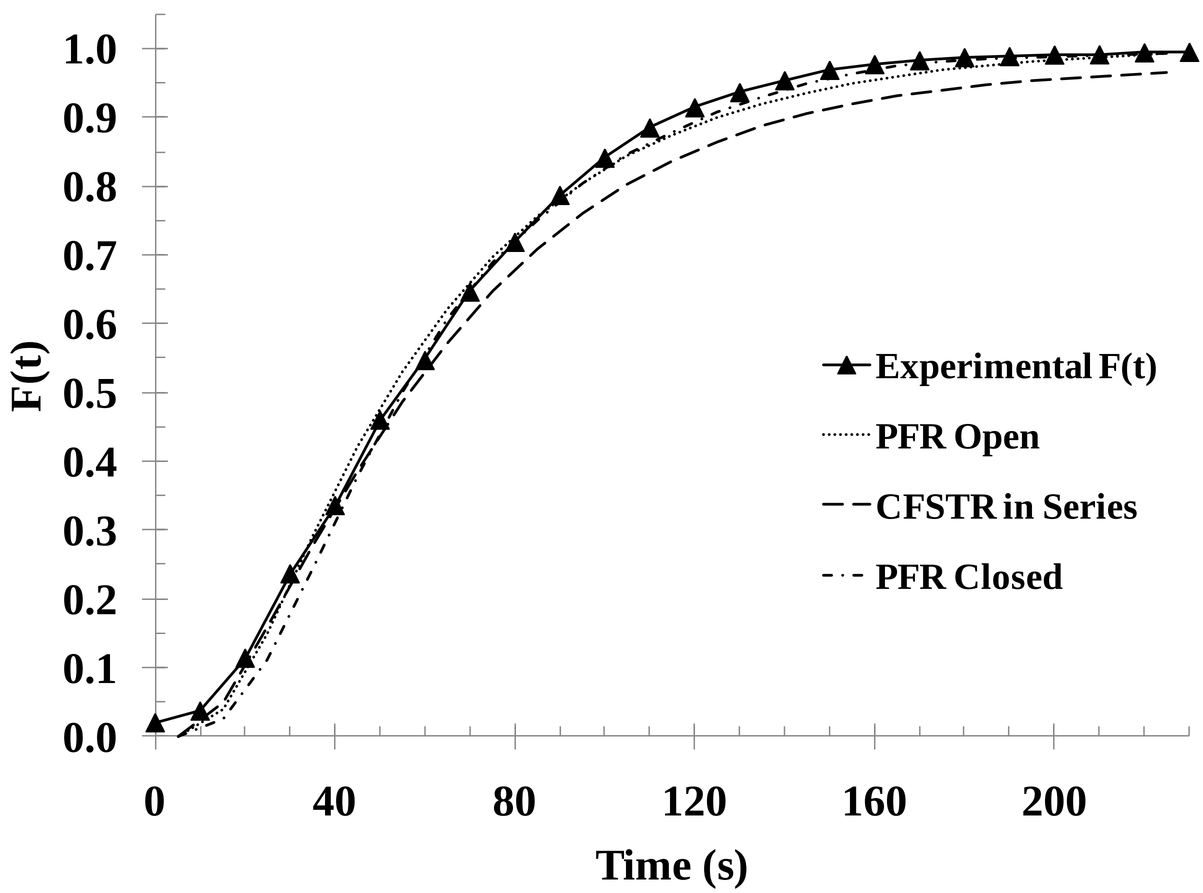
1.0
0.9
0.8
0.7
0.6
0.5
0.4
0.3
0.2
0.1
0.0
F(t)
0
40
80
120
160
200
Time (s)
Experimental F(t)
PFR Open
CFSTR in Series
PFR Closed

Prototype 3 – 1.07 L/min Tracer Data

Volume	900	mL	Time (s)	delta t	t/tau	A_{254} (1/cm)	F(t)	E(t)	tavg	delta F(t)	tavg delta F(t)	Eave(t) delta t	Variance Calc
Input A_{254}	0.51		0			0.005	0.009	0.000					
Flow Rate	1070	mL/min	10	10	0.198	0.048	0.095	0.009	5	0.086	0.428	0.043	1.079
Theoretical Residence Time	50.47		20	10	0.396	0.134	0.262	0.017	15	0.167	2.503	0.126	28.617
Mean Hydraulic Detention Time	38.86		30	10	0.594	0.229	0.450	0.019	25	0.188	4.701	0.177	111.706
Variance	1074		40	10	0.793	0.313	0.615	0.016	35	0.165	5.765	0.176	217.614
Non-dimensional Variance	0.711		50	10	0.991	0.376	0.737	0.012	45	0.122	5.506	0.144	292.742
Nd-cb	0.891	0.711	60	10	1.189	0.423	0.829	0.009	55	0.092	5.079	0.107	327.084
Nd-ob	0.461	0.710	70	10	1.387	0.453	0.888	0.006	65	0.059	3.824	0.076	321.662
tau-cb	38.86		80	10	1.585	0.463	0.907	0.002	75	0.019	1.412	0.039	219.957
tau-ob	20.21		90	10	1.783	0.486	0.952	0.005	85	0.045	3.850	0.032	233.295
N	1.41		100	10	1.981	0.495	0.970	0.002	95	0.018	1.676	0.031	286.069
Gamma Function (1.41)	0.887		110	10	2.180	0.503	0.987	0.002	105	0.017	1.812	0.017	193.784
			120	10	2.378	0.508	0.997	0.001	115	0.010	1.127	0.014	180.216
			130	10	2.576	0.509	0.998	0.000	125	0.002	0.196	0.006	89.488
			140	10	2.774	0.513	1.006	0.001	135	0.007	0.979	0.004	80.984
											38.859	0.993	2584.297

Prototype 3 – 1.07 L/min Modeling Data

PFR Open E(t) (2-71)	E avg delta t	CFSTR E(t) (2-87)	E avg delta t	PFR closed (figure 2-16)	PFR Closed E(t)	E avg delta t	PFR Open F(t)	CFSTR F(t)	PFR Closed F(t)
0.000		0.000		0.000	0.000		0.000	0.000	0.000
0.022	0.110	0.019	0.094	0.900	0.023	0.116	0.110	0.094	0.116
0.021	0.214	0.017	0.181	0.800	0.021	0.219	0.324	0.275	0.335
0.015	0.181	0.014	0.158	0.600	0.015	0.180	0.505	0.433	0.515
0.011	0.134	0.011	0.127	0.400	0.010	0.129	0.638	0.560	0.643
0.008	0.097	0.008	0.098	0.350	0.009	0.097	0.735	0.658	0.740
0.006	0.070	0.006	0.074	0.300	0.008	0.084	0.805	0.732	0.823
0.004	0.051	0.005	0.055	0.200	0.005	0.064	0.856	0.788	0.888
0.003	0.037	0.003	0.041	0.150	0.004	0.045	0.893	0.829	0.933
0.002	0.027	0.003	0.030	0.100	0.003	0.032	0.920	0.859	0.965
0.002	0.020	0.002	0.022	0.100	0.003	0.026	0.940	0.881	0.991
0.001	0.015	0.001	0.016	0.000	0.000	0.013	0.954	0.897	1.004
0.001	0.011	0.001	0.011	0.000	0.000	0.000	0.965	0.908	1.004
0.001	0.008	0.001	0.008	0.000	0.000	0.000	0.973	0.916	1.004
0.000	0.006	0.000	0.006	0.000	0.000	0.000	0.979	0.922	1.004

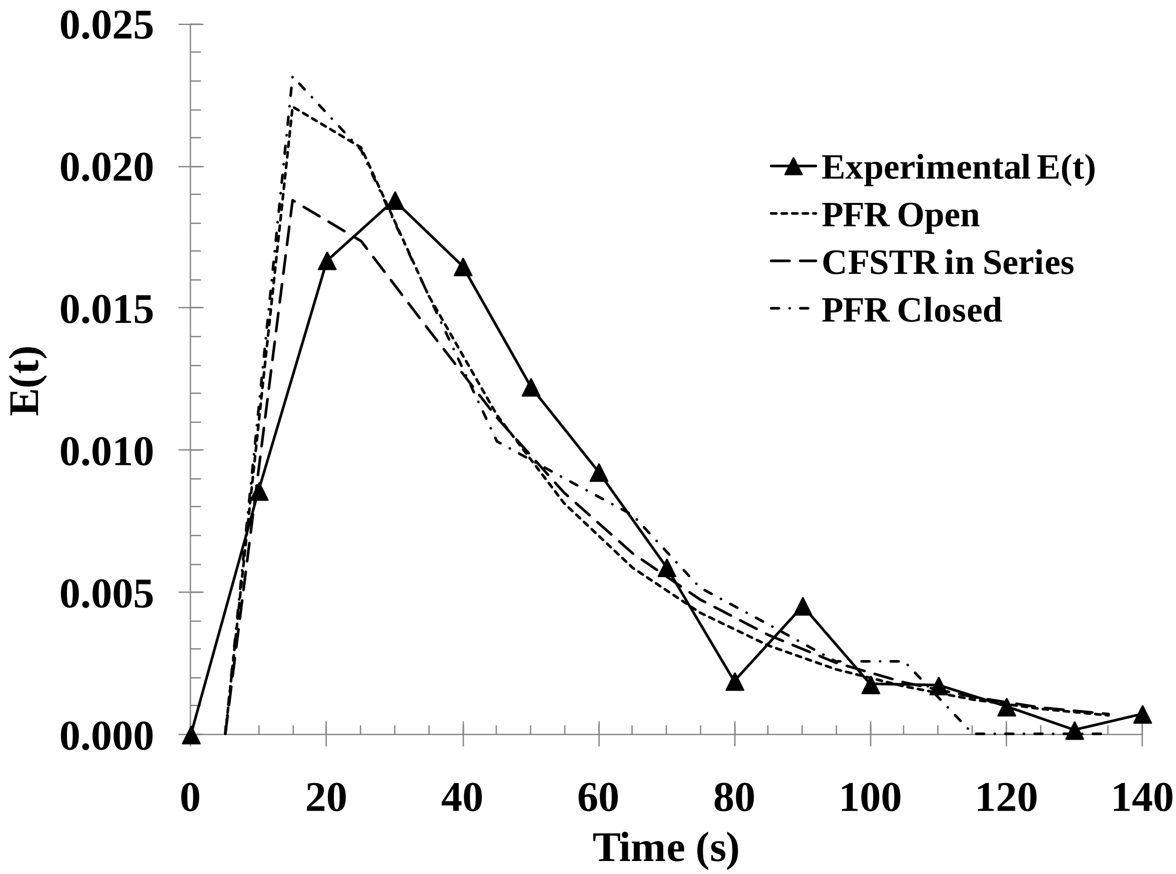
0.025
0.020
0.015
0.010
0.005
0.000
E(t)
0
20
40
60
80
100
120
140
Time (s)
Experimental E(t)
PFR Open
CFSTR in Series
PFR Closed

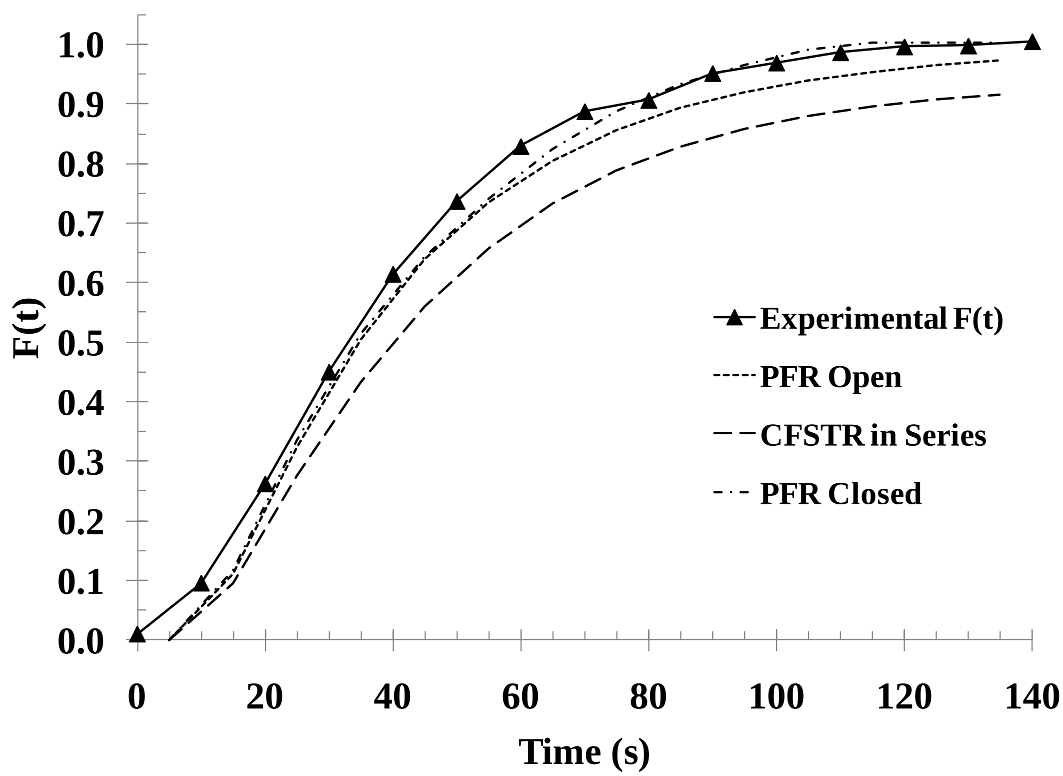
1.0
0.9
0.8
0.7
0.6
0.5
0.4
0.3
0.2
0.1
0.0
F(t)
0
20
40
60
80
100
120
140
Time (s)
Experimental F(t)
PFR Open
CFSTR in Series
PFR Closed

Prototype 3 – 1.21 L/min Tracer Data

Volume	900	mL	Time (s)	delta t	t/tau	A_{254} (1/cm)	F(t)	E(t)	tavg	delta F(t)	tavg delta F(t)	Eave(t) delta t	Variance Calc
Input A_{254}	0.51		0			0.000	0.000	0.000					
Flow Rate	1210	mL/min	10	10	0.224	0.078	0.153	0.015	5	0.153	0.766	0.077	1.908
Theoretical Residence Time	44.63	s	20	10	0.448	0.182	0.357	0.020	15	0.204	3.059	0.179	40.043
Mean Hydraulic Detention Time	34.20		30	10	0.672	0.282	0.552	0.019	25	0.195	4.873	0.199	124.243
Variance	875		40	10	0.896	0.348	0.683	0.013	35	0.131	4.584	0.163	198.979
Non-dimensional Variance	0.748		50	10	1.120	0.402	0.788	0.011	45	0.105	4.738	0.118	238.480
Nd-cb	1.060	0.748	60	10	1.344	0.440	0.862	0.007	55	0.074	4.055	0.090	269.920
Nd-ob	0.498	0.748	70	10	1.569	0.464	0.910	0.005	65	0.048	3.148	0.061	257.249
tau-cb	34.20		80	10	1.793	0.488	0.957	0.005	75	0.047	3.500	0.048	266.627
tau-ob	17.14		90	10	2.017	0.500	0.981	0.002	85	0.024	2.050	0.035	254.909
N	1.34		100	10	2.241	0.502	0.984	0.000	95	0.003	0.279	0.014	121.721
Gamma Function (1.34)	0.892		110	10	2.465	0.508	0.996	0.001	105	0.012	1.297	0.008	84.045
			120	10	2.689	0.508	0.995	0.000	115	-0.001	-0.158	0.005	72.381
			130	10	2.913	0.516	1.011	0.002	125	0.016	2.010	0.007	114.530
								0.101			34.201	1.003	2045.035

Prototype 3 – 1.21 L/min Modeling Data

PFR Open E(t) (2-71)	E avg delta t	CFSTR E(t) (2-87)	E avg delta t	PFR closed (figure 2-16)	PFR Closed E(t)	E avg delta t	PFR Open F(t)	CFSTR F(t)	PFR Closed F(t)
0.000		0.000		0.000	0.000		0.000	0.000	0.000
0.026	0.132	0.022	0.108	0.850	0.025	0.124	0.132	0.108	0.124
0.021	0.238	0.018	0.200	0.750	0.022	0.234	0.370	0.308	0.358
0.015	0.182	0.014	0.164	0.550	0.016	0.190	0.551	0.472	0.548
0.010	0.127	0.011	0.125	0.350	0.010	0.132	0.678	0.597	0.680
0.007	0.088	0.008	0.092	0.300	0.009	0.095	0.767	0.689	0.775
0.005	0.062	0.006	0.067	0.250	0.007	0.080	0.828	0.756	0.855
0.004	0.043	0.004	0.048	0.150	0.004	0.058	0.872	0.804	0.914
0.003	0.031	0.003	0.034	0.100	0.003	0.037	0.902	0.838	0.950
0.002	0.022	0.002	0.024	0.100	0.003	0.029	0.924	0.862	0.980
0.001	0.015	0.001	0.017	0.000	0.000	0.015	0.940	0.879	0.994
0.001	0.011	0.001	0.012	0.000	0.000	0.000	0.951	0.891	0.994
0.001	0.008	0.001	0.008	0.000	0.000	0.000	0.959	0.899	0.994
0.000	0.006	0.000	0.006	0.000	0.000	0.000	0.964	0.905	0.994

APPENDIX B: COLLIMATED BEAM TESTING DATA

T1 Bacteriophage Data

Trial	Dose	Dilution	Count	Sample Volume (mL)	Concentration (PFU/mL)	log N	log N average
A	Blank	0	0	0.1	0.00E+00		
B	Blank	0	0	0.1	0.00E+00		
C	Blank	0	0	0.1	0.00E+00		
D	Blank	0	0	0.1	0.00E+00		
1A	0	4	47	0.1	4.70E+06	6.67	6.55
1B	0	4	28	0.1	2.80E+06	6.45	
1C	0	4	34	0.1	3.40E+06	6.53	
2A	0	4	40	0.1	4.00E+06	6.60	6.58
2B	0	4	33	0.1	3.30E+06	6.52	
2C	0	4	43	0.1	4.30E+06	6.63	
Low Pressure							
1A	5	2	257	0.1	2.57E+05	5.41	5.39
1B	5	2	239	0.1	2.39E+05	5.38	
1C	5	2	235	0.1	2.35E+05	5.37	
2A	5	2	217	0.1	2.17E+05	5.34	5.39
2B	5	2	265	0.1	2.65E+05	5.42	
2C	5	2	264	0.1	2.64E+05	5.42	
1A	10	1	296	0.1	2.96E+04	4.47	4.54
1B	10	1	342	0.1	3.42E+04	4.53	
1C	10	1	413	0.1	4.13E+04	4.62	
2A	10	1	409	0.1	4.09E+04	4.61	4.49
2B	10	1	422	0.1	4.22E+04	4.63	
2C	10	1	175	0.1	1.75E+04	4.24	
1A	15	0	394	0.1	3.94E+03	3.60	3.53
1B	15	0	310	0.1	3.10E+03	3.49	
1C	15	0	312	0.1	3.12E+03	3.49	
2A	15	0	277	0.1	2.77E+03	3.44	3.43
2B	15	0	302	0.1	3.02E+03	3.48	
2C	15	0	229	0.1	2.29E+03	3.36	
1A	20	0	33	0.1	3.30E+02	2.52	2.52
1B	20	0	44	0.1	4.40E+02	2.64	
1C	20	0	25	0.1	2.50E+02	2.40	
2A	20	0	53	0.1	5.30E+02	2.72	2.71
2B	20	0	45	0.1	4.50E+02	2.65	
2C	20	0	55	0.1	5.50E+02	2.74	

MS2 Bacteriophage Data

Trial	Dose	Dilution	Count	Sample Volume (mL)	Concentration (PFU/mL)	log N	log N average
A	Blank	0	0	0.1	0.00E+00		
B	Blank	0	0	0.1	0.00E+00		
C	Blank	0	0	0.1	0.00E+00		
D	Blank	0	0	0.1	0.00E+00		
1A	0	4	48	0.1	4.80E+06	6.68	6.69
1B	0	4	56	0.1	5.60E+06	6.75	
1C	0	4	45	0.1	4.50E+06	6.65	
2A	0	4	61	0.1	6.10E+06	6.79	6.73
2B	0	4	56	0.1	5.60E+06	6.75	
2C	0	4	45	0.1	4.50E+06	6.65	
Low Pressure							
1A	15	3	88	0.1	8.80E+05	5.94	5.94
1B	15	3	83	0.1	8.30E+05	5.92	
1C	15	3	88	0.1	8.80E+05	5.94	
2A	15	3	84	0.1	8.40E+05	5.92	5.90
2B	15	3	76	0.1	7.60E+05	5.88	
2C	15	3	81	0.1	8.10E+05	5.91	
1A	30	2	192	0.1	1.92E+05	5.28	5.29
1B	30	2	190	0.1	1.90E+05	5.28	
1C	30	2	208	0.1	2.08E+05	5.32	
2A	30	2	169	0.1	1.69E+05	5.23	5.27
2B	30	2	183	0.1	1.83E+05	5.26	
2C	30	2	205	0.1	2.05E+05	5.31	
1A	45	1	176	0.1	1.76E+04	4.25	4.25
1B	45	1	154	0.1	1.54E+04	4.19	
1C	45	1	203	0.1	2.03E+04	4.31	
2A	45	1	213	0.1	2.13E+04	4.33	4.33
2B	45	1	229	0.1	2.29E+04	4.36	
2C	45	1	200	0.1	2.00E+04	4.30	

APPENDIX C: BIODOSEMETRY DATA

Prototype 2 98.5% UVT

Trial	Flow Rate (L/min)	Dilution	Count	Sample Volume (mL)	Concentration (PFU/mL)	log N	Logi	log N average	Dose
A	Blank	0	0	0.1	0.00E+00				
B	Blank	0	0	0.1	0.00E+00				
C	Blank	0	0	0.1	0.00E+00				
D	Blank	0	0	0.1	0.00E+00				
1A	0	4	40	0.1	4.00E+06	6.60			
1B	0	4	33	0.1	3.30E+06	6.52		6.58	
1C	0	4	43	0.1	4.30E+06	6.63			
2A	0	4	46	0.1	4.60E+06	6.66			
2B	0	4	45	0.1	4.50E+06	6.65		6.66	
2C	0	4	45	0.1	4.50E+06	6.65			
Reactor (A_{254}=.0067)									
1A	1.23	2	189	0.1	1.89E+05	5.28	1.31		6.46
1B	1.23	2	185	0.1	1.85E+05	5.27	1.32	5.30	6.51
1C	1.23	2	232	0.1	2.32E+05	5.37	1.22		6.02
2A	1.23	2	183	0.1	1.83E+05	5.26	1.39		6.88
2B	1.23	2	222	0.1	2.22E+05	5.35	1.31	5.32	6.47
2C	1.23	2	228	0.1	2.28E+05	5.36	1.30		6.41
1A	1.03	2	150	0.1	1.50E+05	5.18	1.41		6.96
1B	1.03	2	155	0.1	1.55E+05	5.19	1.39	5.17	6.89
1C	1.03	2	137	0.1	1.37E+05	5.14	1.45		7.15
2A	1.03	2	156	0.1	1.56E+05	5.19	1.46		7.23
2B	1.03	2	175	0.1	1.75E+05	5.24	1.41	5.24	6.98
2C	1.03	2	188	0.1	1.88E+05	5.27	1.38		6.83
1A	0.772	2	42	0.1	4.20E+04	4.62	1.96		9.69
1B	0.772	2	37	0.1	3.70E+04	4.57	2.02	4.62	9.96
1C	0.772	2	47	0.1	4.70E+04	4.67	1.91		9.44
2A	0.772	2	52	0.1	5.20E+04	4.72	1.94		9.58
2B	0.772	2	40	0.1	4.00E+04	4.60	2.05	4.68	10.14
2C	0.772	2	51	0.1	5.10E+04	4.71	1.95		9.62

Flow Rate	log N average	logi LP	Dose	Standard Deviation	Critical t	90% Confidence
0	6.58	0.00	0.00	0.00	0.00	0.00
1.23	5.30	1.28	6.33	0.27	2.92	0.55
1.03	5.17	1.42	7.00	0.14	2.92	0.28
0.772	4.62	1.96	9.70	0.26	2.92	0.53
0	6.66	0.00	0.00	0.00	0.00	0.00
1.23	5.32	1.33	6.59	0.51	2.92	1.06
1.03	5.24	1.42	7.01	0.40	2.92	0.83
0.772	4.68	1.98	9.78	0.63	2.92	1.29

Prototype 2 89.3% UVT

Trial	Flow Rate	Dilution	Count	Sample Volume (mL)	Concentration (PFU/mL)	log N	Logi	log N average	Dose
A	Blank	0	0	0.1	0.00E+00				
B	Blank	0	0	0.1	0.00E+00				
C	Blank	0	0	0.1	0.00E+00				
D	Blank	0	0	0.1	0.00E+00				
1A	0	4	49	0.1	4.90E+06	6.69			
1B	0	4	65	0.1	6.50E+06	6.81		6.74	
1C	0	4	53	0.1	5.30E+06	6.72			
2A	0	4	43	0.1	4.30E+06	6.63			
2B	0	4	51	0.1	5.10E+06	6.71		6.66	
2C	0	4	45	0.1	4.50E+06	6.65			
Reactor (A_{254}=.0490)									
1A	1.23	3	72	0.1	7.20E+05	5.86	0.89		4.37
1B	1.23	3	80	0.1	8.00E+05	5.90	0.84	5.87	4.15
1C	1.23	3	71	0.1	7.10E+05	5.85	0.89		4.40
2A	1.23	3	64	0.1	6.40E+05	5.81	0.86		4.24
2B	1.23	3	73	0.1	7.30E+05	5.86	0.80	5.84	3.96
2C	1.23	3	71	0.1	7.10E+05	5.85	0.81		4.02
1A	1.03	3	53	0.1	5.30E+05	5.72	1.02		5.03
1B	1.03	3	45	0.1	4.50E+05	5.65	1.09	5.73	5.38
1C	1.03	3	66	0.1	6.60E+05	5.82	0.92		4.56
2A	1.03	3	43	0.1	4.30E+05	5.63	1.03		5.09
2B	1.03	3	55	0.1	5.50E+05	5.74	0.92	5.69	4.56
2C	1.03	3	50	0.1	5.00E+05	5.70	0.97		4.77
1A	0.772	2	276	0.1	2.76E+05	5.44	1.30		6.43
1B	0.772	2	313	0.1	3.13E+05	5.50	1.25	5.48	6.16
1C	0.772	2	323	0.1	3.23E+05	5.51	1.23		6.09
2A	0.772	2	314	0.1	3.14E+05	5.50	1.17		5.77
2B	0.772	2	313	0.1	3.13E+05	5.50	1.17	5.47	5.77
2C	0.772	2	270	0.1	2.70E+05	5.43	1.23		6.09

Flow Rate (L/min)	log N average	logi	Dose	Standard Deviation	Critical t	90% Confidence
0	6.74	0.00	0.00	0.00	0.00	0.00
1.23	5.87	0.87	4.31	0.14	2.92	0.29
1.03	5.73	1.01	4.99	0.41	2.92	0.85
0.772	5.48	1.26	6.23	0.18	2.92	0.37
0	6.66	0.00	0.00	0.00	0.00	0.00
1.23	5.84	0.82	4.07	0.30	2.92	0.61
1.03	5.69	0.97	4.81	0.53	2.92	1.10
0.772	5.47	1.19	5.88	0.37	2.92	0.76

Prototype 3 86.7% UVT

Trial	Flow Rate (L/min)	Dilution	Count	Sample Volume (mL)	Concentration (PFU/mL)	log N	log N average	logi	Dose
A	Blank	0	0	0.1	0.00E+00				
B	Blank	0	0	0.1	0.00E+00				
C	Blank	0	0	0.1	0.00E+00				
D	Blank	0	0	0.1	0.00E+00				
1A	0	4	50	0.1	5.00E+06	6.70			
1B	0	4	48	0.1	4.80E+06	6.68	6.69		
1C	0	4	49	0.1	4.90E+06	6.69			
2A	0	4	36	0.1	3.60E+06	6.56			
2B	0	4	56	0.1	5.60E+06	6.75	6.67		
2C	0	4	52	0.1	5.20E+06	6.72			
Reactor (A_{254}=.062)									
1A	1.47	2	133	0.1	1.33E+05	5.12		1.57	30.12
1B	1.47	2	168	0.1	1.68E+05	5.23	5.18	1.46	28.17
1C	1.47	2	159	0.1	1.59E+05	5.20		1.49	28.63
2A	1.47	2	162	0.1	1.62E+05	5.21		1.46	28.15
2B	1.47	2	142	0.1	1.42E+05	5.15	5.18	1.52	29.25
2C	1.47	2	151	0.1	1.51E+05	5.18		1.49	28.74
1A	1.36	2	135	0.1	1.35E+05	5.13		1.56	30.00
1B	1.36	2	143	0.1	1.43E+05	5.16	5.14	1.53	29.52
1C	1.36	2	140	0.1	1.40E+05	5.15		1.54	29.69
2A	1.36	2	120	0.1	1.20E+05	5.08		1.59	30.66
2B	1.36	2	110	0.1	1.10E+05	5.04	5.09	1.63	31.39
2C	1.36	2	138	0.1	1.38E+05	5.14		1.53	29.49
1A	1.12	2	93	0.1	9.30E+04	4.97		1.72	33.11
1B	1.12	2	86	0.1	8.60E+04	4.93	4.97	1.76	33.76
1C	1.12	2	104	0.1	1.04E+05	5.02		1.67	32.18
2A	1.12	2	87	0.1	8.70E+04	4.94		1.73	33.35
2B	1.12	2	94	0.1	9.40E+04	4.97	4.97	1.70	32.70
2C	1.12	2	100	0.1	1.00E+05	5.00		1.67	32.18

Flow Rate	log N average	logi LP	Dose	Standard Deviation	Critical t	90% Confidence
0	6.69	0.00	0.00	0.00	0.00	0.00
1.47	5.18	1.51	29.03	1.02	2.92	2.11
1.36	5.14	1.55	29.79	0.24	2.92	0.50
1.12	4.97	1.72	33.08	0.80	2.92	1.65
0	6.67	0.00	0.00	0.00	0.00	0.00
1.47	5.18	1.49	28.77	0.55	2.92	1.14
1.36	5.09	1.59	30.57	0.96	2.92	1.97
1.12	4.97	1.70	32.81	0.58	2.92	1.20

APPENDIX D: FIRST ORDER KINETIC MODELING CALCULATIONS

						T_{10}				tau			
Reactor	Flow Rate (L/min)	k_1 (1/min)	Dispersion # (Open Boundaries)	T_{10} (min)	Tau (min)	a	Cout/Cin	Percent Removal	Log Reduction	a	Cout/Cin	Percent Removal	Log Reduction
2	0.772	3.0374	0.313	0.167	0.240	1.28	0.622	37.8%	0.206	1.38	0.512	48.8%	0.291
2	1.03	3.0374	0.386	0.133	0.180	1.27	0.676	32.4%	0.170	1.36	0.593	40.7%	0.227
2	1.23	3.0374	0.313	0.117	0.150	1.20	0.713	28.7%	0.147	1.25	0.650	35.0%	0.187
3	1.12	0.3205	0.377	0.333	0.804	1.08	0.900	10.0%	0.046	1.18	0.777	22.3%	0.109
3	1.36	0.3205	0.461	0.167	0.662	1.05	0.948	5.2%	0.023	1.18	0.809	19.1%	0.092
3	1.47	0.3205	0.498	0.117	0.612	1.04	0.963	3.7%	0.016	1.18	0.820	18.0%	0.086